Genetic mapping reveals new loci and alleles for flowering time and plant height using the double round-robin population of barley

Authors

Francesco Cosenza[1], Asis Shrestha[1], Delphine Van Inghelandt[1], Federico A. Casale[1], Po-Ya Wu[1], Marius Weisweiler[1], Jinquan Li[2,3], Franziska Wespel[4], and Benjamin Stich[1,2,5*]

[1] Institute of Quantitative Genetics and Genomics of Plants, Heinrich Heine University, 40225 Düsseldorf, Germany

[2] Max Planck Institute for Plant Breeding Research, Köln, Germany

[3] Current address: Strube D&S GmbH, Söllingen, Germany

[4] Saatzucht Josef Breun GmbH Co. KG, Amselweg 1, 91074 Herzogenaurach, Germany

[5] Cluster of Excellence on Plant Sciences (CEPLAS), Heinrich Heine University, 40225 Düsseldorf, Germany

[*] Correspondence (Tel +49 211 81 13395; e-mail benjamin.stich@hhu.de)

ABSTRACT

Flowering time and plant height are two critical determinants of yield potential in barley (*Hordeum vulgare*). Although their role as key traits, a comprehensive understanding of the genetic complexity of flowering time and plant height regulation in barley is still lacking. Through a double round-robin population originated from the crossings of 23 diverse parental inbred lines, we aimed to determine the variance components in the regulation of flowering time and plant height in barley as well as identify new genetic variants by single and multi-population quantitative trait loci (QTL) analyses and allele mining. Despite similar genotypic variance, we observed higher environmental variance components for plant height than flowering time. Furthermore, we detected one new QTL for flowering time and two new QTL for plant height. Finally, we identified a new functional allelic variant of the main regulatory gene *Ppd-H1*. Our results show that the genetic architecture of flowering time and plant height might be more complex than reported earlier and that a number of undetected, small effect or low frequency, genetic variants underlie the control of these two traits.

1 INTRODUCTION

The increase in world population, the reduction of available arable land, and climate change represent some of the greatest challenges that humanity is and will further have to face in the near future (Vyas *et al.*, 2022). One of the answers to these challenges is to reduce the influence of biotic and abiotic stress factors and by that increase crop productivity (Khush, 2013). Of particular importance are yield increases of cereals (Araus *et al.*, 2008), which are essential for human nutrition as they alone contribute about 44.5% of the calory uptake of the world population (FAO, 2019). In addition, they are important for animal feeding and beverage production (FAO, 2020).

Flowering time is one of the critical determinants of yield potential in cereals (Hill and Li, 2016). This is because, at this phenological stage, the plant transits from the vegetative to the reproductive phase, and grain filling starts (Cockram *et al.*, 2007). In turn, the efficiency of grain filling is maximized if it coincides with optimal environmental conditions (Wiegmann *et al.*, 2019). Therefore, plants and farmers have adapted several strategies to synchronize the phenological stages to environmental conditions (Anderson and Song, 2020).

Barley (*Hordeum vulgare* L.) is ranked fourth among the most cultivated cereals worldwide (FAO, 2020). This species is characterized by great environmental plasticity that allows it to be cultivated at different latitudes, with extremely dissimilar conditions of temperature and photoperiod (Dawson *et al.*, 2015). It has been demonstrated that the adaptive success of barley is also due to the selection of favorable allelic variants at the main genes determining the transition from the vegetative to the reproductive phase (Comadran *et al.*, 2012; Göransson *et al.*, 2019; Turner *et al.*, 2005). Three types of genes have been identified to be responsible for the modulation of flowering time in barley: genes that act under the influence of photoperiod, genes that act under the influence of temperature, and genes, called as *earliness per se*, that act independently of environmental variables (Fernández-Calleja *et al.*, 2021).

The main genes whose expression is influenced by the photoperiod are *Ppd-H1* (Turner *et al.*, 2005) and *Ppd-H2* (Kikuchi and Handa, 2009). *Ppd-H1*, which is located on chromosome 2H, has been described as the major determinant of the response to long day conditions in barley, acting jointly with *HvCO1* and *HvCO2* (Campoli *et al.*, 2012). At the same time, *Ppd-H1* indirectly influences the response to vernalization by promoting the expression of *Vrn-H3* (Mulki and von Korff, 2016). *Ppd-H2* is the second main driver of the photoperiod response in barley, but unlike *Ppd-H1* it acts in short day conditions. The non-functional

allelic variant of *Ppd-H2* allowed the expansion of the cultivation area of barley at higher latitudes (Casao *et al.*, 2011).

The major determinants of the response to temperature are genes involved in the vernalization process. *Vrn-H1*, which is located on chromosome 5H, promotes flowering after the plant has satisfied its vernalization requirement (Yan *et al.*, 2003). Furthermore, *Vrn-H1* inhibits the expression of *Vrn-H2*, which is located on chromosome 4H. *Vrn-H2* delays flowering, allowing the plant to fulfill its cold needs (Deng *et al.*, 2015; Yan *et al.*, 2004). The interaction between *Vrn-H1* and *Vrn-H2* is therefore one of the main mechanisms that allow the control of flowering time in winter or facultative barley varieties (Yan *et al.*, 2004). The third gene responsible for the temperature response in barley is *Vrn-H3* on chromosome 7H (Yan *et al.*, 2006). *Vrn-H3*, when not repressed by *Vrn-H2*, promotes flowering by allowing the transition from the vegetative to the reproductive phase in long day conditions (Hemming *et al.*, 2008).

Within the group of *earliness per se* genes, the major determinant is *HvCEN* which is located on chromosome 2H. Because its expression is not directly influenced by environmental variables, the allelic variants of *HvCEN* allowed the expansion and adaptation of barley to new areas through the regulation of flowering time (Comadran *et al.*, 2012). In addition, three other genes have been described as circadian clock-related *earliness per se* genes which, although not directly influencing flowering, alter the expression of *Ppd-H1*: *HvELF3* (Faure *et al.*, 2012), on chromosome 1H, *HvLUX1* (Campoli *et al.*, 2013), on chromosome 3H, and *HvPHYC* (Nishida *et al.*, 2013), on chromosome 5H. Furthermore, mutations in *HvELF3* can also affect the expression of *HvGI* (Dunford *et al.*, 2005), causing earlier flowering (Zakhrabekova *et al.*, 2012). Finally, other genes initially reported to be responsible for controlling other quantitative traits have also been described to have an influence on flowering time or flower development: *HvAP2* (Shoesmith *et al.*, 2021), on chromosome 2H, and *Hv20ox2* (*sdw1/denso*) (Bezant *et al.*, 1996; Jia *et al.*, 2009), on chromosome 3H.

Another key trait responsible for determining production performance in cereal species is plant height (Mikołajczak *et al.*, 2017). An adequate plant height allows to obtain a lower exposure to lodging and a higher harvest index but on the other side, it is essential to keep the spikes far from the soil to reduce the risk of yield losses caused by infectious diseases (Vidal *et al.*, 2018). Plant height and flowering time are two interrelated characters. This is because flowering is possible when the meristem has switched from the vegetative to the reproductive phase. For this reason, many of the genes controlling flowering time, such as *Ppd-H1* (Turner *et al.*, 2005), *Vrn-H1* (Wiegmann *et al.*, 2019), *Vrn-H2* (Rollins *et al.*, 2013), *Vrn-H3* (Arifuzzaman *et al.*, 2016), *Hv20ox2* (Jia *et al.*, 2009), *HvCEN* (Bi *et al.*, 2019), and

HvAP2 (Patil *et al.*, 2019), have a pleiotropic effect on plant height. In addition to these genes, other genes involved in the biosynthesis of brassinosteroids, such as *HvBRD* on chromosome 2H, *HvBRI1* (*uzu*) on chromosome 3H, *HvDWF4*, on chromosome 4H, *HvCPD* and *HvDEP1* on chromosome 5H, and *HvDIM* on chromosome 7H (Dockter *et al.*, 2014; Wendt *et al.*, 2016), have been described to be involved in plant height regulation of barley. Some of the above mentioned genes, such as *HvAP2* and the genes regulating brassinosteroids biosynthesis, have been identified based on mutant approaches (Dockter *et al.*, 2014; Shoesmith *et al.*, 2021). When instead natural variation was exploited, bi-parental (Arifuzzaman *et al.*, 2014; Von Korff *et al.*, 2006; Rollins *et al.*, 2013; Schmalenbach *et al.*, 2009) or nested association mapping populations (Maurer *et al.*, 2015; Nice *et al.*, 2017) were used. When multi-parental populations were examined instead, the experiments comprised a restricted number of inbred lines (Cuesta-Marcos *et al.*, 2008), and/or the selected parental inbreds were from a restricted geographical range (Afsharyan *et al.*, 2020; Cuesta-Marcos *et al.*, 2008). All these factors reduce the likelihood of identifying genes and allelic variants with low population frequency (Yu *et al.*, 2006). Therefore, the utilization of segregating populations derived from genetic resources with high genotypic and phenotypic diversity could allow the identification of further genes that are mechanistically involved in flowering time and plant height regulation. This has the potential to facilitate and speed up breeding and provide new targets for genetic modification through, for example, CRISPR platforms. In turn, this could help to extend the cultivation area of barley by allowing its adaptation to new environmental conditions. Furthermore, the knowledge gained in barley has a high potential to be transferred to other cereal species that are genetically close but have a polyploid chromosomal structure, such as tetraploid (*Triticum turgidum* var. *durum*) and hexaploid (*Triticum aestivum*) wheat (Langridge, 2018).

In this study, a multi-parent population was used to explore the genetic landscape of flowering time and plant height in barley with the objectives of: (i) determining the genetic variance components in the regulation of flowering time and plant height, (ii) obtaining a comprehensive understanding of the genetic complexity of flowering time and plant height in barley by single and multi-population QTL analyses, (iii) identifying candidate genes for the detected QTL regulating flowering time and plant height, and detecting new allelic variants of genes responsible for the control of these two traits.

2 MATERIALS AND METHODS

2.1 Plant material and genotypic evaluation

The plant material used in this study consisted of a population which is designated in the following as *Hordeum vulgare* Double Round-Robin (HvDRR). The population originated from the crossings of 23 parental inbred lines, including eleven cultivars and twelve landraces (Shrestha *et al.*, 2022), in a double round-robin scheme (Stich, 2009) (Supplementary Table 1). The parental inbred lines have been chosen from a diversity panel of 224 spring barley accessions selected from the Barley Core Collection (BCC) (Pasam *et al.*, 2012) to maximize the combined genotypic and phenotypic richness index (Weisweiler *et al.*, 2019).

Starting from the 45 F1s, a single seed descent strategy has been applied to develop between 35 and 146 recombinant inbred lines (RIL) for each of the 45 sub-populations (Casale *et al.*, 2022). The RILs were genotyped at the F4 generation using a 50K SNP genotyping array (Bayer *et al.*, 2017).

2.2 Phenotyping

Flowering time (FT) evaluation was carried out in seven environments in Germany: Cologne from 2017 to 2019, Mechernich from 2018 to 2019, and Quedlinburg from 2018 to 2019. Plant height (PH) was evaluated in the same environments except for Quedlinburg, totaling five environments. At the Cologne and Mechernich environments, 33 seeds were sown in single rows of 1.6 meters length. In Quedlinburg, double rows of the same length were sowed. The inter-row distance was 20 cm. Fertilization and plant protection followed local practices.

In each environment, an augmented design was used. RILs of the HvDRR population and the inbreds of the diversity panel were planted with one replicate and only the parental inbreds of the HvDRR population were replicated 15-20 times per environment.

FT was recorded as days after sowing when 50% of the plants within the (double) row were flowering. PH was measured on average across all available plants within a row as height in cm from the collar to the peak of the plant when the spike was fully developed.

2.3 Statistical analyses

The collected phenotypic data were subject to statistical analysis using the following linear mixed model:

$$Y_{ijk} = \mu + G_i + E_j + e_{ijk} \quad (1)$$

where Y_{ijk} indicated the observed phenotypic value for the i^{th} genotype in the j^{th} environment within the k^{th} replication, μ the general mean of the trait, G_i the effect of the i^{th} genotype, E_j the effect of the j^{th} environment, and e_{ijk} the random error. For the calculation of adjusted entry means, the genotypic effect was considered fixed, while the environmental effect was considered random.

The broad sense heritability (h^2) was calculated as:

$$h^2 = V_g / (V_g + \frac{\bar{c}}{2}) \quad (2)$$

where V_g represented the genotypic variance and $\bar{c}$ the mean of the standard errors of the contrasts among all pairs of genotypes (Piepho and Möhring, 2007). For the calculation of the genotypic variance (V_g), model *(1)* was used, but all effects were considered as random. In addition, we calculated h^2, when applying for each environment a correction based on the augmented design considering different grid sizes, and then estimating V_g and $\bar{c}$ across the environments.

In order to quantify the interaction between genotype and environment, we used a second linear mixed model:

$$Y_{ijk} = \mu + G_i + E_j + (G{:}E)_{ij} + e_{ijk} \quad (3)$$

where $(G{:}E)_{ij}$ represented the interaction between the i^{th} genotype in the j^{th} environment, which was fitted to the data of the parental inbreds.

2.3.1 QTL analyses

Two different QTL analyses were performed in this study on the HvDRR population: multi-parent population (MPP) and single population (SP) analyses.

The estimation of genetic maps necessary for the SP analysis, as well as that of the consensus map used in the MPP, have been described by Casale *et al.* (2022).

For each sub-population and each trait, an SP QTL analysis was performed, based on the adjusted entry means for each RIL calculated with model *(1)*, using the following scheme:

first, standard interval mapping using the Haley-Knott regression algorithm (Knott and Haley, 1992) was applied, followed by forward selection in order to determine the number of QTL to include in the model. Then a forward and backward selection algorithm was applied to perform multiple QTL mapping. Model selection was based on the highest penalized LOD score with penalties determined through 4000 permutations. A two-dimensional genome-wide scan was performed to detect epistatic interactions between all pairs of loci in the genome. The SP analyses were carried out with the R package "qtl" (Broman *et al.*, 2003). The MPP analyses were performed by jointly analyzing all sub-populations using an ancestral model that took into account the degree of relatedness among the parental inbreds (Garin *et al.*, 2017). The degree of relatedness was calculated by clustering the haplotypes. The haplotype window size was chosen as the consensus genetic map distance for which the linkage disequilibrium (LD), measured as r^2, was 0.2 (Giraud *et al.*, 2014) (Supplementary Table 2). The MPP analysis was performed using the R package "mppR" (Garin *et al.*, 2015).

Confidence intervals for the QTL detected via SP and MPP were calculated using a 1.5 LOD drop method (Manichaikul *et al.*, 2006).

2.3.2 Genomic prediction

Genomic predictions of FT and PH in the HvDRR population were performed by genomic best linear unbiased prediction (GBLUP) using the following model (VanRaden, 2008):

$$\boldsymbol{y} = \mathbf{1}\mu + \boldsymbol{Zu} + \boldsymbol{\varepsilon} \quad (4)$$

where $\boldsymbol{y}$ was the vector of the adjusted entry means of the considered trait (FT or PH), $\mathbf{1}$ was a unit vector, μ the general mean, $\boldsymbol{Z}$ the design matrix that assigned the random effects to the genotypes, and $\boldsymbol{u}$ the vector of genotypic effects that were assumed to be normally distributed with $N(0, \boldsymbol{K}\sigma_u^2)$, in which $\boldsymbol{K}$ denoted the realized kinship matrix between inbreds and σ_u^2 the genetic variance of the GBLUP model. In addition, $\boldsymbol{\varepsilon}$ was the vector of residuals following a normal distribution $N(0, I\sigma_e^2)$.

The prediction ability of the GBLUP model was evaluated by Pearson's correlation coefficient (r) between observed and predicted phenotypes. To assess the model performance, five-fold cross-validation (CV) with 20 replications was performed. In that case, the prediction ability was defined as the median of the prediction abilities across the 20 runs of each 5 fold-CV.

2.3.3 Candidate gene analysis and allele mining

The candidate gene analysis was performed for those QTL from the SP analysis that did not carry inside their confidence intervals previously reported genes controlling the corresponding trait, explained ≥ 15% of the phenotypic variance, and had a confidence interval ≤ 30 cM. For the QTL that fulfilled these criteria, all the genes within the confidence interval were extracted using the Morex v3 reference sequence (Mascher *et al.*, 2021). Next, variant calling data of single nucleotide polymorphisms (SNPs), causing tolerated and deleterious mutations, insertion and deletions (INDELs), and predicted structural variants (SV), obtained as described by Weisweiler *et al.* (2022), were used to identify genes that were polymorphic between the two parental inbreds of the sub-population in which the QTL was detected. For each gene, we took into account all the polymorphisms inside the coding, non-coding, and, for SV, potential regulatory regions of the gene within 5 kb up and downstream of the gene.

Subsequently, we performed a weighted gene co-expression network analysis (WGCNA) to identify modules of co-expressed genes that were associated with the phenotypic variability of the traits. The mRNA sequencing experiment of leaf samples of 21 parental inbred lines, described by Weisweiler *et al*. (2019), was the basis for this analysis. The selected soft thresholding power was two, based on the scale-free topology criterion (Zhang and Horvath, 2005). We predicted the gene networks for the three modules with the highest and the three lowest correlations for both traits. In order to have a comprehensive understanding of the networks we selected genes with a gene-module membership p-value < 0.01 and, within them, the top 30% of gene-gene interactions based on the interactions weight. Because of the high number of gene-gene interactions in the module “turquoise”, we selected the top 5% of interactions with the highest weight. For the “lightyellow” and “tan” modules we did not filter the interactions based on weight. Furthermore, for the “black” module we selected the genes with a gene-module membership p-value < 0.05.

In the next step, the results of the WGCNA and SP QTL analyses were combined: we further filtered the polymorphic genes within the confidence intervals based on their membership to a module (Wei *et al.*, 2022). The genes within the three modules with the highest and the three with the lowest correlation with the trait under consideration were evaluated for their functional annotation. We selected as candidate genes those with an annotation similar to that of genes previously reported to control the trait under consideration in barley and those for whom functional annotation has been described to be involved in plant vegetative or

reproductive development. All the analyses for the calculation of the weighted gene co-expression networks were performed with the R package "WGCNA" (Langfelder and Horvath, 2008).

Allele mining was performed for the known genes with pleiotropic effect on FT and PH located within SP QTL confidence intervals. For each gene, polymorphisms between the parental inbreds of the respective segregating sub-populations were extracted from the whole genome sequencing data (Weisweiler *et al.*, 2022). To confirm the accuracy of the whole genome sequencing data, we performed Sanger sequencing of the 23 parental inbreds for *Ppd-H1*. To predict the effect of polymorphisms on the phenotype, we used the SIFT algorithm (Vaser *et al.*, 2016). In addition, we performed PCR, as described in Karsai *et al*. (2005), to check the presence/absence of the three *Vrn-H2* genes.

2.3.4 Fine mapping of QTL by association genetics

We used association genetics in the diversity panel of Pasam *et al*. (2012) to fine map the QTL that did not carry within their confidence intervals genes reported to control the corresponding trait, explained ≥ 15%, and had a confidence interval ≤ 30 cM. We used the phenotypic data of the 224 inbreds collected in our field trials and the genotypic information available from Milner *et al*. (2019). To construct the kinship matrix among the 224 inbreds, we used all the SNPs in the SNP matrix. Association analysis was performed using only polymorphisms from QTL fulfilling the above mentioned criteria. For association analysis, we used a mixed model approach, implemented for the variance component (Kang *et al.*, 2010), with the R package "statgenGWAS" (van Rossum *et al.*, 2022).

3 RESULTS

3.1 Phenotypic variation and covariation

FT and PH were evaluated for each RIL across seven and five environments, respectively. For both traits, the environmental variance (V_e) was about two to three times higher than the genotypic variance (Table 1). Furthermore, for FT, the G:E variance was about half the genotypic variance, while for PH the G:E variance was about 87% of the genotypic variance. The values of broad-sense heritability on an entry means basis were high to very high, ranging from 0.76 for PH to 0.86 for FT (Table 1).

To take into account possible intra-environmental variation, the phenotypic values were adjusted using moving grids of three different sizes, exploiting the possibilities of an augmented design. For all three examined grid sizes, we observed that the resulting heritability values across all environments were reduced compared to the analysis without adjustment. Therefore, we decided to discuss in the following only results from analyses where intra-environmental variation was not corrected for.

Across all environments, the sub-population that was found to be the earliest to flower was HvDRR35, where RILs flowered on average 58 days after sowing. In contrast, the latest sub-population to flower was HvDRR46 for which, on average, RILs reached flowering 79 days after sowing (Figure 1; Supplementary Table 3). HvDRR46 was also the sub-population with the smallest plants, with an average height of 48 cm. In contrast, HvDRR12 was, with an average of 87 cm, the sub-population with the tallest plants (Figure 1; Supplementary Table 3). HvDRR09 was the sub-population with the lowest coefficient of variation (CoV) value for FT (2.73 days), while the highest CoV was observed for HvDRR43 (23.31 days) (Supplementary Table 3). Regarding PH, the sub-population with the smallest variability was HvDRR15 (CoV = 3.83 cm), while the highest CoV, 30.53 cm, was observed for HvDRR46 (Supplementary Table 3). The CoV was, for the diversity panel across the same environments, 7.35 days for FT and 14.01 cm for PH (Supplementary Table 3).

The differences between the mean of the parental inbreds and the mean of the sub-populations were also examined as these are an indicator for the presence of epistasis. For flowering time, the differences between the means of the parental inbred lines and the respective sub-populations were statistically significant ($p < 0.05$) in 22 cases. Among them, the highest differences were observed for sub-populations HvDRR43, with 7.2 days, and HvDRR46, with 10.5 days. For plant height the differences of the means of the sub-populations and the parental inbreds were significant ($p < 0.05$) in 14 cases. The strongest

difference between the parental inbreds and the progeny mean was observed for sub-populations HvDRR10, with 9.62 cm, HvDRR12, with 9.88 cm, and HvDRR11, with 10.60 cm. All these sub-populations had Sanalta as common parental inbred (Figure 1).

Across all sub-populations, the correlation coefficient of FT and PH was -0.012 (Supplementary Figure 1). However, considerable differences were observed for the single sub-populations (Figure 2). HvDRR28 was the sub-population for which the highest correlation coefficient has been observed (0.44), while the sub-population where the two traits were most negatively correlated was HvDRR43 (-0.77) (Supplementary Figure 2).

3.2 Multi-parent population analysis

The multi-parent population analysis identified each 21 QTL for FT and PH, distributed across all seven chromosomes (Figure 3). The analysis was performed using the genetic haplotype window sizes estimated from the extent of linkage disequilibrium (Supplementary Table 2). The percentage of phenotypic variance explained by all the QTL detected in the MPP analysis was 39.1% and 24.9% for FT and PH, respectively. For FT, the confidence interval of 17 QTL overlapped with the interval of at least one QTL identified in the SP analysis (Supplementary Tables 4-5). Out of 21 QTL identified for PH, 16 overlapped with one or more QTL detected in SP analysis (Supplementary Tables 4-6). Among the QTL detected for both traits, the intervals of two pairs of QTL overlapped: *FT-MP-Q3* with *PH-MP-Q3* and *FT-MP-Q19* with *PH-MP-Q20*.

The additive effect of the 23 parental inbreds for the 21 QTL for FT ranged from -2.42 days, observed for Ancap2 at *FT-MP-Q5,* to 5.14 days, for Kombyne at *FT-MP-Q13* (Figure 4). However, in about 92% of cases, the additive effect for FT was between -1 and 1 day (Supplementary Figure 3). For PH, the effect ranged from -3.88 cm for Kombyne at *PH-MP-Q15*, to a maximum of 1.99 cm at *PH-MP-Q5*, for seven parental inbreds (Figure 4). Also in this case more than 90% of the additive effects had a value between -1 and 1 cm (Supplementary Figure 3). The crossings design underlying our population allows to estimate the number of alleles at each QTL. The QTL with the highest number of significantly different allele effects and thereby with presumably alleles were, for FT, *FT-MP-Q20*, with 9 alleles, and, for PH, *PH-MP-Q20*, with 8 detected alleles.

3.3 Genomic prediction ability

The prediction abilities of the GBLUP model across the HvDRR population were high with values of 0.89 and 0.87 for FT and PH respectively (Supplementary Table 7). To compare the prediction performance of the GBLUP model with those of the detected QTL, we used the squared prediction abilities. The coefficient of determinations (r^2) obtained by genomic prediction without CV was 0.79 for FT and 0.76 for PH. The cross-validated prediction abilities were 0.77 for both FT and PH.

3.4 Single population QTL analysis

Through single population analysis, 89 QTL were identified for FT and 80 for PH (Figures 5-6; Supplementary Tables 5-6). The percentages of explained variance by the individual QTL detected for FT sized from 1.02%, for *qHvDRR47-FT-7.1*, to 77.75%, for *qHvDRR27-FT-2.1* (Supplementary Table 5), while for PH the values ranged from 2.52%, for *qHvDRR11-PH-2.2*, to 63.62%, for *qHvDRR10-PH-3.1* (Supplementary Table 6). HvDRR22 was the sub-population with the highest values of explained variance for both FT (70.24%) and PH (78.54%), while the lowest percentages of variance explained by the detected QTL were observed for FT in HvDRR35 (33.49%) and for PH in HvDRR31 (23.65%) (Supplementary Tables 5-6).

Out of 89 QTL identified in the single population analysis for FT, 43 mapped to chromosome 2H (Figure 5). A cluster comprising 21 QTL was located at the beginning of chromosome 2H. The region covered by the confidence interval of these QTL included *Ppd-H1*. Also for other major effect genes, responsible for the control of FT, QTL clusters had been identified: six QTL at the end of chromosome 4H, whose confidence intervals included *Vrn-H2*, ten QTL at the beginning of chromosome 5H, a region in which *Vrn-H1* was positioned, and eleven QTL at the beginning of chromosome 7H in which *Vrn-H3* was located. Other QTL comprised additional genes within their confidence intervals such as *HvELF3*, *HvCEN*, *Hv20ox2* (*sdw1/denso)*, *HvFT4* (Pieper *et al.*, 2021), and *HvAP2* (Supplementary Table 5).

Single population analysis for PH identified 80 QTL, where these QTL were characterized by wider confidence intervals compared to those detected for FT (Figure 6, Supplementary Table 6). As observed for FT, the chromosome with the highest number of QTL was 2H. A cluster, including 14 QTL, comprised within their confidence interval *Ppd-H1*. Other clusters of QTL that included in their confidence interval *HvAP2*, *Hv20ox2* (*sdw1/denso*), *Vrn-H1*, and *Vrn-H3* had been identified (Supplementary Table 6).

However, we identified 16 QTL for FT and 31 QTL for PH for which no genes previously described for the control of the trait were included within their confidence interval

(Supplementary Tables 5-6). Among the 16 QTL detected for FT, the QTL with the lowest number of genes in the confidence interval were *qHvDRR02-FT-5.1* and *qHvDRR31-FT-5.2.* The QTL comprised 52 and 71 genes, respectively, which reduced to 35 and 45 when neglecting the low confidence genes. *qHvDRR31-FT-5.2* was with 3.4 cM the QTL with the shortest genetic confidence interval. For PH, *qHvDRR48-PH*-4.1 was the QTL with the lowest number of genes in its confidence interval (115 low and high confidence or 79 high confidence genes). The QTL with the shortest confidence interval was *qHvDRR22-PH-7.1* with 3.9 cM.

Eight sub-populations showed significant epistatic interactions between loci on a genome-wide scale. In total, ten significant epistatic interactions were detected. Nine interactions were detected for PH and one for FT. Two epistatic interactions each were observed for populations HvDRR34 and HvDRR44 (Supplementary Table 8).

3.5 Allele mining

For FT, 21 sub-populations showed a QTL that included *Ppd-H1*. For 14 of these, a QTL that included *Ppd-H1* was also identified for PH. A total of 16 of the 21 sub-populations were polymorphic for the causal SNP 22 of *Ppd-H1* (Turner *et al.*, 2005). However, five sub-populations (HvDRR02, HvDRR04, HvDRR20, HvDRR23, and HvDRR48), for which the QTL confidence intervals comprised *Ppd-H1*, did not segregate for this polymorphism. All non-polymorphic sub-populations for SNP 22 had HOR1842 or IG128104 as parental inbred lines (Supplementary Table 1). Through Sanger sequencing, we identified the presence of a unique SNP in HOR1842 and IG128104 in the CCT domain of *Ppd-H1* (Figure 7). The primers used to amplify *Ppd-H1* are listed in Supplementary Table 9. Based on the SNP position on the *Ppd-H1* coding sequence of Morex, we refer to it as SNP 1945. SNP 1945 determines the synthesis of a threonine instead of an alanine (Supplementary Figure 4). We then used the SIFT algorithm to predict the effect of this SNP on the phenotype. The effect of this polymorphism was classified by the SIFT algorithm as deleterious.

At the *Vrn-H2* locus, an FT QTL was detected in six sub-populations. We evaluated by PCR, as described in Karsai *et al*. (2005) (Supplementary Table 9), the presence/absence of the three causal *Vrn-H2* genes. Out of six sub-populations, five were polymorphic for the genes regulating the *Vrn-H2* locus. In HvDRR29, both parental inbred lines, HOR8160 and IG128216, had the complete set of genes (Supplementary Figure 5).

3.6 Candidate gene analysis

The candidate gene analysis was performed for the QTL detected in the SP analysis that did not carry in their confidence interval previously reported genes controlling the trait under consideration, explaining ≥ 15% of the phenotypic variance, and having a confidence interval ≤ 30 cM. For these QTL, we combined the results of QTL mapping with variant calling data and results from WGCNA. Through WGCNA, 27 different gene modules were detected across all the expressed genes in the barley genome (Supplementary Figure 6). The correlation of the gene expression of modules and the adjusted entry means ranged from -0.52 to 0.49 for FT and from -0.54 to 0.47 for PH. Interestingly, the module with the highest correlation was the same for both traits. After selecting genes within the QTL range and which were included in one of the three modules with the highest or the lowest correlation (Supplementary Figure 7), we searched for candidate genes. The most represented class of genes for the two traits was that of receptor-like kinase, followed by genes involved in the ethylene pathways, and genes coding for F-box proteins (Supplementary Table 10).

In addition to the functional based candidate gene analysis, we used association genetics in the diversity panel to fine map the selected QTL using the genome-wide genotyping-by-sequencing data of Milner *et al*. (2019). For FT, none of the polymorphisms in the QTL confidence intervals was significantly associated with the phenotype. For PH, we identified four significant SNPs associated with the phenotype (Supplementary Figure 8).

4 DISCUSSION

With this study, we aimed to obtain a comprehensive overview of the environmental and genotypic contributions to the regulation of flowering time and plant height in barley. We performed MPP and SP analysis to elucidate the genetic complexity underlying the control of FT and PH. Finally, we identified candidate genes and new allelic variants using additional approaches such as WGCNA and association genetics.

4.1 Flowering time variation is less environmental sensitive than that of plant height

We observed that relative to the genotypic variance, the variance components of environment and genotype by environment interaction were higher for PH than FT (Table 1). This finding was in discordance with a previous study where the variance component of the genotype-environment interaction was higher for FT than for PH (Rodriguez *et al.*, 2008). This result might be explained thereby by that the environments of our study differed mainly with respect to soil, precipitations, and temperature, which influence PH more strongly than FT (Li *et al.*, 2003). In contrast, latitudinal differences, which heavily impact FT (Kikuchi and Handa, 2009), were very small among our environments. An additional explanation is the limited number of studied genotypes by Rodriguez *et al*. (2008), which reduced the precision to estimate variance components. Nevertheless, we observed for both traits high to very high heritabilities indicating that the adjusted entry means calculated for FT and PH are very suitable to unravel the genetics of both traits (Table 1).

4.2 The double round-robin population shows high variability of flowering time and plant height

We observed in our study, with a range of adjusted entry means of 51.2 to 105.7 days as well as 12.6 to 101.2 cm for FT and PH, respectively, a high phenotypic diversity among the RILs of the HvDRR population (Figure 1). This range was considerably higher than that observed in earlier studies (Afsharyan *et al.*, 2020; Arifuzzaman *et al.*, 2016; Cuesta-Marcos *et al.*, 2008; Maurer *et al.*, 2015; Nice *et al.*, 2017). Also, the standard deviation of the adjusted entry means of the RILs of the HvDRR population was higher for both traits than that described in previous studies (Pauli *et al.*, 2014; Wang *et al.*, 2014) (Supplementary Table 3). These observations might be due to the higher number of RILs but also because of the selection of the 23 parental inbreds with maximal genotypic and phenotypic richness.

In addition, the variation observed for FT and PH in the diversity panel of 224 spring barley inbreds (Pasam *et al.*, 2012) was similar to that observed in individual sub-populations. However, it was considerably smaller (FT) and more influenced by a few outliers (PH) compared to the diversity observed in the entire HvDRR population (Figure 1).

These findings of high phenotypic variability, combined with high heritability values and high-quality genotypic data suggest that the double-round-robin population is a very powerful tool for exploring and detecting new genetic variants underlying the control of agronomic traits in barley, also compared to association mapping panels.

4.3 QTL analyses uncovered the role of the genetic background in determining the correlation between FT and PH

We observed that the correlation between FT and PH was different among the HvDRR sub-populations (Figure 2; Supplementary Figure 2). These results are in agreement with those of previous studies where positive and negative correlations have been identified between FT and PH (Von Korff *et al.*, 2006; Maurer *et al.*, 2016; Nice *et al.*, 2017; Schmalenbach *et al.*, 2009), although only one direction of the correlation index, positive or negative, was observed in each of these studies. The high variability of the correlation values could be due to the great genotypic diversity of the parental inbreds used in our study. In order to understand this aspect better, we considered in detail the co-located QTL for FT and PH in the SP analysis.

Considering the sub-populations in which the adjusted entry means of the two traits had the most negative correlation (HvDRR10, HvDRR11, and HvDRR43), all QTL detected for FT were also detected for PH, although additional QTL were observed for the latter trait (Supplementary Tables 5-6). For four of the five FT/PH QTL pairs, the parental inbred line conferring a positive additive effect for PH revealed a negative additive effect for FT and vice versa (Supplementary Tables 5-6; Supplementary Figure 2). At the same time, the three sub-populations with the highest correlation coefficient between FT and PH (HvDRR19, HvDRR28, and HvDRR29) had QTL falling within the same interval for the two traits (Figures 5-6). In this case, however, for the three overlapping pairs of QTL, the positive additive effect was given by the same parental inbred for both traits (Supplementary Tables 5-6; Supplementary Figure 2).

In order to increase the resolution of the dissection of the genetic origin of the correlation between FT and PH, we exploited the MPP analysis. For each of the two studied traits, we identified 21 QTL through MPP analysis (Figure 3). The QTL profiles obtained through MPP

analysis for both traits had peaks falling within neighboring regions for the main genes previously reported to control FT and PH, such as *Ppd-H1* and the three vernalization genes. The diversity of the parental inbreds and the large number of sub-populations as well as the total RILs resulted in a high mapping resolution that led to narrow confidence intervals. In our study, we observed a pleiotropic effect only for two QTL pairs (*FT-MP-Q3*/*PH-MP-Q3* and *FT-MP-Q19*/*PH-MP-Q20*). *FT-MP-Q3*/*PH-MP-Q3*, included in their common interval HORVU.MOREX.r3.1HG0075860 which was functionally annotated as transcription factor, while *FT-MP-Q19*/*PH-MP-Q20*, which explained a higher percentage of phenotypic variance compared to *FT-MP-Q3*/*PH-MP-Q3*, included in their intervals *Vrn-H3*. For all other QTL, the effect was separated by recombination.

Therewith, our results suggest that FT and PH variations are, with the exception of two QTL, caused by independent genetic factors (Figures 2-3-6-7; Supplementary Tables 4-5-6).

4.4 Multi-parent and single population analyses revealed new genome regions as well as genomic variants involved in the control of flowering time and plant height

The number of QTL identified through MPP analysis (Figure 3; Supplementary Table 4) was, with 21 each, higher compared to the maximum number of QTL, 13 for FT and 20 for PH, that were detected in earlier studies using bi- and multi-parental populations of spring barley (Arifuzzaman *et al.*, 2014; Cuesta-Marcos *et al.*, 2008; Von Korff *et al.*, 2006; Maurer *et al.*, 2015; Nice *et al.*, 2017; Pauli *et al.*, 2014; Rollins *et al.*, 2013; Schmalenbach *et al.*, 2009). The only exception was the study of Hemshrot *et al*. (2019) where a total of 23 QTL were identified for FT. However, in Hemshrot *et al*. (2019), QTL with the same genetic position were detected which reduced the number of QTL with different genetic positions to 13. The reasons for the higher number of QTL detected in our study compared to earlier studies were most probably the greater number of RILs and environments as well as the selection of very diverse parental inbreds (Weisweiler *et al.*, 2019) which both increased the statistical power to detect QTL (Stich, 2009). Our observation suggested that the genetic complexity of FT and PH is higher than initially reported. This conclusion is furthermore supported by the observation that for both traits the percentage of explained variance by a genomic prediction model was about twice the value of the variance explained by the QTL detected in the MPP analysis (Supplementary Table 7). This result suggested that even with about 4000 RILs many small effect QTL remain undetected.

The difference between the percentage of variance explained by a genomic prediction model and the variance explained by the QTL detected in the MPP analysis was greater in the case

of PH compared to FT (Supplementary Table 7). This observation suggests that PH is more strongly influenced by small (and undetected) effect QTL than FT. In addition, the total proportion of variance explained by the detected QTL was with 25.7% lower for PH than for FT (37.4%). This trend was in agreement with the observation that epistatic interaction played a bigger role for PH than for FT (Supplementary Table 8).

The SP QTL analyses detected 89 QTL for FT and 80 for PH (Figures 5-6; Supplementary Tables 5-6). We determined the physical position of QTL reported in earlier studies (Afsharyan *et al.*, 2020; Druka *et al.*, 2011; Hemshrot *et al.*, 2019; Laurie *et al.*, 1994; Maurer *et al.*, 2015; Nice *et al.*, 2017; Pauli *et al.*, 2014), wherever possible, and compared it to the QTL observed in our study. We observed for 166 QTL detected in our study a co-localization with earlier reported QTL. However, three QTL detected with SP analyses, one for FT and two for PH, did not overlap with other previously reported QTL. The novel QTL detected by SP were *qHvDRR30-FT*-3.1, *qHvDRR24-PH-3.1*, and *qHvDRR48-PH-4.1*. The percentage of variance explained by these QTL was relatively low for *qHvDRR30-FT*-3.1 (4.3%) but higher for *qHvDRR24-PH-3.1* (26.2%) and *qHvDRR48-PH-4.1* (19.5%). Because of the high percentage of variance explained by *qHvDRR24-PH-3.1*, we started fine mapping project of this QTL, as well as for *qHvDRR28-FT-2.2*, *qHvDRR41-FT-2.2, qHvDRR42-FT-3.1, qHvDRR22-PH-7.1, qHvDRR29-PH-2.1*, and *qHvDRR47-PH-2.1*.

We observed for 21 sub-populations an FT QTL whose confidence interval included the *Ppd-H1* locus. Five of these sub-populations (HvDRR02, HvDRR04, HvDRR20, HvDRR23, and HvDRR48) were not polymorphic for SNP 22 (Figure 7; Supplementary Table 1). SNP 22 is located within the CCT domain of *Ppd-H1*, one of the two main regulatory regions of the *Ppd-H1* causal gene (Turner *et al.*, 2005). SNP 22 was described as the polymorphism responsible for the difference between the dominant and recessive allelic variant of *Ppd-H1* (Turner *et al.*, 2005). Although more than 80 variants had been detected for *Ppd-H1* (Jones *et al.*, 2008), SNP 22 was so far the only functionally characterized polymorphism for which a difference in phenotype has been reported. A further polymorphism of *Ppd-H1*, SNP 48 (Jones *et al.*, 2008), had previously been associated with FT variation. However, the study of Sharma *et al*. (2020) did not observe hints that SNP 48 was the causal SNP of the *Ppd-H1* mutation. In addition, in none of the above mentioned five sub-populations, SNP 48 was segregating. All five sub-populations had HOR1842 or IG128104 as parental inbreds (Supplementary Table 1). From the whole genome sequencing data of the parental inbreds (Weisweiler *et al.*, 2022), followed by Sanger sequencing, we identified a not previously reported polymorphism, SNP 1945, unique to HOR1842 and IG128104 (Figure 7). SNP 1945 is located within the CCT domain of *Ppd-H1* and it causes the synthesis of threonine

instead of alanine (Supplementary Figure 4). This amino acid change was predicted by the SIFT algorithm as deleterious. In the sub-population HvDRR24, whose parental inbreds were HOR1842 and IG128104, we did not detect a QTL either for FT or for PH in the genome region of *Ppd-H1*. Together with the fact that HOR1842 and IG128104 originated from the same geographical region (south-central Asia), these observations support the hypothesis that HOR1842 and IG128104 might carry the same causal polymorphism. In addition, we observed that the additive effect for FT QTL co-locating with *Ppd-H1* was, with about 3.5 days, higher in sub-populations that segregated for SNP 22 compared to about 2.3 days for the five sub-populations that did not segregate for SNP 22 (Supplementary Table 5). For the latter sub-populations, the additive effect assumed a positive value for the RILs that inherited the *Ppd-H1* allele from HOR1842 or IG128104. These findings suggest that SNP 1945 is the causal polymorphism for the QTL in those sub-populations that are monomorphic for SNP 22 as well as a new functional allelic variant of *Ppd-H1*.

A similar observation was made for the QTL co-localizing with *Vrn-H2*. The *Vrn-H2* locus has been described as one of the main loci responsible for the difference between winter and spring barley varieties (Distelfeld *et al.*, 2009). This difference is caused by the total deletion of a complex of three genes (*ZCCT-Ha, ZCCT-Hb*, and *ZCCT-Hc*) in the spring barley genotypes or, in the case of facultative genotypes, of a partial deletion (Fernández-Calleja *et al.*, 2021; Karsai *et al.*, 2005). Surprisingly, we observed for four of the HvDRR parental inbreds the complete set of *Vrn-H2* causal genes in spring varieties of barley (Supplementary Figure 5), which was previously reported only for winter varieties (Fernández-Calleja *et al.*, 2021). This observation suggests that the plant response to the vernalization requirement may be more complex than previously assumed and not merely based on the presence/absence of the *Vrn-H2* genes. In addition, among the six sub-populations for which an FT QTL was detected at the *Vrn-H2* genome position, one sub-population, HvDRR29, was monomorphic for the number of *Vrn-H2* genes. Both parental lines, HOR8160 and IG128126 carried three *Vrn-H2* causal genes (Supplementary Figure 5). Similarly to *Ppd-H1*, it could be hypothesized that one of the parental lines of sub-population HvDRR29 carried a new functional allelic variant or that an additional gene, that acted on the phenotype in a similar way to *ZCCT-Ha:c*, was present within the same QTL confidence interval.

These two examples suggest that the genetic complexity of the studied traits might be higher than anticipated from the simple comparison of the list of co-localizing QTL and can now be resolved using multiple segregating populations together with next-generation sequencing

of the parental inbreds. In addition, the cloning of the underlying genes will complement our understanding of the regulatory mechanisms of flowering time and plant height.

4.5 Candidate gene analysis for a subset of the QTL

We first extracted the polymorphic genes among the parental inbred lines within the confidence interval of the QTL that explained ≥ 15% of the phenotypic variance, had a confidence interval ≤ 30 cM, and did not carry in their confidence interval any previously reported gene controlling the trait under consideration. Then, we combined this screening with the results obtained from the WGCNA, selecting the three modules that showed each the lowest and highest correlation with FT and PH (Supplementary Figure 6).

Among the QTL detected for FT, *qHvDRR28-FT-2.2* was the one that had the highest percentage of explained variance and, at the same time, had the shortest genetic confidence interval. Two, out of the five candidate genes identified for this QTL, encoded for the pseudo-response regulator 3 (PRR3) HORVU.MOREX.r3.2HG0170150 and the ethylene-responsive transcription factor HORVU.MOREX.r3.2HG0170460 (Supplementary Table 10). Pseudo-response regulator is the same class of genes to which *Ppd-H1* belongs. The role of these genes is critical for the regulation of the plant circadian clock (Eriksson and Millar, 2003; Mizuno and Nakamichi, 2005) and it has been described, among the other functions, to be involved in the control of flowering time (Hayama and Coupland, 2004). Five different sub-groups belonging to this class of genes have been reported: PRR1, PRR3, PRR5, PRR7 (to which *Ppd-H1* belongs), and PRR9 (Matsushika *et al.*, 2000). Phylogenetic analyses grouped the five sub-groups into three main clusters: PRR1, PRR5-PRR9, and PRR3-PRR7 (Nakamichi *et al.*, 2020). Although genes belonging to all three clusters have been described to control flowering time or to be influenced by the photoperiod, the only cluster containing genes from grass species described to be dependent on the photoperiod and at the same time to control flowering time was PRR3-PRR7 (Nakamichi *et al.*, 2020). Therewith this gene is an interesting target for further functional studies.

Genes responsible for ethylene biosynthesis are instead involved in a multitude of developmental processes throughout the plant life cycle, ranging from the early stages of plant development to the regulation of senescence (Bleecker and Kende, 2000). The concentration of ethylene also influences gene networks that regulate flowering in order to optimize the timing of the transition from the vegetative to the reproductive stage in relation to endogenous and external stimuli (Iqbal *et al.*, 2017). Although further studies are needed to identify the pathways regulated by ethylene in barley, in rice, overexpression of an

ethylene receptor (*ETR2*) was associated with delayed flowering (Hada *et al.*, 2009). The delay was associated with an up-regulation of a homologous gene of GIGANTEA and TERMINAL FLOWER 1/CENTRORADIALIS (Hada *et al.*, 2009), both of these classes of genes are involved in barley in the control of flowering since *HvGI* (Dunford *et al.*, 2005) and *HvCEN* (Comadran *et al.*, 2012) belong to them. Ethylene is also involved in plant growth (Dubois *et al.*, 2018) and its role in vegetative development in plants has been described in barley (Patil *et al.*, 2019). In addition to the one found in *qHvDRR28-FT-2.2*, we also identified two ethylene-responsive transcription factors (HORVU.MOREX.r3.7HG0685230 and HORVU.MOREX.r3.2HG0182430) in *qHvDRR22-PH-7.1* and *qHvDRR29-PH-2.1*. Besides being an ethylene-responsive transcription factor, HORVU.MOREX.r3.2HG0182430 also belongs to the same class of genes as *HvAP2*.

In addition to functional data, we used association genetics to fine map the detected QTL using the diversity panel which was evaluated in the same set of environments as the HvDRR population. For FT, none of the polymorphisms from Milner *et al*. (2019) that were located in the QTL confidence intervals were significantly associated ($p < 0.05$) with FT variation. The reason for this discrepancy was most probably that association mapping panels have a low power to detect marker-trait associations in the case of low frequency alleles (Myles *et al.*, 2009), which is overcome by using segregating populations as in the HvDRR population. For PH, low significant marker-trait associations have been detected. However, only one of the polymorphisms was in proximity (< 150 kbp) to HORVU.MOREX.r3.3HG0222500, a candidate gene detected for *qHvDRR24-PH-3.1* using the WGCNA approach (Supplementary Table 10; Supplementary Figure 8).

These results suggest that the integration of QTL analyses with other omics data sets supports the detection of candidate genes regulating traits of agronomic interest.

5 CONCLUSIONS

The great phenotypic variability observed for FT and PH in the HvDRR population suggests that this population will be a powerful genetic resource to detect new regulatory mechanisms that could allow to extend the barley cultivation area or its adaptation in changing environmental conditions. Furthermore, it was observed how environmental variables affected these traits and how the environmental component had a greater influence on plant height compared to flowering time. In addition, our study provides a comprehensive summary of the genetic architecture of FT and PH and serves as basis for future QTL cloning studies. Finally, the detection of novel QTL but also the observation that additional alleles or genes segregate at known loci like *Ppd-H1* and *Vrn-H2* suggests that the studied traits are genetically more complex than previously reported.

6 ACKNOWLEDGMENTS

We would like to thank our former colleagues George Alskief and Florian Esser for their technical support and for organizing and managing the field trials of the HvDRR population in the Cologne and Eifel location. We acknowledge Muenteha Yilmaz and Srinivasa Reddy Mothukuri for contribution to data collection and analyses. We thank the team of Saatzucht Breun for running the field trials in Quedlinburg. Computational infrastructure and support were provided by the Centre for Information and Media Technology at Heinrich Heine University, Düsseldorf.

7 AUTHORS CONTRIBUTIONS

Conceptualization: F.C., A.S. and B.S.

Data analysis: F.C., A.S., D.V.I., F.Ca., P.W., M.W and B.S.

Investigation: F.C and B.S.

Resources: J.L., F.W. and B.S.

Funding acquisition: B.S.

Writing: F.C. and B.S.

8 CONFLICT OF INTEREST

The authors declare no conflict of interest.

9 FUNDING

This work was supported by Deutsche Forschungsgemeinschaft (DFG, German Research Foundation) in the frame of an International Research Training Group (GRK 2466, Project ID: 391465903).

10 DATA AVAILABILITY

The codes used for the calculation of the adjusted entry means, the single and multi-parent population QTL analyses, the epistatic QTL models, the WGCNA analysis, as well as the data sets of the adjusted entry means of the HvDRR population, the genetic haplotypes used to build the ancestral model, and the genotypic and phenotypic data used in the QTL analyses are deposited at https://github.com/cosenzaf/HvDRR_FT_PH. The data of membership of genes to gene modules used in the WGCNA are deposited in https://zenodo.org/record/7525604#.Y7_VgxXMLIW. Genetic maps and variant calling data can be obtained from Casale *et al*. (2022) and Weisweiler *et al*. (2022). Seeds of the RILs of the HvDRR population can be requested from the corresponding author.

738 **11 REFERENCES**

739

740 Afsharyan, N.P., Sannemann, W., Léon, J., and Ballvora, A. (2020) *Effect of epistasis and*
741 *environment on flowering time in barley reveals a novel flowering-delaying QTL allele*.
742 *J. Exp. Bot.*, **71**, 893–906.
743 Anderson, J.T. and Song, B.H. (2020) *Plant adaptation to climate change—Where are we?*
744 *J. Syst. Evol.*, **58**, 533–545.
745 Araus, J.L., Slafer, G.A., Royo, C., and Serret, M.D. (2008) *Breeding for yield potential and*
746 *stress adaptation in cereals*. *CRC. Crit. Rev. Plant Sci.*, **27**, 377–412.
747 Arifuzzaman, M., Günal, S., Bungartz, A., Muzammil, S., Afsharyan, N.P., Léon, J., and
748 Naz, A.A. (2016) *Genetic mapping reveals broader role of vrn-h3 gene in root and*
749 *shoot development beyond heading in barley*. *PLoS One*, **11**, 1–16.
750 Arifuzzaman, M., Sayed, M.A., Muzammil, S., Pillen, K., Schumann, H., Naz, A.A., and
751 Léon, J. (2014) *Detection and validation of novel QTL for shoot and root traits in*
752 *barley (Hordeum vulgare L.)*. *Mol. Breed.*, **34**, 1373–1387.
753 Bayer, M.M., Rapazote-Flores, P., Ganal, M., Hedley, P.E., Macaulay, M., Plieske, J., et al.
754 (2017) *Development and evaluation of a barley 50k iSelect SNP array*. *Front. Plant*
755 *Sci.*, **8**, 1–10.
756 Bezant, J., Laurie, D., Pratchett, N., Chojecki, J., and Kearsey, M. (1996) *Marker*
757 *regression mapping of QTL controlling flowering time and plant height in a spring*
758 *barley (Hordeum vulgare L.) cross*. *Heredity (Edinb).*, **77**, 64–73.
759 Bi, X., Esse, W. Van, Mulki, M.A., Kirschner, G., Zhong, J., Simon, R., and Korff, M. Von
760 (2019) *Centroradialis interacts with flowering locus t-like genes to control floret*
761 *development and grain number*. *Plant Physiol.*, **180**, 1013–1030.
762 Bleecker, A.B. and Kende, H. (2000) *Ethylene: A gaseous signal molecule in plant*. *Annu.*
763 *Rev. Cell Dev. Biol.*, **16**, 1–18.
764 Broman, K.W., Wu, H., Sen, Ś., and Churchill, G.A. (2003) *R/qtl: QTL mapping in*
765 *experimental crosses*. *Bioinformatics*, **19**, 889–890.
766 Campoli, C., Drosse, B., Searle, I., Coupland, G., and Von Korff, M. (2012) *Functional*
767 *characterisation of HvCO1, the barley (Hordeum vulgare) flowering time ortholog of*
768 *CONSTANS*. *Plant J.*, **69**, 868–880.
769 Campoli, C., Pankin, A., Drosse, B., Casao, C.M., Davis, S.J., and Von Korff, M. (2013)
770 *HvLUX1 is a candidate gene underlying the early maturity 10 locus in barley:*
771 *Phylogeny, diversity, and interactions with the circadian clock and photoperiodic*
772 *pathways*. *New Phytol.*, **199**, 1045–1059.

773 Casale, F., Van Inghelandt, D., Weisweiler, M., Li, J., and Stich, B. (2022) *Genomic*
774 *prediction of the recombination rate variation in barley – A route to highly*
775 *recombinogenic genotypes*. *Plant Biotechnol. J.*, **20**, 676–690.
776 Casao, M.C., Karsai, I., Igartua, E., Gracia, M.P., Veisz, O., and Casas, A.M. (2011)
777 *Adaptation of barley to mild winters: A role for PPDH2*. *BMC Plant Biol.*, **11**.
778 Cockram, J., Jones, H., Leigh, F.J., O'Sullivan, D., Powell, W., Laurie, D.A., and
779 Greenland, A.J. (2007) *Control of flowering time in temperate cereals: Genes,*
780 *domestication, and sustainable productivity*. *J. Exp. Bot.*, **58**, 1231–1244.
781 Comadran, J., Kilian, B., Russell, J., Ramsay, L., Stein, N., Ganal, M., et al. (2012) *Natural*
782 *variation in a homolog of Antirrhinum CENTRORADIALIS contributed to spring growth*
783 *habit and environmental adaptation in cultivated barley*. *Nat. Genet.*, **44**, 1388–1391.
784 Cuesta-Marcos, A., Casas, A.M., Yahiaoui, S., Gracia, M.P., Lasa, J.M., and Igartua, E.
785 (2008) *Joint analysis for heading date QTL in small interconnected barley populations*.
786 *Mol. Breed.*, **21**, 383–399.
787 Dawson, I.K., Russell, J., Powell, W., Steffenson, B., Thomas, W.T.B., and Waugh, R.
788 (2015) *Barley: A translational model for adaptation to climate change*. *New Phytol.*,
789 **206**, 913–931.
790 Deng, W., Casao, M.C., Wang, P., Sato, K., Hayes, P.M., Finnegan, E.J., and Trevaskis, B.
791 (2015) *Direct links between the vernalization response and other key traits of cereal*
792 *crops*. *Nat. Commun.*, **6**.
793 Distelfeld, A., Li, C., and Dubcovsky, J. (2009) *Regulation of flowering in temperate*
794 *cereals*. *Curr. Opin. Plant Biol.*, **12**, 178–184.
795 Dockter, C., Gruszka, D., Braumann, I., Druka, A., Druka, I., Franckowiak, J., et al. (2014)
796 *Induced variations in brassinosteroid genes define barley height and sturdiness, and*
797 *expand the green revolution genetic toolkit*. *Plant Physiol.*, **166**, 1912–1927.
798 Druka, A., Franckowiak, J., Lundqvist, U., Bonar, N., Alexander, J., Houston, K., et al.
799 (2011) *Genetic dissection of barley morphology and development*. *Plant Physiol.*, **155**,
800 617–627.
801 Dubois, M., Van den Broeck, L., and Inzé, D. (2018) *The Pivotal Role of Ethylene in Plant*
802 *Growth*. *Trends Plant Sci.*, **23**, 311–323.
803 Dunford, R.P., Griffiths, S., Christodoulou, V., and Laurie, D.A. (2005) *Characterisation of a*
804 *barley (Hordeum vulgare L.) homologue of the Arabidopsis flowering time regulator*
805 *GIGANTEA*. *Theor. Appl. Genet.*, **110**, 925–931.
806 Eriksson, M.E. and Millar, A.J. (2003) *The circadian clock. A plant's best friend in a*
807 *spinning world*. *Plant Physiol.*, **132**, 732–738.

Food and Agriculture Organization of the United Nations. (2019). FAOSTAT statistical database. [Rome] :FAO

Food and Agriculture Organization of the United Nations. (2020). FAOSTAT statistical database. [Rome] :FAO

Faure, S., Turner, A.S., Gruszka, D., Christodoulou, V., Davis, S.J., Von Korff, M., and Laurie, D.A. (2012) *Mutation at the circadian clock gene EARLY MATURITY 8 adapts domesticated barley (Hordeum vulgare) to short growing seasons*. *Proc. Natl. Acad. Sci. U. S. A.*, **109**, 8328–8333.

Fernández-Calleja, M., Casas, A.M., and Igartua, E. (2021) *Major flowering time genes of barley: allelic diversity, effects, and comparison with wheat*. Springer Berlin Heidelberg.

Garin, V., Wimmer, V., and Malosetti, M. (2015) *mppR : An R Package for QTL Analysis in Multi-parent Populations using Linear Mixed Models*.

Garin, V., Wimmer, V., Mezmouk, S., Malosetti, M., and van Eeuwijk, F. (2017) *How do the type of QTL effect and the form of the residual term influence QTL detection in multi-parent populations? A case study in the maize EU-NAM population*. *Theor. Appl. Genet.*, **130**, 1753–1764.

Giraud, H., Lehermeier, C., Bauer, E., Falque, M., Segura, V., Bauland, C., et al. (2014) *Linkage disequilibrium with linkage analysis of multiline crosses reveals different multiallelic QTL for hybrid performance in the flint and dent heterotic groups of maize*. *Genetics*, **198**, 1717–1734.

Göransson, M., Hallsson, J.H., Lillemo, M., Orabi, J., Backes, G., Jahoor, A., et al. (2019) *Identification of ideal allele combinations for the adaptation of spring barley to northern latitudes*. *Front. Plant Sci.*, **10**, 1–13.

Hada, W., Bo, Z., Cao, W.H., Biao, M., Gang, L., Liu, Y.F., et al. (2009) *The Ethylene Receptor ETR2 delays floral transition and affects starch accumulation in rice*. *Plant Cell*, **21**, 1473–1494.

Hayama, R. and Coupland, G. (2004) *The molecular basis of diversity in the photoperiodic flowering responses of arabidopsis and rice*. *Plant Physiol.*, **135**, 677–684.

Hemming, M.N., Peacock, W.J., Dennis, E.S., and Trevaskis, B. (2008) *Low-temperature and daylength cues are integrated to regulate Flowering Locus T in barley*. *Plant Physiol.*, **147**, 355–366.

Hemshrot, A., Poets, A.M., Tyagi, P., Lei, L., Carter, C.K., Hirsch, C.N., et al. (2019) *Development of a multiparent population for genetic mapping and allele discovery in six-row barley*. *Genetics*, **213**, 595–613.

Hill, C.B. and Li, C. (2016) *Genetic architecture of flowering phenology in cereals and opportunities for crop improvement*. *Front. Plant Sci.*, **7**, 1–23.

Iqbal, N., Khan, N.A., Ferrante, A., Trivellini, A., Francini, A., and Khan, M.I.R. (2017) *Ethylene role in plant growth, development and senescence: interaction with other phytohormones*. *Front. Plant Sci.*, **8**, 1–19.

Jia, Q.J., Zhang, J.J., Westcott, S., Zhang, X.Q., Bellgard, M., Lance, R., and Li, C.D. (2009) *GA-20 oxidase as a candidate for the semidwarf gene sdw1/denso in barley*. *Funct. Integr. Genomics*, **9**, 255–262.

Jones, H., Leigh, F.J., Mackay, I., Bower, M.A., Smith, L.M.J., Charles, M.P., et al. (2008) *Population-based resequencing reveals that the flowering time adaptation of cultivated barley originated east of the fertile crescent*. *Mol. Biol. Evol.*, **25**, 2211–2219.

Kang, H.M., Sul, J.H., Service, S.K., Zaitlen, N.A., Kong, S.Y., Freimer, N.B., et al. (2010) *Variance component model to account for sample structure in genome-wide association studies*. *Nat. Genet.*, **42**, 348–354.

Karsai, I., Szucs, P., Mészáros, K., Filichkina, T., Hayes, P.M., Skinner, J.S., et al. (2005) *The Vrn-H2 locus is a major determinant of flowering time in a facultative x winter growth habit barley (Hordeum vulgare L.) mapping population*. *Theor. Appl. Genet.*, **110**, 1458–1466.

Khush, G.S. (2013) *Strategies for increasing the yield potential of cereals: Case of rice as an example*. *Plant Breed.*, **132**, 433–436.

Kikuchi, R. and Handa, H. (2009) *Photoperiodic control of flowering in barley*. *Breed. Sci.*, **59**, 546–552.

Knott, S.A. and Haley, C.S. (1992) *A simple regression method for mapping quantitative trait loci in line crosses using flanking markers*. *Heredity (Edinb).*, **69**, 315–324.

Von Korff, M., Wang, H., Léon, J., and Pillen, K. (2006) *AB-QTL analysis in spring barley: II. Detection of favourable exotic alleles for agronomic traits introgressed from wild barley (H. vulgare ssp. spontaneum)*. *Theor. Appl. Genet.*, **112**, 1221–1231.

Langfelder, P. and Horvath, S. (2008) *WGCNA: An R package for weighted correlation network analysis*. *BMC Bioinformatics*, **9**.

Langridge (2018), Peter. *Economic and academic importance of barley. In The barley genome. Springer, Cham,* 1-10.

Laurie, D.A., Pratchett, N., Bezant, J.H., and Snape, J.W. (1994) *Genetic analysis of a photoperiod response gene on the short arm of chromosome 2(2h) of Hordeum vulgare (barley)*. *Heredity (Edinb).*, **72**, 619–627.

878 Li, Z.K., Yu, S.B., Lafitte, H.R., Huang, N., Courtois, B., Hittalmani, S., et al. (2003) *QTL x*
879 *environment interactions in rice. I. Heading date and plant height*. *Theor. Appl. Genet.*,
880 **108**, 141–153.
881 Manichaikul, A., Dupuis, J., Sen, Ś., and Broman, K.W. (2006) *Poor performance of*
882 *bootstrap confidence intervals for the location of a quantitative trait locus*. *Genetics*,
883 **174**, 481–489.
884 Mascher, M., Wicker, T., Jenkins, J., Plott, C., Lux, T., Koh, C.S., et al. (2021) *Long-read*
885 *sequence assembly: A technical evaluation in barley*. *Plant Cell*, **33**, 1888–1906.
886 Matsushika, A., Makino, S., Kojima, M., and Mizuno, T. (2000) *Circadian waves of*
887 *expression of the APRR1/TOC1 family of pseudo-response regulators in Arabidopsis*
888 *thaliana: Insight into the plant circadian clock*. *Plant Cell Physiol.*, **41**, 1002–1012.
889 Maurer, A., Draba, V., Jiang, Y., Schnaithmann, F., Sharma, R., Schumann, E., et al.
890 (2015) *Modelling the genetic architecture of flowering time control in barley through*
891 *nested association mapping*. *BMC Genomics*, **16**, 1–12.
892 Maurer, A., Draba, V., and Pillen, K. (2016) *Genomic dissection of plant development and*
893 *its impact on thousand grain weight in barley through nested association mapping*. *J.*
894 *Exp. Bot.*, **67**, 2507–2518.
895 Mikołajczak, K., Kuczyńska, A., Krajewski, P., Sawikowska, A., Surma, M., Ogrodowicz, P.,
896 et al. (2017) *Quantitative trait loci for plant height in Maresi × CamB barley population*
897 *and their associations with yield-related traits under different water regimes*. *J. Appl.*
898 *Genet.*, **58**, 23–35.
899 Sharma, R., Shaaf, S., Neumann, K., Go, Y., Mascher, M., David, M., et al. (2020) *On the*
900 *origin of photoperiod non-responsiveness in barley*. *bioRxiv*, 2020.07.02.185488.
901
902 Mizuno, T. and Nakamichi, N. (2005) *Pseudo-response regulators (PRRs) or true oscillator*
903 *components (TOCs)*. *Plant Cell Physiol.*, **46**, 677–685.
904 Mulki, M.A. and von Korff, M. (2016) *CONSTANS controls floral repression by up-*
905 *regulating VERNALIZATION2 (VRN-H2) in Barley1*. *Plant Physiol.*, **170**, 325–337.
906 Myles, S., Peiffer, J., Brown, P.J., Ersoz, E.S., Zhang, Z., Costich, D.E., and Buckler, E.
907 (2009) *Association mapping: Critical considerations shift from genotyping to*
908 *experimental design*. *Plant Cell*, **21**, 2194–2202.
909 Nakamichi, N., Kudo, T., Makita, N., Kiba, T., Kinoshita, T., and Sakakibara, H. (2020)
910 *Flowering time control in rice by introducing Arabidopsis clock-associated PSEUDO-*
911 *RESPONSE REGULATOR 5*. *Biosci. Biotechnol. Biochem.*, **84**, 970–979.
912 Nice, L.M., Steffenson, B.J., Blake, T.K., Horsley, R.D., Smith, K.P., and Muehlbauer, G.J.

(2017) *Mapping agronomic traits in a wild barley advanced backcross–nested association mapping population*. *Crop Sci.*, **57**, 1199–1210.

Nishida, H., Ishihara, D., Ishii, M., Kaneko, T., Kawahigashi, H., Akashi, Y., et al. (2013) *Phytochrome C is a key factor controlling long-day flowering in barley*. *Plant Physiol.*, **163**, 804–814.

Pasam, R.K., Sharma, R., Malosetti, M., van Eeuwijk, F. a, Haseneyer, G., Kilian, B., and Graner, A. (2012) *Genome-wide association studies for agronomical traits in a world wide spring barley collection*. *BMC Plant Biol.*, **12**, 16.

Patil, V., McDermott, H.I., McAllister, T., Cummins, M., Silva, J.C., Mollison, E., et al. (2019) *APETALA2 control of barley internode elongation*. *Dev.*, **146**.

Pauli, D., Muehlbauer, G.J., Smith, K.P., Cooper, B., Hole, D., Obert, D.E., et al. (2014) *Association Mapping of Agronomic QTLs in U.S. Spring Barley Breeding Germplasm*. *Plant Genome*, **7**.

Pieper, R., Tomé, F., Pankin, A., and Von Korff, M. (2021) *FLOWERING LOCUS T4 delays flowering and decreases floret fertility in barley*. *J. Exp. Bot.*, **72**, 107–121.

Piepho, H.P. and Möhring, J. (2007) *Computing heritability and selection response from unbalanced plant breeding trials*. *Genetics*, **177**, 1881–1888.

Rodriguez, M., Rau, D., Papa, R., and Attene, G. (2008) *Genotype by environment interactions in barley (Hordeum vulgare L.): Different responses of landraces, recombinant inbred lines and varieties to Mediterranean environment*. *Euphytica*, **163**, 231–247.

Rollins, J.A., Drosse, B., Mulki, M.A., Grando, S., Baum, M., Singh, M., et al. (2013) *Variation at the vernalisation genes Vrn-H1 and Vrn-H2 determines growth and yield stability in barley (Hordeum vulgare) grown under dryland conditions in Syria*. *Theor. Appl. Genet.*, **126**, 2803–2824.

van Rossum, B.J., Kruijer, W., van Eeuwijk, F., Boer, M., Malosetti, M., Bustos-Korts, D., and Wehrens, R. (2022) *Package ‘ statgenGWAS .’ R Packag. version*, **1**.

Schmalenbach, I., Léon, J., and Pillen, K. (2009) *Identification and verification of QTLs for agronomic traits using wild barley introgression lines*. *Theor. Appl. Genet.*, **118**, 483–497.

Sharma, R., Shaaf, S., Neumann, K., Go, Y., Mascher, M., David, M., et al. (2020) *On the origin of photoperiod non-responsiveness in barley*. *bioRxiv*, 2020.07.02.185488.

Shoesmith, J.R., Solomon, C.U., Yang5, X., Wilkinson, L.G., Sheldrick, S., Eijden, E. Van, et al. (2021) *APETALA2 functions as a temporal factor together with BLADE-ON-PETIOLE2 and MADS29 to control flower and grain development in barley*. *Dev.*, **148**.

948 Shrestha, A., Cosenza, F., van Inghelandt, D., Wu, P.-Y., Li, J., Casale, F.A., et al. (2022)
949 *The double round-robin population unravels the genetic architecture of grain size in*
950 *barley*. *J. Exp. Bot.*, **73**, 7344–7361.
951 Stich, B. (2009) *Comparison of mating designs for establishing nested association*
952 *mapping populations in maize and Arabidopsis thaliana*. *Genetics*, **183**, 1525–1534.
953 Turner, A., Beales, J., Faure, S., Dunford, R.P., and Laurie, D.A. (2005) *The pseudo-*
954 *response regulator Ppd-H1 provides adaptation to photoperiod in barley*. *Science*
955 *(80-.).*, **310**, 1031–1034.
956 VanRaden, P.M. (2008) *Efficient methods to compute genomic predictions*. *J. Dairy Sci.*,
957 **91**, 4414–4423.
958 Vaser, R., Adusumalli, S., Leng, S.N., Sikic, M., and Ng, P.C. (2016) *SIFT missense*
959 *predictions for genomes*. *Nat. Protoc.*, **11**, 1–9.
960 Vidal, T., Gigot, C., De Vallavieille-Pope, C., Huber, L., and Saint-Jean, S. (2018)
961 *Contrasting plant height can improve the control of rain-borne diseases in wheat*
962 *cultivar mixture: Modelling splash dispersal in 3-D canopies*. *Ann. Bot.*, **121**, 1299–
963 1308.
964 Vyas, S., Khatri-Chhetri, A., Aggarwal, P., Thornton, P., and Campbell, B.M. (2022)
965 *Perspective: The gap between intent and climate action in agriculture*. *Glob. Food*
966 *Sec.*, **32**, 100612.
967 Wang, J., Yang, J., Jia, Q., Zhu, J., Shang, Y., Hua, W., and Zhou, M. (2014) *A new QTL*
968 *for plant height in barley (hordeum vulgare l.) showing no negative effects on grain*
969 *yield*. *PLoS One*, **9**.
970 Wei, J., Fang, Y., Jiang, H., Wu, X. ting, Zuo, J. hong, Xia, X. chun, et al. (2022)
971 *Combining QTL mapping and gene co-expression network analysis for prediction of*
972 *candidate genes and molecular network related to yield in wheat*. *BMC Plant Biol.*, **22**,
973 1–14.
974 Weisweiler, M., Arlt, C., Wu, P.-Y., Van Inghelandt, D., Hartwig, T., Stich, B., et al. (2022)
975 *Structural variants in the barley gene pool: precision and sensitivity to detect them*
976 *using short-read sequencing and their association with gene expression and*
977 *phenotypic variation*. *bioRxiv*, 2022.04.25.489331.
978 Weisweiler, M., Montaigu, A. De, Ries, D., Pfeifer, M., and Stich, B. (2019) *Transcriptomic*
979 *and presence/absence variation in the barley genome assessed from multi-tissue*
980 *mRNA sequencing and their power to predict phenotypic traits*. *BMC Genomics*, **20**,
981 1–15.
982 Wendt, T., Holme, I., Dockter, C., Preu, A., Thomas, W., Druka, A., et al. (2016) *HvDep1 Is*

a Positive regulator of culm elongation and grain size in barley and impacts yield in an environment-dependent manner. *PLoS One*, **11**, 1–21.

Wiegmann, M., Maurer, A., Pham, A., March, T.J., Al-Abdallat, A., Thomas, W.T.B., et al. (2019) *Barley yield formation under abiotic stress depends on the interplay between flowering time genes and environmental cues*. *Sci. Rep.*, **9**, 1–16.

Yan, L., Fu, D., Li, C., Blechl, A., Tranquilli, G., Bonafede, M., et al. (2006) *The wheat and barley vernalization gene VRN3 is an orthologue of FT*. *Proc. Natl. Acad. Sci. U. S. A.*, **103**, 19581–19586.

Yan, L., Loukoianov, A., Blechl, A., Tranquilli, G., Ramakrishna, W., SanMiguel, P., et al. (2004) *The Wheat VRN2 Gene Is a Flowering Repressor Down-Regulated by Vernalization*. *Science (80-.).*, **303**, 1640–1644.

Yan, L., Loukoianov, A., Tranquilli, G., Helguera, M., Fahima, T., and Dubcovsky, J. (2003) *Positional cloning of the wheat vernalization gene VRN1*. *Proc. Natl. Acad. Sci. U. S. A.*, **100**, 6263–6268.

Yu, J., Pressoir, G., Briggs, W.H., Bi, I.V., Yamasaki, M., Doebley, J.F., et al. (2006) *A unified mixed-model method for association mapping that accounts for multiple levels of relatedness*. *Nat. Genet.*, **38**, 203–208.

Zakhrabekova, S., Gough, S.P., Braumann, I., MuЇller, A.H., Lundqvist, J., Ahmann, K., et al. (2012) *Induced mutations in circadian clock regulator Mat-a facilitated short-season adaptation and range extension in cultivated barley*. *Proc. Natl. Acad. Sci. U. S. A.*, **109**, 4326–4331.

Zhang, B. and Horvath, S. (2005) *A general framework for weighted gene co-expression network analysis*. *Stat. Appl. Genet. Mol. Biol.*, **4**.

12 TABLES AND FIGURES LEGENDS

Table 1: Variance components of the multi-environment linear mixed model and heritability values for flowering time and plant height. G represents the genetic variance, E the environmental variance, G:E the variance explained by the interaction between G and E, and e the residual error.

Figure 1: Violin plots for adjusted entry means for flowering time and plant height of each HvDRR sub-population and for the 224 inbreds of the diversity panel. The flowering time is presented as days after sowing (DAS) and the plant height values are reported in cm. The green dots represent the adjusted entry means of the parental inbreds of the sub-population. The orange lines represent the average of the adjusted entry means of the recombinant inbred lines of the respective sub-population.

Figure 2: Distribution of correlation coefficients between flowering time and plant height calculated for the HvDRR sub-populations. On the x axis the correlation coefficients are represented and on the y axis the number of sub-populations.

Figure 3: Negative decadic logarithm of the p-value of the multi-parent population analysis for flowering time (top) and plant height (bottom) using an ancestral model. On the x axis, the position on the consensus genetic map is reported. Each dashed line indicates the peak position of the corresponding QTL.

Figure 4: Heat map of the effects of the parental inbreds at the QTL detected through multi-parent population analysis for flowering time (top, in days after sowing) and for plant height (bottom, in cm). Indexed letters indicate the significance of the difference ($p < 0.05$) between the effects of the same QTL.

Figure 5: Genetic position of the QTL detected in single population analyses for flowering time projected to the consensus map. The position of the QTL confidence intervals is represented as a vertical bar parallel to the right of the chromosome. The color of the bar indicates if the sub-population was obtained by crossing two landraces (yellow), two cultivars (blue), or a landrace and a cultivar (green). The genetic positions of the known genes regulating flowering time in barley are shown in red. The positions of the markers that flank each QTL are also reported.

Figure 6: Genetic position of the QTL detected in single population analysis for plant height projected to the consensus map. The position of the QTL confidence intervals is shown as a vertical bar to the right of the chromosome. The color of the bar indicates if the sub-population was obtained by crossing two landraces (yellow), two cultivars (blue), or a landrace and a cultivar (green). The known regulatory genes previously described to be responsible for plant height regulation and their genetic position are reported in red. The positions of the markers at the borders of each QTL are also reported.

Figure 7: Genomic sequence of the last exon of *Ppd-H1* of Morex, Igri, Optic, Golden Promise, Triumph, and the 23 parental inbreds of the HvDRR population. SNP 22 is highlighted in yellow, SNP 1945 in orange. On top, the gene structure of *Ppd-H1* is given. Lines indicate the positions of SNP 21, SNP 22 (Turner *et al*, 2005), and SNP 1945 within the last exon.

Supplementary Table 1: Crossing scheme of the 45 HvDRR sub-populations. The name of the sub-populations is reported in the first column. In the second and third column are indicated the inbred lines that originated the sub-populations.

Supplementary Table 2: Genetic and physical distances for which the linkage disequilibrium measured r^2 reached a value of 0.2.

Supplementary Table 3: Average of the adjusted entry means, standard deviations (SD), and coefficients of variation (CoV) across all 45 sub-populations for flowering time, in days after sowing, and plant height, in cm.

Supplementary Table 4: Summary of the results of the multi-parent population analysis for flowering time and plant height. Chr indicates the chromosome on which the QTL was detected, LOD the logarithm of odds, PVE the percentage of variance explained by the QTL.

Supplementary Table 5: Summary of the results of the single population analysis for flowering time. The information regarding the peak and the borders of the confidence interval of each QTL are reported. Chr represents the chromosome on which the QTL was detected, LOD the logarithm of odds, and PVE the percentage of variance explained by the QTL individually and in a simultaneous fit. The additive effect is given in days after sowing.

Supplementary Table 6: Summary of the results of the single population analysis for plant height. The information regarding the peak and the borders of the confidence interval of each QTL are reported. Chr represents the chromosome on which the QTL was detected, LOD the logarithm of odds, and PVE the percentage of variance explained by the QTL individually and in a simultaneous fit. The additive effect is given in cm.

Supplementary Table 7: Prediction ability of the genomic SNP marker data for flowering time and plant height without cross-validation (CV) and with five fold cross-validation across all sub-populations. SD indicates the standard deviation.

Supplementary Table 8: Genome-wide epistatic loci detected in the HvDRR population. LOD indicates the logarithm of odds of the interaction.

Supplementary Table 9: Lists of primers used to amplify *Ppd-H1* and *Vrn-H2*. The *Ppd-H1* primers are listed for each parental inbred. N-ter primers were used to amplify the start while the C-ter primers the end of the coding sequences. The primers pairs marked with * amplified the whole genet. Primers used to amplify *Vrn-H2* have the same nomenclature as described in Karsai *et al*. (2005).

Supplementary Table 10: List of candidate genes in the confidence interval of selected QTL that carried a polymorphism among the parental lines. IN/DEL indicates an insertion or a deletion, SV indicates predicted structural variants.

Supplementary Figure 1: Histogram and correlation plot between flowering time (FT) and plant height (PH) across all 45 HvDRR sub-populations. Flowering time is reported in days after sowing (DAS) and plant height in cm.

Supplementary Figure 2: Histograms and correlation plots between flowering time (FT, in days after sowing) and plant height (PH, in cm), for each of the 45 HvDRR sub-populations.

Supplementary Figure 3: Effect size of the QTL detected through multi-parent population analysis for flowering time (top, in days after sowing) and plant height (bottom, in cm), for each of the parental lines.

Supplementary Figure 4: Amino acid sequence of the terminal region of *Ppd-H1* of Morex, Igri, Optic, Golden Promise, Triumph, and the 23 parental inbreds of the HvDRR population. The amino acid synthesized by the triplet containing SNP 22 is highlighted in yellow, the one synthesized by the triplet containing SNP 1945 is highlighted in blue.

Supplementary Figure 5: Gel pictures of PCRs performed to detect the presence/absence of *ZCCT-Ha:b* (top) and *ZCCT-Hc* (bottom) as described in Karsai *et al*. (2005). The analyzed genotypes are Bowman (control spring variety), Antonella (control winter variety), Igri (control winter variety), and the parental inbreds of the sub-populations for which a QTL co-localizing with *Vrn-H2* was detected.

Supplementary Figure 6: Heat map of the module-trait relationships for plant height (PH) and flowering time (FT). On the y axis, the 27 detected modules are reported. For each module-trait correlation p-values are given in brackets.

Supplementary Figure 7: Network predictions for modules “orange” (a), “black” (b), “darkgreen” (c), “purple” (d), “tan” (e), “lightyellow” (f), “green” (g), “blue” (h), and “turquoise” (i). Gene names with a gene-module membership p-value < 0.01 are indicated in the orange circles. Gene-gene interactions are represented by grey lines.

Supplementary Figure 8: Negative decadic logarithm of the p-value for association tests of sequence variants in QTL without previously reported genes for the control of the trait within their interval, explaining ≥ 15% variance, and with interval ≤ 30 cM for flowering time (left) and plant height (right). The QTL confidence intervals from single population analyses are indicated by colored bars.

Table 1: Variance components of the multi-environment linear mixed model and heritability values for flowering time and plant height. G represents the genetic variance, E the environmental variance, G:E the variance explained by the interaction between G and E, and e the residual error.

Trait	Groups	Variance	h^2
Flowering time	G	41.33	0.86
	E	77.12	
	G:E	22.31	
	e	17.02	
Plant height	G	41.46	0.76
	E	128.55	
	G:E	36.32	
	e	56.04	

Figure 1: Violin plots for adjusted entry means for flowering time and plant height of each HvDRR sub-population and for the 224 inbreds of the diversity panel. The flowering time is presented as days after sowing (DAS) and the plant height values are reported in cm. The green dots represent the adjusted entry means of the parental inbreds of the sub-population. The orange lines represent the average of the adjusted entry means of the recombinant inbred lines of the respective sub-population.

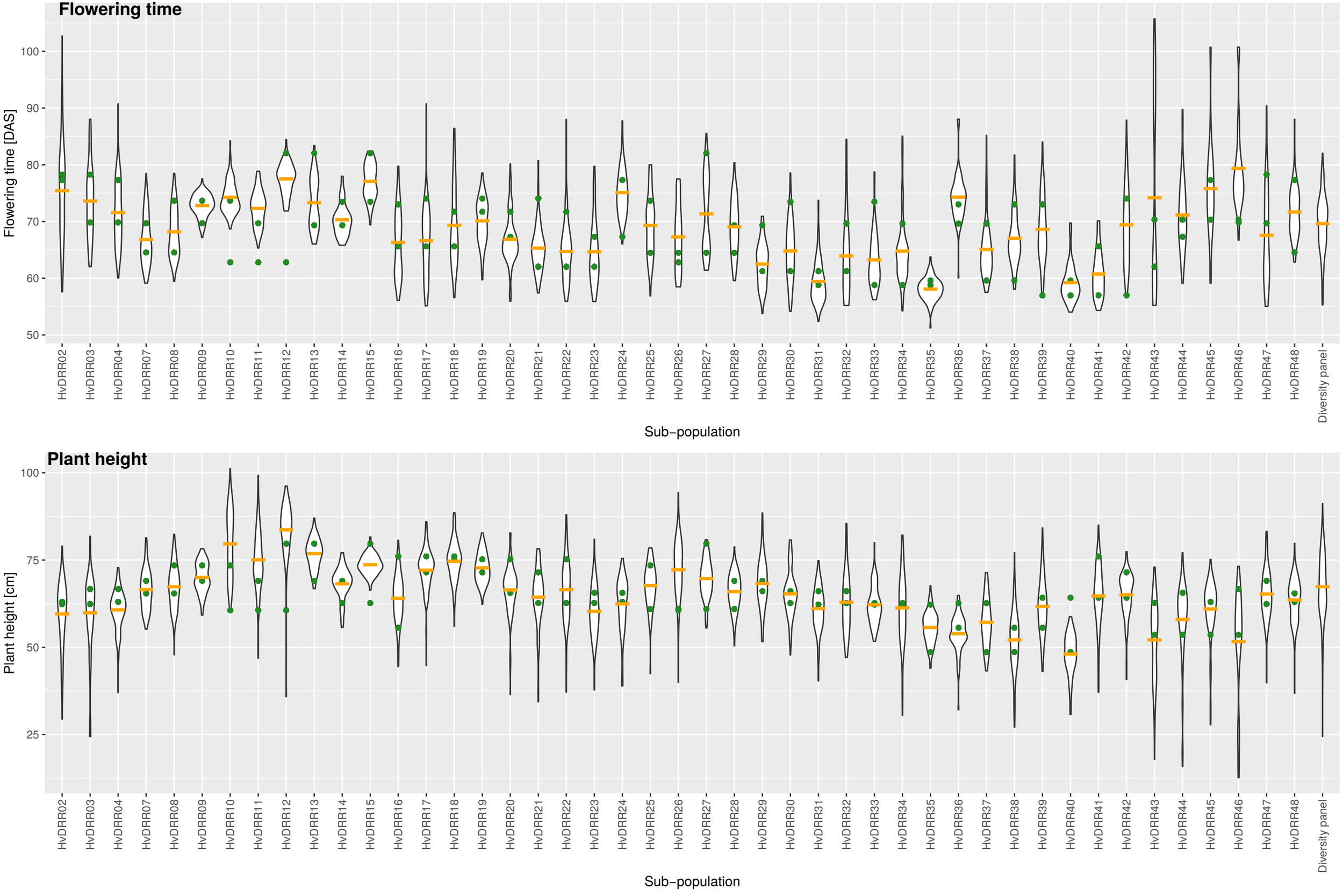

Figure 2: Distribution of correlation coefficients between flowering time and plant height calculated for the HvDRR sub-populations. On the x axis the correlation coefficients are represented and on the y axis the number of sub-populations.

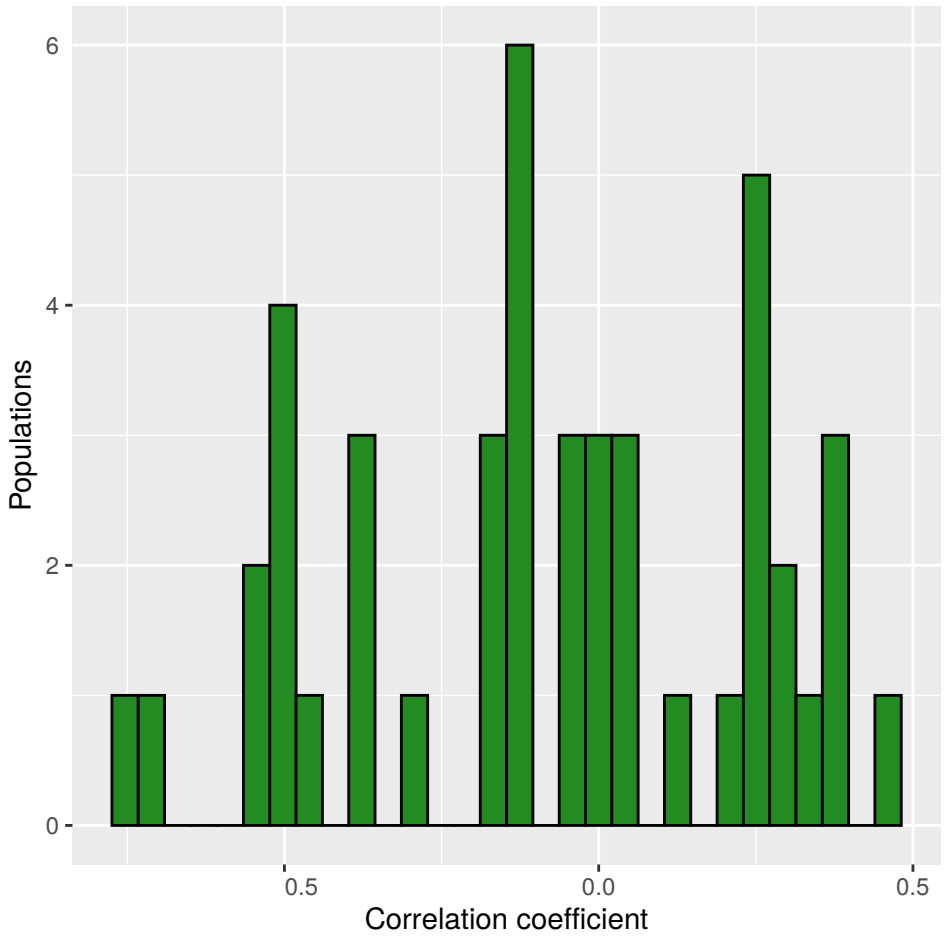

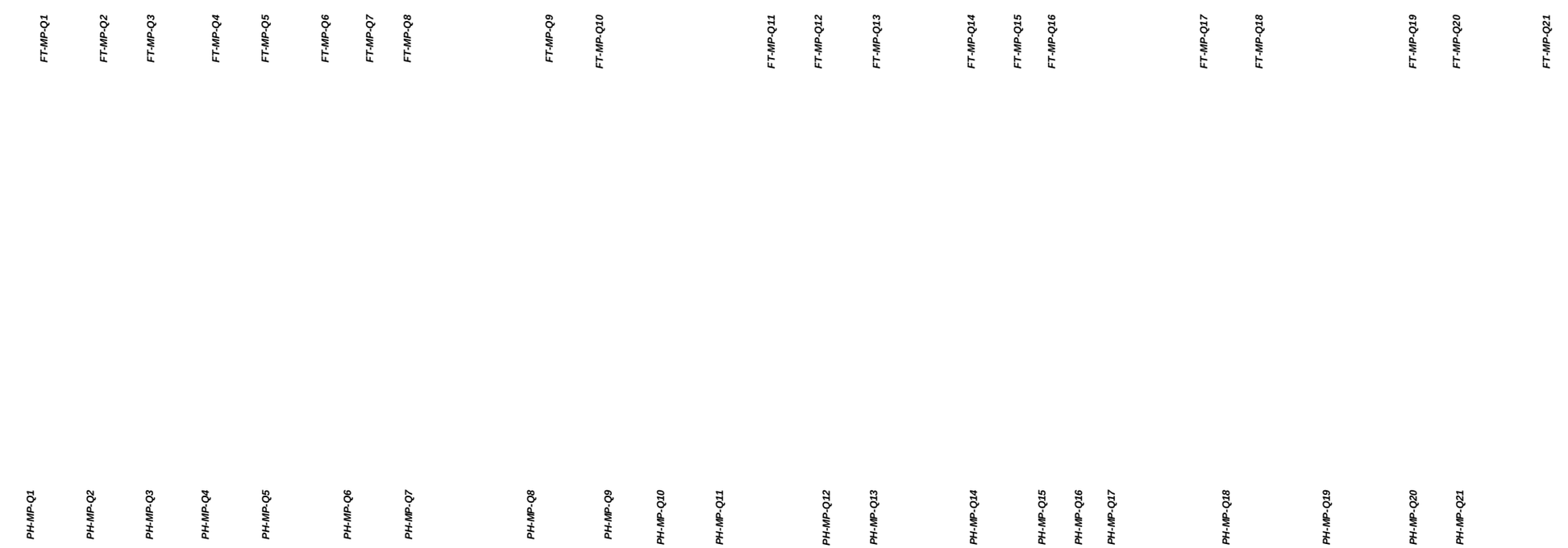

Figure 3: Negative decadic logarithm of the p-value of the multi-parent population analysis for flowering time (top) and plant height (bottom) using an ancestral model. On the x axis, the position on the consensus genetic map is reported. Each dashed line indicates the peak position of the corresponding QTL.

Figure 4: Heat map of the effects of the parental inbreds at the QTL detected through multi-parent population analysis for flowering time (top, in days after sowing) and for plant height (bottom, in cm). Indexed letters indicate the significance of the difference ($p < 0.05$) between the effects of the same QTL.

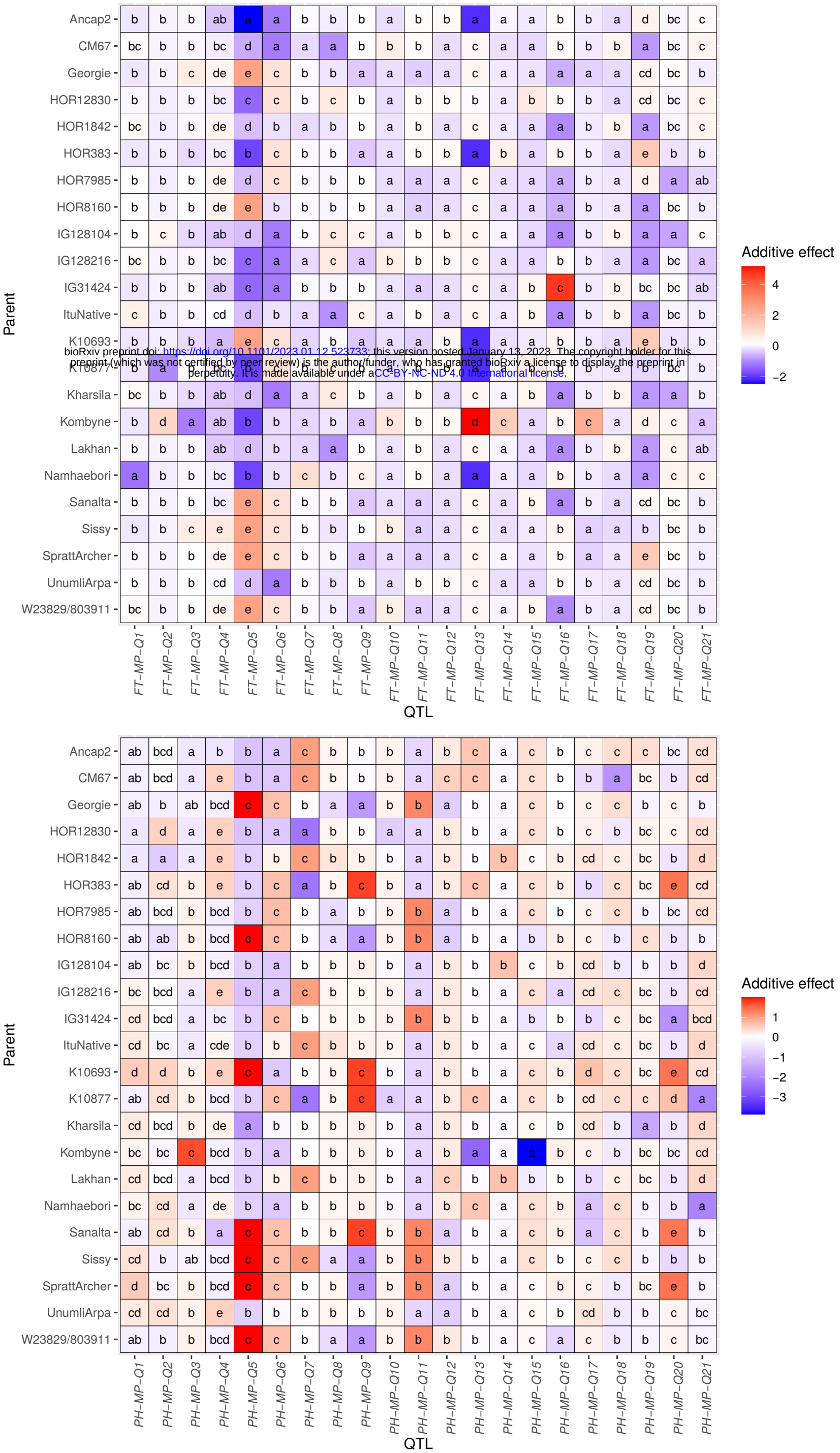

Figure 5: Genetic position of the QTL detected in single population analyses for flowering time projected to the consensus map. The position of the QTL confidence intervals is represented as a vertical bar parallel to the right of the chromosome. The color of the bar indicates if the sub-population was obtained by crossing two landraces (yellow), two cultivars (blue), or a landrace and a cultivar (green). The genetic positions of the known genes regulating flowering time in barley are shown in red. The positions of the markers that flank each QTL are also reported.

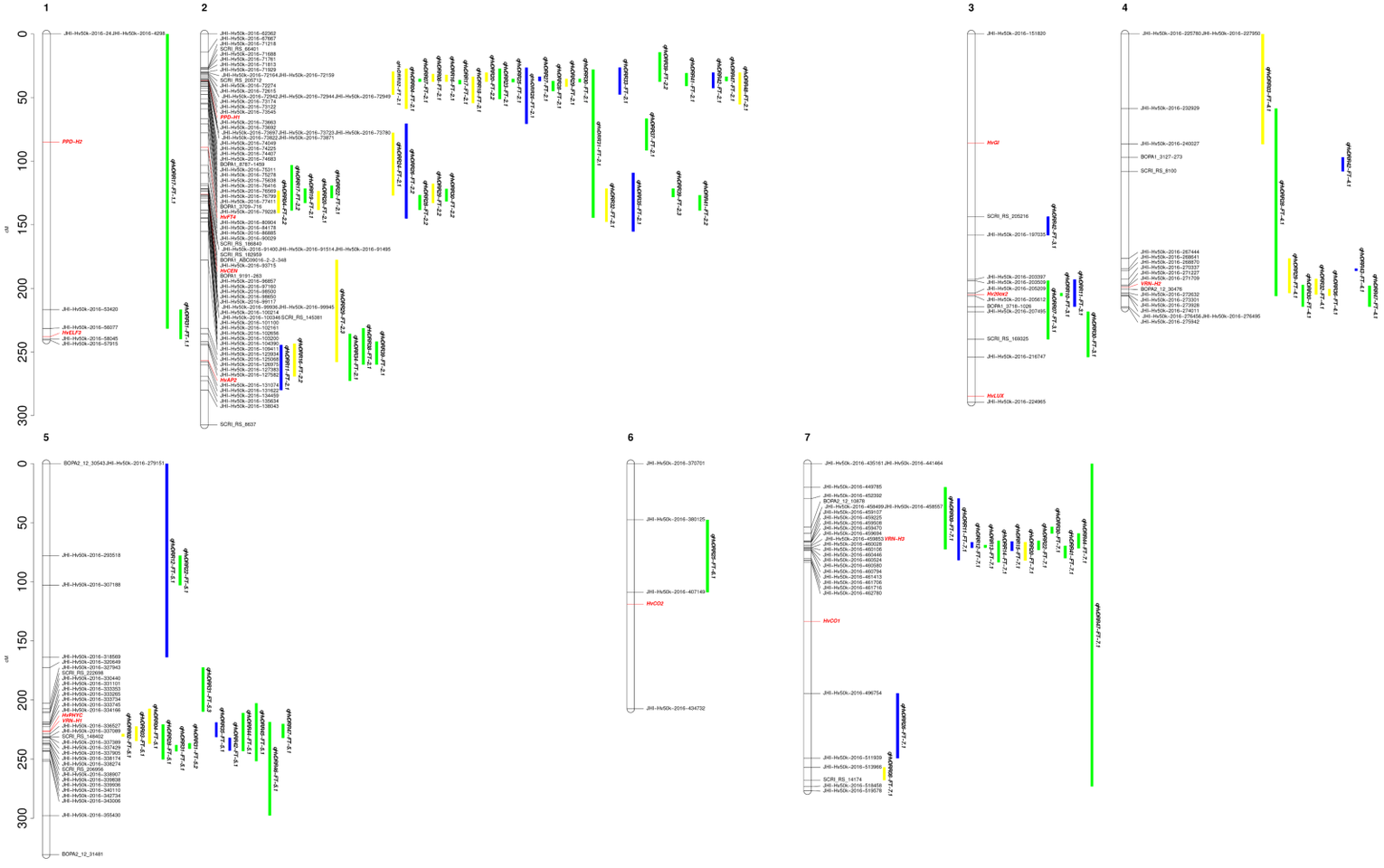

Figure 6: Genetic position of the QTL detected in single population analysis for plant height projected to the consensus map. The position of the QTL confidence intervals is shown as a vertical bar to the right of the chromosome. The color of the bar indicates if the sub-population was obtained by crossing two landraces (yellow), two cultivars (blue), or a landrace and a cultivar (green). The known regulatory genes previously described to be responsible for plant height regulation and their genetic position are reported in red. The positions of the markers at the borders of each QTL are also reported.

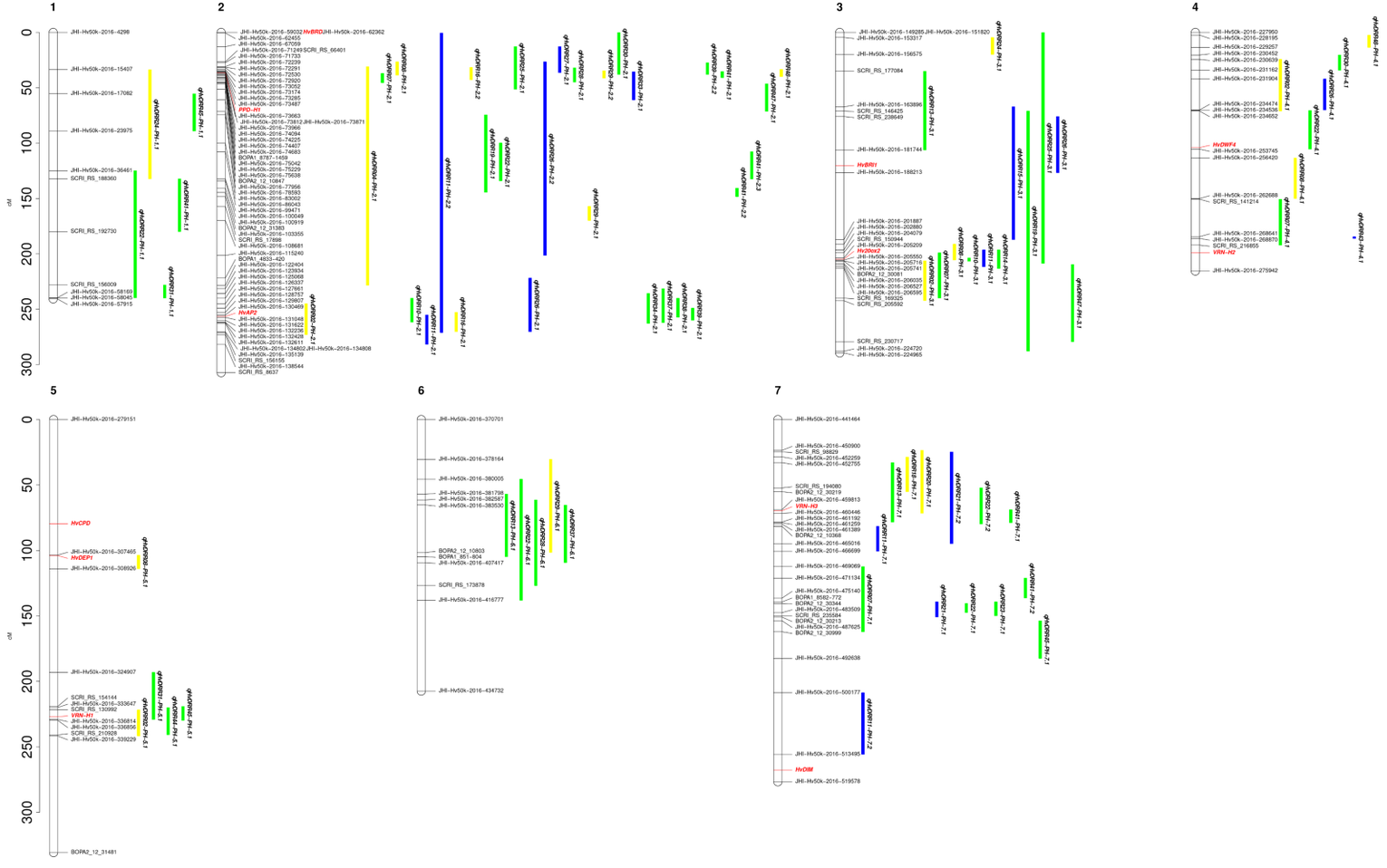

Figure 7: Genomic sequence of the last exon of *Ppd-H1* of Morex, Igri, Optic, Golden Promise, Triumph, and the 23 parental inbreds of the HvDRR population. SNP 22 is highlighted in yellow, SNP 1945 in orange. On top, the gene structure of *Ppd-H1* is given. Lines indicate the positions of SNP 21, SNP 22 (Turner *et al.*, 2005), and SNP 1945 within the last exon.

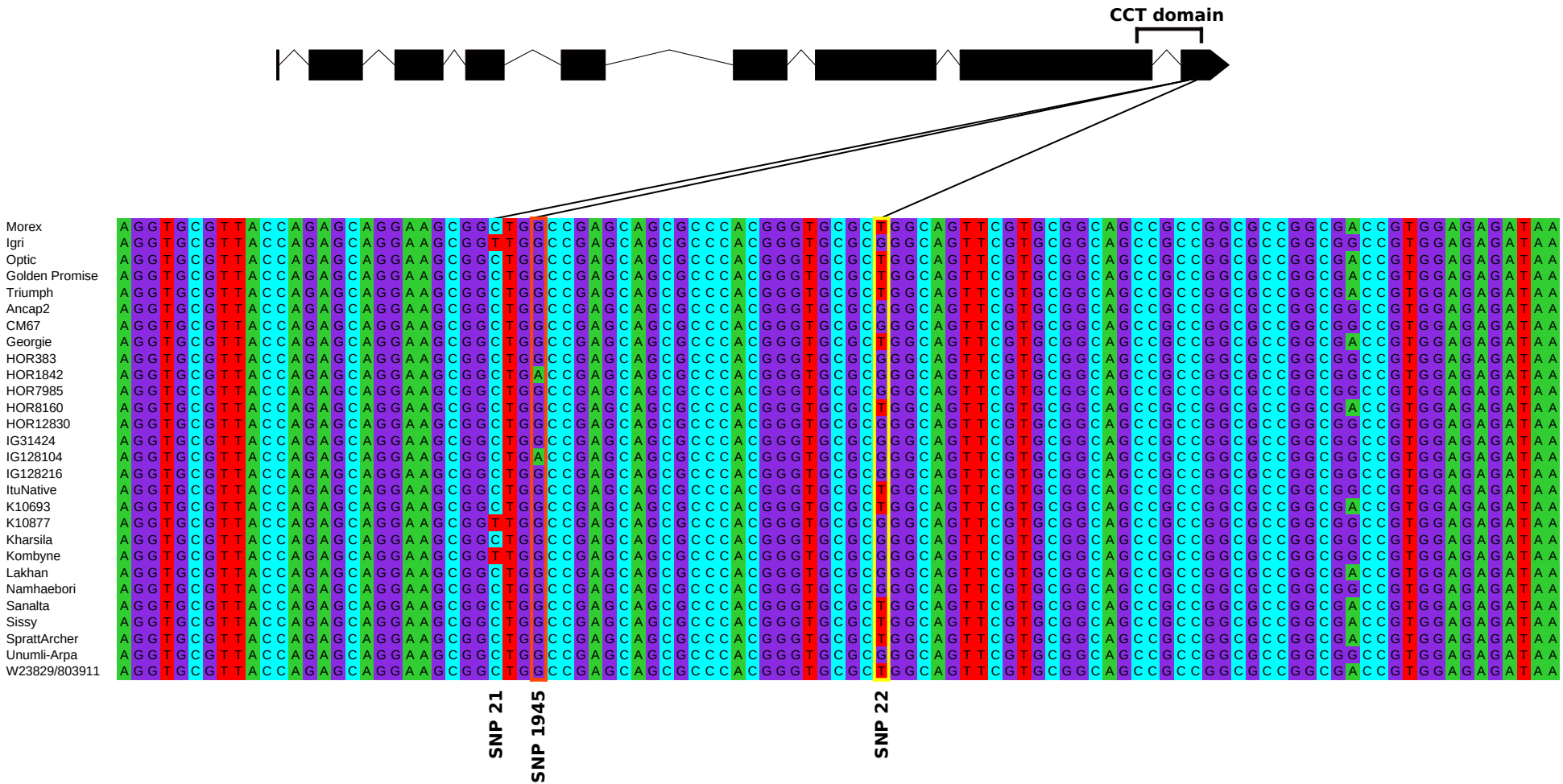

Supplementary Table 1: Crossing scheme of the 45 HvDRR sub-populations. The name of the sub-populations is reported in the first column. In the second and third column are indicated the inbred lines that originated the sub-populations.

Sub-population	Parent A	Parent B
HvDRR02	HOR1842	IG31424
HvDRR03	Kharsila	IG31424
HvDRR04	HOR1842	Kharsila
HvDRR07	Sissy	HOR7985
HvDRR08	HOR7985	W23829/803911
HvDRR09	Sissy	W23829/803911
HvDRR10	Sanalta	W23829/803911
HvDRR11	Sanalta	Sissy
HvDRR12	SprattArcher	Sanalta
HvDRR13	SprattArcher	HOR8160
HvDRR14	Georgie	HOR8160
HvDRR15	SprattArcher	Georgie
HvDRR16	K10693	HOR12830
HvDRR17	K10693	Ancap2
HvDRR18	HOR383	K10693
HvDRR19	HOR383	Ancap2
HvDRR20	IG128104	HOR383
HvDRR21	Ancap2	Namhaebori
HvDRR22	HOR383	Namhaebori
HvDRR23	IG128104	Namhaebori
HvDRR24	IG128104	HOR1842
HvDRR25	W23829/803911	Unumli-Arpa
HvDRR26	Unumli-Arpa	Sanalta
HvDRR27	Unumli-Arpa	SprattArcher
HvDRR28	Unumli-Arpa	HOR8160
HvDRR29	HOR8160	IG128216
HvDRR30	IG128216	Georgie
HvDRR31	Lakhan	IG128216
HvDRR32	IG128216	K10877
HvDRR33	Georgie	Lakhan
HvDRR34	K10877	Lakhan
HvDRR35	Lakhan	CM67
HvDRR36	HOR12830	K10877
HvDRR37	K10877	CM67
HvDRR38	HOR12830	CM67
HvDRR39	HOR12830	ItuNative
HvDRR40	ItuNative	CM67
HvDRR41	ItuNative	K10693
HvDRR42	Ancap2	ItuNative
HvDRR43	Kombyne	Namhaebori
HvDRR44	IG128104	Kombyne
HvDRR45	HOR1842	Kombyne
HvDRR46	Kharsila	Kombyne
HvDRR47	IG31424	Sissy
HvDRR48	HOR1842	HOR7985

Supplementary Table 2: Genetic and physical distances for which the linkage disequilibrium measured r^2 reached a value of 0.2.

Chromosome	cM	bp
1H	3.03	1462496
2H	2.21	1214368
3H	1.85	1254651
4H	1.75	998605
5H	2.05	898399
6H	1.51	915485
7H	3.15	1077964

Supplementary Table 3: Average of the adjusted entry means, standard deviations (SD), and coefficients of variation (CoV) across all 45 sub-populations for flowering time, in days after sowing, and plant height, in cm.

Sub-population	Flowering time (DAS)			Plant height (cm)		
	Mean	SD	CoV	Mean	SD	CoV
HvDRR02	75.42	8.61	11.41	59.57	9.45	15.86
HvDRR03	73.61	6.57	8.93	59.87	11.16	18.65
HvDRR04	71.59	5.87	8.20	60.74	5.72	9.42
HvDRR07	66.82	4.44	6.65	66.51	5.66	8.51
HvDRR08	68.19	4.36	6.39	67.38	6.32	9.37
HvDRR09	72.81	1.99	2.73	70.02	4.28	6.11
HvDRR10	74.27	2.81	3.78	79.62	9.72	12.20
HvDRR11	72.31	3.07	4.24	75.07	8.42	11.21
HvDRR12	77.52	2.72	3.51	83.64	8.29	9.91
HvDRR13	73.32	4.45	6.07	76.84	4.31	5.61
HvDRR14	70.32	2.79	3.96	68.18	4.60	6.74
HvDRR15	77.08	3.07	3.98	73.66	2.82	3.83
HvDRR16	66.33	5.89	8.88	64.06	7.02	10.95
HvDRR17	66.62	6.24	9.36	72.10	6.37	8.84
HvDRR18	69.34	7.20	10.39	74.67	5.90	7.90
HvDRR19	70.12	3.91	5.57	72.75	4.27	5.87
HvDRR20	66.89	4.44	6.64	66.44	7.17	10.80
HvDRR21	65.32	4.14	6.33	64.37	8.32	12.92
HvDRR22	64.71	5.11	7.89	66.50	8.82	13.26
HvDRR23	64.69	5.68	8.78	60.31	7.47	12.38
HvDRR24	75.11	4.13	5.50	62.45	7.78	12.45
HvDRR25	69.32	5.42	7.82	67.68	6.28	9.28
HvDRR26	67.30	5.87	8.72	72.20	9.23	12.78
HvDRR27	71.36	6.77	9.49	69.71	5.55	7.96
HvDRR28	69.08	4.87	7.04	65.94	5.23	7.93
HvDRR29	62.49	3.79	6.07	68.28	7.20	10.55
HvDRR30	64.81	5.27	8.13	65.31	6.75	10.33
HvDRR31	59.43	3.71	6.24	61.09	6.35	10.39
HvDRR32	63.93	7.26	11.36	62.89	8.78	13.96
HvDRR33	63.25	4.64	7.33	62.17	5.43	8.73
HvDRR34	64.78	5.79	8.94	61.29	10.01	16.33
HvDRR35	58.09	2.00	3.44	55.69	4.58	8.23
HvDRR36	74.31	4.30	5.79	53.87	5.40	10.03
HvDRR37	65.08	5.25	8.06	57.15	6.90	12.07
HvDRR38	67.04	4.68	6.98	52.11	8.83	16.94
HvDRR39	68.62	5.80	8.46	61.73	8.12	13.15
HvDRR40	59.23	3.32	5.60	48.10	5.85	12.17
HvDRR41	60.76	4.03	6.63	64.73	9.18	14.18
HvDRR42	69.42	6.91	9.96	65.06	6.51	10.01
HvDRR43	74.19	17.29	23.31	52.10	11.48	22.03
HvDRR44	71.14	6.25	8.79	57.96	11.51	19.86
HvDRR45	75.79	8.50	11.22	60.96	8.47	13.89
HvDRR46	79.35	8.21	10.34	51.62	15.76	30.53
HvDRR47	67.57	8.42	12.47	65.24	7.40	11.35
HvDRR48	71.68	4.37	6.09	63.54	6.29	9.91
Diversity panel	69.63	5.12	7.35	67.38	9.44	14.01

Supplementary Table 4: Summary of the results of the multi-parent population analysis for flowering time and plant height. Chr indicates the chromosome on which the QTL was detected, LOD the logarithm of odds, PVE the percentage of variance explained by the QTL.

Trait	QTL	Chr	Peak marker	Peak cM	Marker position (bp)	LOD	Left border marker	Left border cM	Left border bp	Right border marker	Right border cM	Right border marker bp	PVE
Flowering time	*FT-MP-Q1*	1H	JHI-Hv50k-2016-15152	31.2	20945275	5.1	JHI-Hv50k-2016-15113	31.1	20931089	JHI-Hv50k-2016-15160	31.2	20945741	0.47
Flowering time	*FT-MP-Q2*	1H	JHI-Hv50k-2016-29220	101.4	383491828	3.2	JHI-Hv50k-2016-29224	101.4	383487512	JHI-Hv50k-2016-29301	101.5	383908136	0.41
Flowering time	*FT-MP-Q3*	1H	JHI-Hv50k-2016-40963	158.5	473573522	4.5	JHI-Hv50k-2016-40966	158.5	473572474	BOPA1_8867-459	158.6	473633633	0.20
Flowering time	*FT-MP-Q4*	1H	JHI-Hv50k-2016-57415	237.0	514738633	5.0	JHI-Hv50k-2016-57153	235.4	514047135	SCRI_RS_195067	237.5	514995168	0.09
Flowering time	*FT-MP-Q5*	2H	JHI-Hv50k-2016-73174	35.2	25327192	134.5	JHI-Hv50k-2016-73052	34.6	25023220	JHI-Hv50k-2016-73184	35.3	25332315	11.31
Flowering time	*FT-MP-Q6*	2H	JHI-Hv50k-2016-96906	126.9	471939672	41.8	SCRI_RS_231725	126.7	470678535	JHI-Hv50k-2016-97380	127.1	474383159	3.63
Flowering time	*FT-MP-Q7*	2H	JHI-Hv50k-2016-113511	195.4	601391766	4.1	JHI-Hv50k-2016-113490	195.2	601232283	JHI-Hv50k-2016-113518	195.4	601395368	0.57
Flowering time	*FT-MP-Q8*	2H	JHI-Hv50k-2016-129773	252.5	633228569	8.5	JHI-Hv50k-2016-129562	252.0	633013755	JHI-Hv50k-2016-129785	252.5	633229906	0.70
Flowering time	*FT-MP-Q9*	3H	JHI-Hv50k-2016-186187	119.2	462714357	4.7	JHI-Hv50k-2016-186122	118.9	462283595	JHI-Hv50k-2016-186284	119.5	463381185	0.16
Flowering time	*FT-MP-Q10*	3H	JHI-Hv50k-2016-203283	192.7	555799017	7.7	JHI-Hv50k-2016-203302	192.6	555747286	JHI-Hv50k-2016-203280	192.7	555799748	0.60
Flowering time	*FT-MP-Q11*	4H	JHI-Hv50k-2016-240101	86.6	98719384	3.3	JHI-Hv50k-2016-239980	86.5	96686737	JHI-Hv50k-2016-240141	86.8	103960077	0.27
Flowering time	*FT-MP-Q12*	4H	JHI-Hv50k-2016-260654	138.2	566586983	3.3	JHI-Hv50k-2016-260734	138.2	566569810	JHI-Hv50k-2016-260896	138.5	566780698	0.36
Flowering time	*FT-MP-Q13*	4H	JHI-Hv50k-2016-272205	200.3	602110401	89.1	JHI-Hv50k-2016-272207	200.3	602110153	JHI-Hv50k-2016-272270	200.5	602228904	8.09
Flowering time	*FT-MP-Q14*	5H	JHI-Hv50k-2016-305151	93.6	408438294	4.4	JHI-Hv50k-2016-305116	93.2	406868619	BOPA1_1910-1343	93.6	408439377	0.34
Flowering time	*FT-MP-Q15*	5H	JHI-Hv50k-2016-320334	170.0	494941401	3.5	BOPA1_6315-914	169.7	494772390	JHI-Hv50k-2016-320591	172.4	496478147	0.59
Flowering time	*FT-MP-Q16*	5H	JHI-Hv50k-2016-335345	225.2	527249716	68.0	JHI-Hv50k-2016-335374	225.1	527215217	JHI-Hv50k-2016-335344	225.2	527249879	6.53
Flowering time	*FT-MP-Q17*	6H	JHI-Hv50k-2016-384060	67.4	37903550	3.8	JHI-Hv50k-2016-384032	67.3	37813552	JHI-Hv50k-2016-384334	68.1	38660657	0.06
Flowering time	*FT-MP-Q18*	6H	SCRI_RS_187506	125.2	505526557	3.7	JHI-Hv50k-2016-413770	125.1	505418085	JHI-Hv50k-2016-413779	125.3	505747019	0.26
Flowering time	*FT-MP-Q19*	7H	BOPA2_12_30893	69.6	42285518	31.2	JHI-Hv50k-2016-459744	68.9	41824854	JHI-Hv50k-2016-460024	71.0	43186352	2.16
Flowering time	*FT-MP-Q20*	7H	JHI-Hv50k-2016-473460	130.0	107115320	4.7	JHI-Hv50k-2016-473455	130.0	107102377	JHI-Hv50k-2016-473673	130.7	109831240	0.33
Flowering time	*FT-MP-Q21*	7H	JHI-Hv50k-2016-513247	254.2	617492723	4.1	JHI-Hv50k-2016-513245	254.2	617492616	JHI-Hv50k-2016-513260	254.4	617569820	0.31
Plant height	*PH-MP-Q1*	1H	JHI-Hv50k-2016-11753	15.5	13379830	3.4	JHI-Hv50k-2016-11824	15.5	13388270	JHI-Hv50k-2016-11704	15.6	13343738	0.32
Plant height	*PH-MP-Q2*	1H	BOPA2_12_10489	87.9	304792051	3.2	BOPA2_12_30562	87.5	298992332	BOPA1_ABC11913-1-1-104	88.1	306458264	0.30
Plant height	*PH-MP-Q3*	1H	JHI-Hv50k-2016-40963	158.5	473573522	5.6	JHI-Hv50k-2016-40966	158.5	473572474	BOPA1_8867-459	158.6	473633633	0.82
Plant height	*PH-MP-Q4*	1H	JHI-Hv50k-2016-55210	225.8	509418137	5.5	JHI-Hv50k-2016-54826	223.9	508501007	JHI-Hv50k-2016-55434	226.2	509597380	0.33
Plant height	*PH-MP-Q5*	2H	JHI-Hv50k-2016-73562	36.6	25931885	42.6	BOPA2_12_30871	36.5	25877164	JHI-Hv50k-2016-73570	36.6	25936707	4.90
Plant height	*PH-MP-Q6*	2H	JHI-Hv50k-2016-106330	161.9	567013913	9.9	JHI-Hv50k-2016-106282	161.8	566933880	JHI-Hv50k-2016-106390	162.0	567072224	1.20
Plant height	*PH-MP-Q7*	2H	SCRI_RS_121952	256.4	635204036	36.4	JHI-Hv50k-2016-130926	256.2	635123928	JHI-Hv50k-2016-131006	256.6	635315429	3.33
Plant height	*PH-MP-Q8*	3H	JHI-Hv50k-2016-166560	94.4	119616143	3.6	BOPA2_12_31015	93.4	105848215	JHI-Hv50k-2016-166737	94.6	122286959	0.28
Plant height	*PH-MP-Q9*	3H	JHI-Hv50k-2016-205550	205.6	564418824	31.2	JHI-Hv50k-2016-205539	205.6	564416604	JHI-Hv50k-2016-205562	205.9	564609618	3.64
Plant height	*PH-MP-Q10*	3H	JHI-Hv50k-2016-223901	281.6	612465708	3.8	JHI-Hv50k-2016-223777	281.5	612375068	JHI-Hv50k-2016-224069	283.2	613316424	0.27
Plant height	*PH-MP-Q11*	4H	JHI-Hv50k-2016-231027	31.5	15657353	11.4	JHI-Hv50k-2016-230951	30.2	15129543	JHI-Hv50k-2016-231059	32.4	16054056	1.72
Plant height	*PH-MP-Q12*	4H	JHI-Hv50k-2016-262480	146.7	572549098	4.7	JHI-Hv50k-2016-262456	146.7	572543403	JHI-Hv50k-2016-262558	146.9	572678710	0.32
Plant height	*PH-MP-Q13*	4H	JHI-Hv50k-2016-271589	197.7	600782790	13.9	JHI-Hv50k-2016-271581	197.7	600782213	JHI-Hv50k-2016-271592	197.7	600783028	1.36
Plant height	*PH-MP-Q14*	5H	JHI-Hv50k-2016-306384	98.3	420841523	3.0	JHI-Hv50k-2016-306366	98.3	420833104	JHI-Hv50k-2016-306385	98.3	420841822	0.24
Plant height	*PH-MP-Q15*	5H	JHI-Hv50k-2016-330572	210.1	519056336	16.0	JHI-Hv50k-2016-330602	210.1	519050727	JHI-Hv50k-2016-330549	210.2	519110040	1.66
Plant height	*PH-MP-Q16*	5H	JHI-Hv50k-2016-347448	271.0	553116131	3.1	JHI-Hv50k-2016-347397	270.6	552925862	JHI-Hv50k-2016-347557	271.0	553150806	0.20
Plant height	*PH-MP-Q17*	5H	JHI-Hv50k-2016-363863	325.3	581272563	6.1	JHI-Hv50k-2016-363837	324.9	581089442	JHI-Hv50k-2016-363883	325.3	581277156	0.71
Plant height	*PH-MP-Q18*	6H	JHI-Hv50k-2016-394110	90.4	187857305	8.9	JHI-Hv50k-2016-394106	90.4	187847223	JHI-Hv50k-2016-394159	90.5	189994776	0.89
Plant height	*PH-MP-Q19*	6H	SCRI_RS_152414	194.3	555135170	3.4	JHI-Hv50k-2016-429401	193.9	554931535	JHI-Hv50k-2016-429588	194.6	555268907	0.46
Plant height	*PH-MP-Q20*	7H	JHI-Hv50k-2016-459853	69.6	42283766	15.5	JHI-Hv50k-2016-459744	68.9	41824854	BOPA2_12_10218	70.1	42640729	1.58
Plant height	*PH-MP-Q21*	7H	JHI-Hv50k-2016-481104	133.8	123257426	12.6	JHI-Hv50k-2016-481152	133.8	123251196	JHI-Hv50k-2016-474847	134.9	128949958	1.19

Supplementary Table 5: Summary of the results of the single population analysis for flowering time. The information regarding the peak and the borders of the confidence interval of each QTL are reported. Chr represents the chromosome on which the QTL was detected, LOD the logarithm of odds, and PVE the percentage of variance explained by the QTL individually and in a simultaneous fit. The additive effect is given in days after sowing.

QTL / Population	Chr	Peak			LOD	Start			Stop			Additive effect	Parent	PVE	Locus
		Associated marker	Peak (cM)	Marker position (bp)		Start marker	Start (cM)	Start position (bp)	Stop marker	Stop (cM)	Stop position (bp)				
qHvDRR02-FT-2.1	2H	JHI-Hv50k-2016-73780	56.3	26380311	8.4	JHI-Hv50k-2016-71929	50.7	22342142	JHI-Hv50k-2016-75278	61.8	31307172	3.0	HOR1842	11.2	*Ppd-H1*
qHvDRR02-FT-5.1	5H	JHI-Hv50k-2016-336770	205.3	529432664	29.1	JHI-Hv50k-2016-336527	202.6	529178521	JHI-Hv50k-2016-337089	214.0	530327920	6.7	IG31424	56.7	*eam5*
HvDRR02														66.1	
qHvDRR03-FT-5.1	5H	JHI-Hv50k-2016-335902	242.0	528058903	13.9	JHI-Hv50k-2016-334166	239.4	525813906	JHI-Hv50k-2016-337905	247.0	532356493	4.8	IG31424	50.7	*Vrn-H1*
qHvDRR03-FT-4.1	4H	JHI-Hv50k-2016-234502	73.7	34574624	3.6	JHI-Hv50k-2016-225780	0.6	1399990	JHI-Hv50k-2016-240027	82.0	97435598	2.1	Kharsila	9.1	*Qft.HEB25-4a*
HvDRR03														66.8	
qHvDRR04-FT-2.1	2H	JHI-Hv50k-2016-73615	54.6	25944268	4.3	JHI-Hv50k-2016-71761	46.5	21294256	JHI-Hv50k-2016-76799	77.8	36552741	1.9	HOR1842	9.3	*Ppd-H1*
qHvDRR04-FT-5.1	5H	BOPA2_12_31202	212.0	526335233	5.9	SCRI_RS_222698	199.7	517515363	JHI-Hv50k-2016-338274	224.9	533637328	2.2	Kharsila	12.9	*Vrn-H1*
qHvDRR04-FT-2.2	2H	BOPA1_5233-1070	122.5	428835705	4.5	BOPA1_ABC09016-2-2-348	121.3	346735328	JHI-Hv50k-2016-101100	142.3	537701109	1.9	HOR1842	9.6	*HvCEN*
HvDRR04														38.0	
qHvDRR07-FT-2.1	2H	BK_14	43.8	25877164	16.6	JHI-Hv50k-2016-73122	43	25381159	JHI-Hv50k-2016-73697	45.1	26363248	3.0	Sissy	45.2	*Ppd-H1*
qHvDRR07-FT-3.1	3H	SCRI_RS_150944	155.0	560042502	6.7	JHI-Hv50k-2016-203509	147.3	556739164	SCRI_RS_169325	187.2	588226210	1.8	Sissy	14.2	*sdw1*
HvDRR07														61.7	
qHvDRR08-FT-2.1	2H	JHI-Hv50k-2016-73500	58.4	25802728	16.4	JHI-Hv50k-2016-72274	55.5	23612704	JHI-Hv50k-2016-73697	60.7	26363248	3.3	W23829/803911	52.7	*Ppd-H1*
qHvDRR08-FT-7.1	7H	SCRI_RS_14174	3.5	624114922	3.5	JHI-Hv50k-2016-513966	303.4	618890340	SCRI_RS_14174	342.5	624114922	1.3	HOR7985	8.0	*7_02 (Hemshrot et al., 2019)*
HvDRR08														56.4	
qHvDRR09-FT-7.1	7H	SCRI_RS_220780	90.0	40279198	7	JHI-Hv50k-2016-449785	32.2	15413819	JHI-Hv50k-2016-460524	100.9	44088334	1.1	W23829/803911	27.4	*Vrn-H3*
qHvDRR10-FT-3.1	3H	JHI-Hv50k-2016-205404	123.7	564118077	14.9	JHI-Hv50k-2016-205209	121.5	563172279	JHI-Hv50k-2016-205612	124.2	564697182	2.1	W23829/803911	53.6	*sdw1*
qHvDRR11-FT-2.1	2H	JHI-Hv50k-2016-131359	166.0	636275614	7.8	JHI-Hv50k-2016-127582	151.5	629176434	JHI-Hv50k-2016-138043	176.2	648214097	1.4	Sanalta	20.1	*HvAP2*
qHvDRR11-FT-3.1	3H	JHI-Hv50k-2016-204079	107.3	558351096	8.8	JHI-Hv50k-2016-203397	105.2	556048946	BOPA1_3718-1026	114.9	571209231	1.6	Sissy	23.3	*sdw1*
qHvDRR11-FT-7.1	7H	JHI-Hv50k-2016-460580	53.4	44393592	3.9	JHI-Hv50k-2016-452392	31.2	20554909	JHI-Hv50k-2016-461706	60.0	50031910	1.0	Sanalta	9.2	*Vrn-H3*
HvDRR11														55.2	
qHvDRR12-FT-5.1	5H	JHI-Hv50k-2016-278416	8.0	3692924	3.3	BOPA2_12_30543	0	338140	JHI-Hv50k-2016-318569	103.0	491068447	0.9	Sanalta	10.7	*HvHeading-5H-SA*
qHvDRR12-FT-7.1	7H	BOPA2_12_30893	41.5	42285518	10.7	JHI-Hv50k-2016-459470	39.4	40274346	JHI-Hv50k-2016-460106	44.0	43288624	1.8	SprattArcher	45.9	*Vrn-H3*
HvDRR12														59.4	
qHvDRR13-FT-7.1	7H	BOPA2_12_10218	55.0	42640729	16.6	JHI-Hv50k-2016-459694	54.4	41778424	JHI-Hv50k-2016-460028	55.6	43186739	3.8	SprattArcher	67.5	*Vrn-H3*
qHvDRR14-FT-7.1	7H	SCRI_RS_121774	71.0	49048644	5.9	JHI-Hv50k-2016-459107	56.9	39462837	JHI-Hv50k-2016-462780	74.6	51169072	1.5	Georgie	30.1	*Vrn-H3*
qHvDRR15-FT-7.1	7H	JHI-Hv50k-2016-460172	45.5	43317456	9.7	JHI-Hv50k-2016-459225	38.8	39790897	JHI-Hv50k-2016-460794	48.6	44882536	2.4	SprattArcher	61.5	*Vrn-H3*
qHvDRR16-FT-2.1	2H	JHI-Hv50k-2016-73581	59.2	25938609	19.8	JHI-Hv50k-2016-72615	44.9	23984263	JHI-Hv50k-2016-73697	61.2	26363248	5.0	K10693	63.7	*Ppd-H1*
qHvDRR16-FT-2.2	2H	JHI-Hv50k-2016-129807	264.2	633397466	4.6	JHI-Hv50k-2016-127383	260.1	628668500	JHI-Hv50k-2016-134459	285.1	642392428	2.0	HOR12830	9.6	*HvAP2*
HvDRR16														64.2	
qHvDRR17-FT-1.1	1H	JHI-Hv50k-2016-51526	222.6	499028262	1.4	JHI-Hv50k-2016-24	0	84161	JHI-Hv50k-2016-56077	265.7	512145022	0.9	Ancap2	2.0	*mat-f*
qHvDRR17-FT-2.1	2H	JHI-Hv50k-2016-73780	53.1	26380311	23.4	JHI-Hv50k-2016-73545	48.8	25800459	JHI-Hv50k-2016-74049	56.0	27287895	4.6	K10693	53.2	*Ppd-H1*
qHvDRR17-FT-2.2	2H	JHI-Hv50k-2016-87930	107.5	108053739	5.7	JHI-Hv50k-2016-84178	102.0	79964580	SCRI_RS_145381	123.3	532823915	1.9	K10693	8.8	*HvCEN*
HvDRR17														66.2	
qHvDRR18-FT-2.1	2H	JHI-Hv50k-2016-73692	51.9	26152710	9	JHI-Hv50k-2016-72942	33.7	24594197	JHI-Hv50k-2016-76416	68.1	34425590	5.0	K10693	40.8	*Ppd-H1*
qHvDRR19-FT-2.1	2H	BOPA1_ABC08774-1-1-752	100.0	447579727	7.2	JHI-Hv50k-2016-91400	97.6	200103165	JHI-Hv50k-2016-99936	105.7	514610106	2.3	HOR383	33.0	*HvCEN*
qHvDRR20-FT-2.1	2H	BOPA1_ABC08774-1-1-752	114.9	447579727	7.9	JHI-Hv50k-2016-93715	113.6	404912006	JHI-Hv50k-2016-100214	121.3	531718337	2.5	HOR383	26.5	*HvCEN*
qHvDRR20-FT-2.2	2H	JHI-Hv50k-2016-73370	33.2	25761089	7	JHI-Hv50k-2016-72164	28.1	23156158	JHI-Hv50k-2016-73780	35.3	26380311	2.4	IG128104	22.8	*Ppd-H1*
qHvDRR20-FT-7.1	7H	BOPA2_12_30894	42.5	42285311	4	JHI-Hv50k-2016-459508	39.1	40243638	JHI-Hv50k-2016-461716	63.0	50132127	1.9	HOR383	12.2	*Vrn-H3*
HvDRR20														41.3	
HvDRR21	NO QTL														
qHvDRR22-FT-2.1	2H	JHI-Hv50k-2016-90437	88.1	357413708	7.6	SCRI_RS_186840	79.9	166116285	JHI-Hv50k-2016-98650	89.5	491963798	2.0	HOR383	14.3	*HvCEN*
qHvDRR22-FT-5.1	5H	SCRI_RS_223712	79.2	338641277	4.1	JHI-Hv50k-2016-293518	70.1	92336105	JHI-Hv50k-2016-307188	96.1	428832402	1.5	HOR383	6.9	*5_01 (Hemshrot et al., 2019)*
qHvDRR22-FT-7.1	7H	JHI-Hv50k-2016-460104	63.1	43288076	16.3	JHI-Hv50k-2016-459107	60.3	39462837	JHI-Hv50k-2016-460580	66.8	44393592	3.3	HOR383	38.7	*Vrn-H3*
HvDRR22														70.2	
qHvDRR23-FT-2.1	2H	BOPA2_12_30870	37.9	25878042	3.5	JHI-Hv50k-2016-71688	23.1	21266654	JHI-Hv50k-2016-75638	64.8	33040970	2.4	IG128104	16.9	*Ppd-H1*

qHvDRR24-FT-2.1	2H	JHI-Hv50k-2016-87488	97.0	102240001	3.8	JHI-Hv50k-2016-79228	78.6	47882932	JHI-Hv50k-2016-97160	107.3	473146023	2.0	HOR1842	23.7	*HvCEN*
qHvDRR25-FT-2.1	2H	BK_14	43.9	25877164	16.5	JHI-Hv50k-2016-73122	39.6	25381159	JHI-Hv50k-2016-73822	47.0	26540524	4.7	W23829/803911	63.1	*Ppd-H1*
qHvDRR25-FT-6.1	6H	JHI-Hv50k-2016-382481	75.6	33514697	3.6	JHI-Hv50k-2016-380125	61.7	26327004	JHI-Hv50k-2016-407149	100.9	447687783	1.7	Unumli-Arpa	8.9	*ert-v*
HvDRR25														63.9	
qHvDRR26-FT-2.1	2H	JHI-Hv50k-2016-73562	34.3	25931885	4.4	SCRI_RS_66401	28.1	20871415	BOPA1_3709-716	60.9	43264415	2.7	Sanalta	13.6	*Ppd-H1*
qHvDRR26-FT-7.1	7H	JHI-Hv50k-2016-497524	157.9	581874096	2.5	JHI-Hv50k-2016-496754	149.0	578906347	JHI-Hv50k-2016-511939	190.4	614823443	1.8	Unumli-Arpa	7.0	*mnd5*
qHvDRR26-FT-2.2	2H	JHI-Hv50k-2016-78164	70.0	44129204	3.8	BOPA1_3709-716	60.9	43264415	JHI-Hv50k-2016-102656	134.7	545723577	2.1	Sanalta	11.4	*HvCEN*
HvDRR26														70.1	
qHvDRR27-FT-2.1	2H	BOPA2_12_30870	44.4	25878042	30.3	JHI-Hv50k-2016-72944	41.8	24596379	JHI-Hv50k-2016-73692	45.8	26152710	6.0	SprattArcher	77.7	*Ppd-H1*
qHvDRR28-FT-2.1	2H	JHI-Hv50k-2016-74702	48.3	28827313	6.6	JHI-Hv50k-2016-73692	45.1	26152710	BOPA1_8787-1459	50.4	30044023	2.1	HOR8160	16.7	*Ppd-H1*
qHvDRR28-FT-2.2	2H	BOPA1_4136-869	123.2	516046308	7.5	BOPA1_9191-263	117.1	470676341	JHI-Hv50k-2016-100214	127.6	531718337	2.4	HOR8160	19.4	*Qft.HEB25-2c*
qHvDRR28-FT-5.1	5H	JHI-Hv50k-2016-335896	186.0	527898012	3.8	JHI-Hv50k-2016-333745	181.9	524805307	JHI-Hv50k-2016-342734	200.0	541120940	1.6	Unumli-Arpa	8.9	*Vrn-H1*
qHvDRR28-FT-4.1	4H	JHI-Hv50k-2016-250940	70.6	500815893	3.5	JHI-Hv50k-2016-232929	49.9	27305200	JHI-Hv50k-2016-274011	171.7	605081758	1.4	Unumli-Arpa	8.1	*Vrn-H2*
HvDRR28														63.6	
qHvDRR29-FT-2.1	2H	JHI-Hv50k-2016-73584	41.9	25938729	17.6	JHI-Hv50k-2016-73174	41.2	25327192	JHI-Hv50k-2016-74407	47.5	28202988	2.5	HOR8160	41.8	*Ppd-H1*
qHvDRR29-FT-2.2	2H	JHI-Hv50k-2016-94652	109.0	432869619	5.4	JHI-Hv50k-2016-90029	103.0	146772819	JHI-Hv50k-2016-99945	120.2	514612781	1.2	HOR8160	9.7	*HvCEN*
qHvDRR29-FT-4.1	4H	JHI-Hv50k-2016-272251	169.8	602047895	5.4	JHI-Hv50k-2016-267444	150.8	590465290	JHI-Hv50k-2016-272632	171.4	603700158	1.2	IG128216	9.7	*Vrn-H2*
qHvDRR29-FT-2.3	2H	JHI-Hv50k-2016-126298	224.7	626703141	3	JHI-Hv50k-2016-109411	162.3	585633374	JHI-Hv50k-2016-131074	236.8	635950528	0.9	IG128216	5.2	*HvAP2*
HvDRR29														61.1	
qHvDRR30-FT-2.1	2H	JHI-Hv50k-2016-73566	42.8	25934047	15.8	JHI-Hv50k-2016-73174	42.1	25327192	JHI-Hv50k-2016-73871	49.0	26542729	2.9	Georgie	28.1	*Ppd-H1*
qHvDRR30-FT-7.1	7H	SCRI_RS_160723	76.8	31766007	8.3	BOPA2_12_10878	75.1	31483632	JHI-Hv50k-2016-458499	79.6	34113655	2.0	Georgie	12.7	*Qft.HEB25-7a*
qHvDRR30-FT-3.1	3H	SCRI_RS_169325	230.3	588226210	3.1	JHI-Hv50k-2016-207495	209.9	574021612	JHI-Hv50k-2016-216747	243.9	595847162	1.1	Georgie	4.3	
qHvDRR30-FT-4.1	4H	JHI-Hv50k-2016-272270	232.8	602228904	9	JHI-Hv50k-2016-271227	227.6	600591532	JHI-Hv50k-2016-276456	238.3	609247127	2.0	IG128216	13.9	*Vrn-H2*
qHvDRR30-FT-2.2	2H	JHI-Hv50k-2016-97657	122.8	477301174	4.5	SCRI_RS_182959	116.6	205588975	JHI-Hv50k-2016-99117	128.3	508011086	1.4	Georgie	6.4	*HvCEN*
HvDRR30														65.0	
qHvDRR31-FT-5.1	5H	JHI-Hv50k-2016-338907	212.9	535802677	7.3	SCRI_RS_206956	211.5	534240130	JHI-Hv50k-2016-340110	213.5	537093432	6.8	IG128216	13.5	*Vrn-H1*
qHvDRR31-FT-1.1	1H	JHI-Hv50k-2016-55370	263.4	509641983	6.2	JHI-Hv50k-2016-53420	258.1	505296418	JHI-Hv50k-2016-58045	269.8	516079896	1.2	IG128216	11.1	*HvELF3*
qHvDRR31-FT-2.1	2H	JHI-Hv50k-2016-91422	155.0	200469849	5.3	JHI-Hv50k-2016-71813	24.5	21559000	JHI-Hv50k-2016-102161	179.9	544572700	1.1	Lakhan	9.5	*HvCEN*
qHvDRR31-FT-5.2	5H	JHI-Hv50k-2016-338278	209.8	533639298	4.8	JHI-Hv50k-2016-338174	209.5	533435507	JHI-Hv50k-2016-338907	212.9	535802677	5.4	Lakhan	8.5	*eam5*
qHvDRR31-FT-5.3	5H	JHI-Hv50k-2016-321854	171.3	500427524	5	JHI-Hv50k-2016-320649	169.1	496537582	JHI-Hv50k-2016-330440	192.3	518881864	1.1	IG128216	8.9	*eam5*
HvDRR31														54.8	
qHvDRR32-FT-4.1	4H	JHI-Hv50k-2016-273301	202.5	604261236	5.5	JHI-Hv50k-2016-270337	184.4	598246191	JHI-Hv50k-2016-273301	202.5	604261236	4.7	IG128216	38.6	*Vrn-H2*
qHvDRR32-FT-2.1	2H	JHI-Hv50k-2016-99627	101.3	513466965	3.6	JHI-Hv50k-2016-91514	84.1	201408273	JHI-Hv50k-2016-103200	109.5	549570111	3.4	K10877	21.8	*HvCEN*
HvDRR32														59.5	
qHvDRR33-FT-2.1	2H	JHI-Hv50k-2016-73510	61.8	25802287	6	JHI-Hv50k-2016-71218	54.5	20825473	JHI-Hv50k-2016-75311	69.2	31264487	2.5	Georgie	29.1	*Ppd-H1*
qHvDRR34-FT-2.1	2H	JHI-Hv50k-2016-132317	289.6	637977625	3.9	JHI-Hv50k-2016-125068	223.5	624622312	JHI-Hv50k-2016-135634	311.4	644195578	4.6	K10877	41.2	*HvAP2*
qHvDRR35-FT-5.1	5H	JHI-Hv50k-2016-333666	253.4	524450825	5.1	JHI-Hv50k-2016-333265	250.7	523858991	SCRI_RS_148402	261.4	530490087	0.9	CM67	21.2	*Vrn-H1*
qHvDRR35-FT-2.1	2H	JHI-Hv50k-2016-99962	175.8	514746577	3.6	JHI-Hv50k-2016-86885	134.0	97901851	JHI-Hv50k-2016-104390	198.6	559662952	0.8	Lakhan	14.2	*HvCEN*
HvDRR35														33.5	
qHvDRR36-FT-4.1	4H	JHI-Hv50k-2016-273434	196.5	604293070	5	BOPA2_12_30476	189.5	602249110	JHI-Hv50k-2016-273928	198.9	604961427	2.1	HOR12830	32.7	*Vrn-H2*
qHvDRR37-FT-2.1	2H	SCRI_RS_207244	75.9	43626804	3.3	JHI-Hv50k-2016-77411	66.3	40933207	JHI-Hv50k-2016-80904	95.7	60696083	2.5	K10877	21.7	*HvFT4*
qHvDRR38-FT-2.1	2H	SCRI_RS_147230	363.3	633228850	4.2	JHI-Hv50k-2016-123934	348.2	622368414	JHI-Hv50k-2016-131622	378.4	637093530	2.6	HOR12830	22.6	*HvAP2*
qHvDRR39-FT-2.1	2H	SCRI_RS_121952	239.7	635204036	7.3	JHI-Hv50k-2016-126975	235.4	627838967	JHI-Hv50k-2016-131622	243.6	637093530	2.5	HOR12830	18.0	*HvAP2*
qHvDRR39-FT-2.2	2H	JHI-Hv50k-2016-69230	23.8	17261817	6.6	JHI-Hv50k-2016-67667	19.5	14076281	JHI-Hv50k-2016-73723	50.3	26372182	2.5	ItuNative	16.0	*Ppd-H1*
qHvDRR39-FT-2.3	2H	JHI-Hv50k-2016-94897	121.1	440899866	4.9	JHI-Hv50k-2016-91495	117.1	201420899	JHI-Hv50k-2016-98500	124.6	484522285	2.0	HOR12830	11.4	*HvCEN*
HvDRR39														52.4	
HvDRR40	NO QTL														
qHvDRR41-FT-2.1	2H	JHI-Hv50k-2016-73417	45.8	25879034	12.3	SCRI_RS_205712	41.1	23346149	JHI-Hv50k-2016-74225	49.0	27980386	2.5	K10693	35.5	*Ppd-H1*
qHvDRR41-FT-2.2	2H	SCRI_RS_141789	129.6	484678185	6.9	JHI-Hv50k-2016-96857	127.3	471271325	JHI-Hv50k-2016-100346	138.8	532815321	1.8	K10693	17.0	*Qft.HEB25-2c*
qHvDRR41-FT-7.1	7H	JHI-Hv50k-2016-460797	52.6	44881543	5.5	JHI-Hv50k-2016-459853	47.8	42283766	JHI-Hv50k-2016-461413	56.8	48866586	1.6	K10693	13.1	*Vrn-H3*
HvDRR41														57.9	
qHvDRR42-FT-2.1	2H	JHI-Hv50k-2016-72896	67.6	24497103	4	JHI-Hv50k-2016-72164	65.1	23156158	JHI-Hv50k-2016-74683	83.5	28819655	2.4	ItuNative	9.4	*Ppd-H1*
qHvDRR42-FT-3.1	3H	JHI-Hv50k-2016-196425	286.4	525404837	7.3	JHI-Hv50k-2016-193988	266.9	511021783	JHI-Hv50k-2016-197035	292.8	528466597	3.3	Ancap2	19.3	*sld5*

qHvDRR42-FT-4.1	4H	JHI-Hv50k-2016-253833	155.7	523801355	2.7	BOPA1_3127-273	141.6	483208363	JHI-Hv50k-2016-255019	162.3	531420971	1.9	Ancap2	6.1	*ari-q*
qHvDRR42-FT-5.1	5H	JHI-Hv50k-2016-338482	455.7	534377940	5.9	JHI-Hv50k-2016-337429	449.5	530982821	JHI-Hv50k-2016-339838	459.0	536729125	3.0	Ancap2	14.6	*Vrn-H1*
HvDRR42														67.8	
qHvDRR43-FT-4.1	4H	JHI-Hv50k-2016-268870	131.1	595132794	12	JHI-Hv50k-2016-268641	129.0	594360356	No more polymorphisms upstream of peak marker			10.9	Kombyne	36.6	
qHvDRR44-FT-5.1	5H	JHI-Hv50k-2016-334016	258.8	525535984	5.6	JHI-Hv50k-2016-331101	248.0	519493734	JHI-Hv50k-2016-339936	273	537016242	3.8	Kombyne	21.7	*Vrn-H1*
qHvDRR44-FT-7.1	7H	JHI-Hv50k-2016-459818	74.7	41807357	4.5	JHI-Hv50k-2016-458557	72.9	34116480	JHI-Hv50k-2016-460446	80.1	43517682	2.7	Kombyne	16.8	*Vrn-H3*
HvDRR44														34.8	
qHvDRR45-FT-5.1	5H	JHI-Hv50k-2016-337093	200.9	530329021	6.1	JHI-Hv50k-2016-327943	175.3	514628747	JHI-Hv50k-2016-343006	220.7	541947536	5.4	Kombyne	30.5	*Vrn-H1*
qHvDRR46-FT-5.1	5H	JHI-Hv50k-2016-335345	355.3	527249716	3.1	JHI-Hv50k-2016-333353	347.8	523824571	JHI-Hv50k-2016-355430	428.2	567924333	5.6	Kombyne	34.4	*Vrn-H1*
qHvDRR47-FT-2.1	2H	JHI-Hv50k-2016-73422	40.7	25877853	11.8	JHI-Hv50k-2016-72949	38.7	24597354	JHI-Hv50k-2016-73663	41.5	26107957	4.5	Sissy	27.0	*Ppd-H1*
qHvDRR47-FT-4.1	4H	SCRI_RS_221876	242.2	604259662	10.5	JHI-Hv50k-2016-271709	238.0	600927835	JHI-Hv50k-2016-276495	243.4	609268367	4.3	IG31424	23.5	*Vrn-H2*
qHvDRR47-FT-5.1	5H	SCRI_RS_193529	272.4	525928975	9.2	JHI-Hv50k-2016-333734	268.6	524587621	JHI-Hv50k-2016-337389	281.5	530890859	4.0	IG31424	19.9	*Vrn-H1*
qHvDRR47-FT-7.1	7H	JHI-Hv50k-2016-475698	200.0	187984054	0.6	JHI-Hv50k-2016-435161	0	2549430	JHI-Hv50k-2016-518458	360.9	627531040	0.9	Sissy	1.0	*Vrn-H3*
HvDRR47														62.4	
qHvDRR48-FT-2.1	2H	JHI-Hv50k-2016-75250	50.6	31093363	4.2	JHI-Hv50k-2016-72159	23.5	23156664	JHI-Hv50k-2016-76569	59.1	34867730	2.0	HOR1842	20.8	*Ppd-H1*

Supplementary Table 6: Summary of the results of the single population analysis for plant height. The information regarding the peak and the borders of the confidence interval of each QTL are reported. Chr represents the chromosome on which the QTL was detected, LOD the logarithm of odds, and PVE the percentage of variance explained by the QTL individually and in a simultaneous fit. The additive effect is given in cm.

QTL / Population	Chr	Peak			LOD	Start			Stop			Additive effect	Parent	PVE	Locus
		Associated marker	Peak (cM)	Marker position (bp)		Start marker	Start (cM)	Start position (bp)	Stop marker	Stop (cM)	Stop position (bp)				
qHvDRR02-PH-2.1	2H	JHI-Hv50k-2016-132262	242.7	637974692	3.9	JHI-Hv50k-2016-127661	233.7	629444744	SCRI_RS_156155	254.8	644348170	2.8	HOR1842	8.2	*HvAP2*
qHvDRR02-PH-5.1	5H	JHI-Hv50k-2016-338436	216.9	534224386	7.4	SCRI_RS_130992	198.1	525431316	JHI-Hv50k-2016-339229	222.0	536164535	3.9	HOR1842	16.4	*Vrn-H1*
qHvDRR02-PH-3.1	3H	JHI-Hv50k-2016-207933	196.5	576804876	4.7	JHI-Hv50k-2016-205716	183.9	564905926	SCRI_RS_205592	216.2	589574347	3.2	IG31424	9.9	*sdw1*
qHvDRR02-PH-4.1	4H	JHI-Hv50k-2016-231100	44.1	16384199	3.5	JHI-Hv50k-2016-230639	37.1	13052112	JHI-Hv50k-2016-234652	71.1	35448323	2.6	IG31424	7.3	*brh9*
HvDRR02														41.6	
HvDRR03	NO QTL														
qHvDRR04-PH-2.1	2H	JHI-Hv50k-2016-116511	209.6	608449388	3.3	JHI-Hv50k-2016-72239	49.8	23346162	JHI-Hv50k-2016-122404	239.1	620783775	1.9	HOR1842	10.3	*Ppd-H1*
qHvDRR07-PH-2.1	2H	SCRI_RS_170337	46.0	27283212	11.1	JHI-Hv50k-2016-73663	44.3	26107957	JHI-Hv50k-2016-75042	50.1	30307054	2.7	Sissy	22.8	*Ppd-H1*
qHvDRR07-PH-3.1	3H	JHI-Hv50k-2016-205562	158.2	564609618	11.2	SCRI_RS_150944	152.6	560042502	SCRI_RS_169325	187.2	588226210	2.7	HOR7985	23	*sdw1*
qHvDRR07-PH-4.1	4H	JHI-Hv50k-2016-268537	124.1	592785835	3.0	SCRI_RS_141214	93.3	575753195	SCRI_RS_216855	138.4	598006884	1.3	Sissy	5.0	*ari-q*
qHvDRR07-PH-7.1	7H	JHI-Hv50k-2016-475138	129.4	137977116	6.3	JHI-Hv50k-2016-469069	121.3	74922565	BOPA2_12_30999	139.5	509069522	1.9	HOR7985	11.4	*brh7*
HvDRR07														66.8	
qHvDRR08-PH-2.1	2H	JHI-Hv50k-2016-72853	57.6	24508569	7.9	JHI-Hv50k-2016-71249	51.6	20862461	JHI-Hv50k-2016-73966	64.2	26842811	2.7	W23829/803911	16.5	*Ppd-H1*
qHvDRR08-PH-3.1	3H	JHI-Hv50k-2016-205257	223.6	563231300	8.1	JHI-Hv50k-2016-202880	211.0	554784656	JHI-Hv50k-2016-205550	225.4	564418824	2.6	HOR7985	17.0	*sdw1*
qHvDRR08-PH-4.1	4H	SCRI_RS_176669	135.2	566061970	6.8	JHI-Hv50k-2016-256420	120.7	541858127	JHI-Hv50k-2016-262688	146.9	575372062	2.5	W23829/803911	13.9	*ari-q*
qHvDRR08-PH-5.1	5H	JHI-Hv50k-2016-307515	118.1	430059350	4.1	JHI-Hv50k-2016-307465	116.2	429632399	JHI-Hv50k-2016-308926	146.4	441596516	1.8	W23829/803911	7.8	*HvDep1*
HvDRR08														64.5	
HvDRR09	NO QTL														
qHvDRR10-PH-3.1	3H	JHI-Hv50k-2016-205404	123.7	564118077	23.3	JHI-Hv50k-2016-205209	121.5	563172279	JHI-Hv50k-2016-205741	124.8	565023140	7.8	Sanalta	63.6	*sdw1*
qHvDRR10-PH-2.1	2H	JHI-Hv50k-2016-130123	189.2	633688209	4.4	JHI-Hv50k-2016-126337	181.7	626889809	JHI-Hv50k-2016-132236	197.9	637973669	2.7	W23829/803911	7.0	*HvAP2*
HvDRR10														72.8	
qHvDRR11-PH-2.1	2H	JHI-Hv50k-2016-135139	175.3	643345831	10.8	JHI-Hv50k-2016-130469	165.1	634659802	JHI-Hv50k-2016-138544	177.1	649502780	4.2	Sissy	21.2	*HvAP2*
qHvDRR11-PH-3.1	3H	JHI-Hv50k-2016-205774	112.8	567242962	17.9	JHI-Hv50k-2016-204079	107.3	558351096	JHI-Hv50k-2016-206527	113.6	569278995	6.1	Sanalta	42.2	*sdw1*
qHvDRR11-PH-2.2	2H	BOPA1_4833-420	136.9	617233959	1.6	JHI-Hv50k-2016-62455	5.1	5549885	JHI-Hv50k-2016-135139	175.3	643345831	1.5	Sanalta	2.5	*HvCEN*
qHvDRR11-PH-7.1	7H	JHI-Hv50k-2016-464308	76.8	55406818	3.8	BOPA2_12_10368	60.0	49964856	JHI-Hv50k-2016-466699	81.2	63672450	2.2	Sanalta	6.2	*brh7*
qHvDRR11-PH-7.2	7H	JHI-Hv50k-2016-505814	160.3	601772379	3.8	JHI-Hv50k-2016-500177	142.7	590201204	JHI-Hv50k-2016-513495	185.0	618285111	2.2	Sanalta	6.3	*mnd5*
HvDRR11														68.5	
HvDRR12	NO QTL														
qHvDRR13-PH-3.1	3H	JHI-Hv50k-2016-164723	66.7	44836033	4.8	SCRI_RS_177084	45.5	20531937	JHI-Hv50k-2016-181744	73.9	418703261	2.0	SprattArcher	17.7	*sdw1*
qHvDRR13-PH-6.1	6H	JHI-Hv50k-2016-383599	69.0	36341989	3.6	JHI-Hv50k-2016-381798	61.1	31180257	BOPA1_851-804	78.9	413234840	1.7	SprattArcher	12.6	*ert-k*
qHvDRR13-PH-7.1	7H	JHI-Hv50k-2016-458766	53.1	34687802	3.6	JHI-Hv50k-2016-452755	34.8	21937819	JHI-Hv50k-2016-461192	59.6	47753959	1.6	SprattArcher	12.8	*Vrn-H3*
HvDRR13														54.2	
qHvDRR14-PH-3.1	3H	BOPA1_ABC07496-pHv1343-02	177.0	562581369	3.8	JHI-Hv50k-2016-204079	172.1	558351096	JHI-Hv50k-2016-206595	183.3	570352909	2.0	HOR8160	20.8	*sdw1*
qHvDRR15-PH-3.1	3H	JHI-Hv50k-2016-183463	98.0	443119491	3.4	JHI-Hv50k-2016-163896	87.9	35406401	JHI-Hv50k-2016-201887	139.0	551776522	1.5	SprattArcher	28.6	*ari-a*
qHvDRR16-PH-2.1	2H	JHI-Hv50k-2016-131048	268.9	635724995	7.9	JHI-Hv50k-2016-129807	264.6	633397466	JHI-Hv50k-2016-134802	287.0	642978551	4.2	K10693	26.0	*HvAP2*
qHvDRR16-PH-2.2	2H	BOPA2_12_30872	47.5	25879588	5.1	JHI-Hv50k-2016-72291	41.4	23609188	JHI-Hv50k-2016-74683	68.0	28819655	2.9	K10693	15.4	*Ppd-H1*
HvDRR16														48.6	
HvDRR17	NO QTL														
qHvDRR18-PH-7.1	7H	JHI-Hv50k-2016-454940	37.1	27942550	3.5	JHI-Hv50k-2016-452259	27.4	19265644	BOPA2_12_30219	41.2	32279583	2.6	HOR383	18.4	*brh1*
qHvDRR19-PH-2.1	2H	JHI-Hv50k-2016-98990	103.6	502130218	3.6	JHI-Hv50k-2016-78593	72.0	45543263	BOPA2_12_31383	113.9	544622565	1.7	HOR383	14.1	*HvCEN*
qHvDRR19-PH-3.1	3H	JHI-Hv50k-2016-203690	192.2	557107513	2.9	JHI-Hv50k-2016-163568	58.5	33364832	JHI-Hv50k-2016-224720	290.4	616302985	1.5	HOR383	11.3	*sdw1*
HvDRR19														36.2	
qHvDRR20-PH-7.1	7H	JHI-Hv50k-2016-455231	29.6	28232124	3.7	JHI-Hv50k-2016-450900	16.5	17063873	JHI-Hv50k-2016-460446	45.9	43517682	2.8	HOR383	15.9	*Vrn-H3*
qHvDRR21-PH-7.1	7H	JHI-Hv50k-2016-481738	135.0	323336489	6.9	BOPA1_8582-772	128.5	160630477	BOPA2_12_30213	140.7	445207235	4.8	Ancap2	31.5	*brh7*
qHvDRR21-PH-7.2	7H	JHI-Hv50k-2016-459234	65.5	39788787	3.1	SCRI_RS_98829	39.1	17593266	JHI-Hv50k-2016-465016	88.1	58991477	3.0	Ancap2	12.7	*Vrn-H3*

HvDRR21														43.9	
qHvDRR22-PH-7.1	7H	JHI-Hv50k-2016-479763	119.3	280304048	20.8	BOPA2_12_30344	117.3	172307219	JHI-Hv50k-2016-483509	121.2	386505847	5.5	HOR383	40.7	*brh7*
qHvDRR22-PH-1.1	1H	SCRI_RS_147318	214.1	510414373	2.4	JHI-Hv50k-2016-36461	126.9	437726587	JHI-Hv50k-2016-58169	220.7	516001848	1.6	HOR383	2.8	*eam8*
qHvDRR22-PH-2.1	2H	JHI-Hv50k-2016-93257	85.2	385833711	5.9	JHI-Hv50k-2016-83002	66.5	73195772	JHI-Hv50k-2016-100049	93.6	518890224	2.4	HOR383	7.5	*HvCEN*
qHvDRR22-PH-7.2	7H	JHI-Hv50k-2016-460104	63.1	43288076	7.6	SCRI_RS_194080	53.0	30808856	JHI-Hv50k-2016-461389	69.0	48714131	2.8	HOR383	10.1	*Vrn-H3*
qHvDRR22-PH-4.1	4H	JHI-Hv50k-2016-242645	64.4	406709482	6.4	JHI-Hv50k-2016-234536	54.4	34760445	JHI-Hv50k-2016-253745	79.2	523027560	2.5	Namhaebori	8.3	*brh9*
qHvDRR22-PH-6.1	6H	SCRI_RS_118381	57.5	161943460	4.3	JHI-Hv50k-2016-380005	34.5	25548365	JHI-Hv50k-2016-416777	97.5	521286626	2.1	Namhaebori	5.3	*ert-k*
HvDRR22														78.5	
qHvDRR23-PH-7.1	7H	JHI-Hv50k-2016-479764	115.9	280303948	7.3	BOPA1_8582-772	106.4	160630477	SCRI_RS_235584	129.3	435303585	4.3	IG128104	32.4	*brh7*
qHvDRR24-PH-3.1	3H	JHI-Hv50k-2016-154007	20.0	8888089	5.1	JHI-Hv50k-2016-153317	12.3	6784714	JHI-Hv50k-2016-156575	32.0	13791261	3.9	IG128104	26.2	
qHvDRR24-PH-1.1	1H	JHI-Hv50k-2016-34594	105.9	425018349	3.4	JHI-Hv50k-2016-15407	56.1	22087681	SCRI_RS_188360	116.3	447057229	3.1	IG128104	16.4	*ari-t*
HvDRR24														41.2	
qHvDRR25-PH-2.1	2H	BOPA1_2646-1277	48.8	28086868	5.5	JHI-Hv50k-2016-67059	15.9	13308057	JHI-Hv50k-2016-75638	55.9	33040970	3.1	W23829/803911	23.1	*Ppd-H1*
qHvDRR25-PH-3.1	3H	JHI-Hv50k-2016-205406	152.4	564114289	4.6	JHI-Hv50k-2016-149285	0	1799813	BOPA2_12_30081	162.7	567161897	2.8	Unumli-Arpa	18.5	*sdw1*
HvDRR25														43.5	
qHvDRR26-PH-2.1	2H	BOPA2_12_30396	217.9	634394889	5.8	BOPA1_4833-420	196.3	617233959	JHI-Hv50k-2016-134808	222.9	642978976	4.4	Unumli-Arpa	22.0	*HvAP2*
qHvDRR26-PH-3.1	3H	JHI-Hv50k-2016-186194	87.4	462670492	4.9	SCRI_RS_238649	64.1	42458039	JHI-Hv50k-2016-188213	90.4	479908157	3.8	Sanalta	18.1	*HvBRI1*
qHvDRR26-PH-4.1	4H	JHI-Hv50k-2016-232799	67.4	24125272	5.4	JHI-Hv50k-2016-231904	55.8	19763786	JHI-Hv50k-2016-234474	74.5	34288184	4.1	Sanalta	20.1	*brh9*
qHvDRR26-PH-2.2	2H	JHI-Hv50k-2016-109198	161.3	582019742	2.5	SCRI_RS_66401	28.1	20871415	JHI-Hv50k-2016-115240	171.8	605942036	2.7	Sanalta	8.0	*Ppd-H1*
HvDRR26														65.4	
qHvDRR27-PH-2.1	2H	JHI-Hv50k-2016-71249	33.0	20862461	4.4	JHI-Hv50k-2016-67059	14.4	13308057	JHI-Hv50k-2016-73487	43.4	25810005	2.5	SprattArcher	19.6	*Ppd-H1*
qHvDRR28-PH-2.1	2H	JHI-Hv50k-2016-73692	45.1	26152710	10.6	JHI-Hv50k-2016-72530	40.1	23831226	BOPA1_8787-1459	50.4	30044023	3.3	HOR8160	36.5	*Ppd-H1*
qHvDRR28-PH-6.1	6H	JHI-Hv50k-2016-408338	89.3	461666718	3.2	JHI-Hv50k-2016-382587	68.3	33857352	SCRI_RS_207284	97.5	511223129	1.7	Unumli-Arpa	8.8	*ert-k*
HvDRR28														55.9	
qHvDRR29-PH-2.1	2H	BOPA2_12_30897	146.2	570803230	8.9	SCRI_RS_17898	139.4	561858220	JHI-Hv50k-2016-108681	152.3	574833138	3.6	HOR8160	23.1	*ert-j*
qHvDRR29-PH-2.2	2H	JHI-Hv50k-2016-73780	43.4	26380311	5.9	JHI-Hv50k-2016-73052	40.1	25023220	JHI-Hv50k-2016-74407	47.5	28202988	2.8	HOR8160	14.4	*Ppd-H1*
qHvDRR29-PH-6.1	6H	JHI-Hv50k-2016-395685	73.8	289251842	3.8	JHI-Hv50k-2016-378164	38.2	19699707	BOPA2_12_10803	95.9	396967363	2.2	IG128216	8.8	*ert-k*
HvDRR29														48.3	
qHvDRR30-PH-2.1	2H	JHI-Hv50k-2016-67694	20.0	14065564	4.3	JHI-Hv50k-2016-59032	0	566575	JHI-Hv50k-2016-73871	49.0	26542729	2.5	Georgie	12.9	*Ppd-H1*
qHvDRR30-PH-4.1	4H	SCRI_RS_98443	49.0	13871241	4.8	JHI-Hv50k-2016-230452	40.9	11788248	JHI-Hv50k-2016-231162	52.5	16680700	2.6	Georgie	14.8	*QHt4H.26*
HvDRR30														25.8	
qHvDRR31-PH-1.1	1H	JHI-Hv50k-2016-58045	269.8	516079896	5.6	SCRI_RS_156009	264.8	510473721	JHI-Hv50k-2016-58045	269.8	516079896	2.6	IG128216	17.0	*eam8*
qHvDRR31-PH-5.1	5H	JHI-Hv50k-2016-335543	201.8	527185413	3.4	JHI-Hv50k-2016-324907	181.8	508775487	JHI-Hv50k-2016-336814	204.1	529367527	2.0	IG128216	9.9	*Vrn-H1*
HvDRR31														23.6	
HvDRR32	NO QTL														
qHvDRR33-PH-2.1	2H	JHI-Hv50k-2016-75950	93.9	33607845	6.9	JHI-Hv50k-2016-73285	60.7	25434173	BOPA2_12_10847	100.6	37534650	3.1	Georgie	32.7	*Ppd-H1*
qHvDRR34-PH-2.1	2H	SCRI_RS_55841	250.2	629407561	4.0	JHI-Hv50k-2016-125068	223.5	624622312	JHI-Hv50k-2016-132611	301.9	638549040	5.3	Lakhan	42.1	*HvAP2*
HvDRR35	NO QTL														
HvDRR36	NO QTL														
qHvDRR37-PH-2.1	2H	JHI-Hv50k-2016-131048	285.7	635724995	5.8	JHI-Hv50k-2016-123934	276.0	622368414	JHI-Hv50k-2016-132428	319.2	638148957	4.1	CM67	29.6	*HvAP2*
qHvDRR37-PH-6.1	6H	JHI-Hv50k-2016-401443	111.5	377513797	3.9	JHI-Hv50k-2016-383530	84.7	36126314	JHI-Hv50k-2016-407417	131.5	449902392	3.1	K10877	18.4	*ert-k*
HvDRR37														44.5	
qHvDRR38-PH-2.1	2H	SCRI_RS_147230	363.3	633228850	10.0	JHI-Hv50k-2016-126337	354.7	626889809	JHI-Hv50k-2016-131048	372.7	635724995	6.5	CM67	45.4	*HvAP2*
qHvDRR39-PH-2.1	2H	JHI-Hv50k-2016-130184	238.8	633708485	14.1	JHI-Hv50k-2016-128757	237.5	631502800	JHI-Hv50k-2016-131622	243.6	637093530	5.2	ItuNative	41.0	*HvAP2*
qHvDRR39-PH-2.2	2H	JHI-Hv50k-2016-73618	41.6	25941826	4.5	JHI-Hv50k-2016-71733	35.3	21290528	JHI-Hv50k-2016-73812	53.4	26541621	2.7	ItuNative	10.5	*Ppd-H1*
HvDRR39														52.3	
HvDRR40	NO QTL														
qHvDRR41-PH-1.1	1H	BOPA2_12_30191	147.4	485117907	3.4	SCRI_RS_188360	112.3	447057229	SCRI_RS_192730	155.1	488343190	2.0	K10693	4.4	*ert-b*

qHvDRR41-PH-2.1	2H	JHI-Hv50k-2016-73417	45.8	25879034	18.5	JHI-Hv50k-2016-73174	45.3	25327192	JHI-Hv50k-2016-74225	49.0	27980386	5.8	K10693	35.7	*Ppd-H1*
qHvDRR41-PH-2.2	2H	JHI-Hv50k-2016-102289	148.6	544834817	5.9	JHI-Hv50k-2016-100919	146.7	537247142	JHI-Hv50k-2016-103355	152.3	550508509	3.4	ItuNative	8.1	*ari-g*
qHvDRR41-PH-7.1	7H	JHI-Hv50k-2016-460797	52.6	44881543	9.7	JHI-Hv50k-2016-459813	46.9	41804923	JHI-Hv50k-2016-461259	56.3	48091239	4.4	K10693	14.7	*Vrn-H3*
qHvDRR41-PH-2.3	2H	BOPA2_12_10330	115.2	154488197	3.8	JHI-Hv50k-2016-86043	109.2	93370860	JHI-Hv50k-2016-99471	132.9	511935305	2.6	K10693	4.9	*HvCEN*
qHvDRR41-PH-7.2	7H	JHI-Hv50k-2016-472845	97.9	97980146	6.0	JHI-Hv50k-2016-471134	94.4	86628232	JHI-Hv50k-2016-475140	110.6	137976713	3.0	ItuNative	8.3	*brh7*
HvDRR41														76.1	
HvDRR42	NO QTL														
qHvDRR43-PH-4.1	4H	JHI-Hv50k-2016-268870	131.1	595132794	5.5	JHI-Hv50k-2016-268641	129.0	594360356	No more polymorphisms upstream of peak marker			5.1	Namhaebori	18.0	
qHvDRR44-PH-5.1	5H	JHI-Hv50k-2016-338130	264.8	533307510	7.0	JHI-Hv50k-2016-333647	257.4	524452711	SCRI_RS_210928	267.9	535693146	7.5	IG128104	28.2	*Vrn-H1*
qHvDRR45-PH-5.1	5H	JHI-Hv50k-2016-333733	195.2	524587700	9.6	SCRI_RS_154144	194.2	523996363	JHI-Hv50k-2016-336856	198.9	529735901	5.9	HOR1842	38.1	*Vrn-H1*
qHvDRR45-PH-1.1	1H	JHI-Hv50k-2016-20787	90.7	116772750	4.2	JHI-Hv50k-2016-17082	73.3	31502343	JHI-Hv50k-2016-23975	98.7	316156722	3.1	Kombyne	14.1	*ari-t*
qHvDRR45-PH-7.1	7H	JHI-Hv50k-2016-491516	139.5	539028571	3.6	JHI-Hv50k-2016-487625	127.5	473171587	JHI-Hv50k-2016-492638	146.4	565539004	2.8	Kombyne	11.8	*brh7*
HvDRR45														51.2	
HvDRR46	NO QTL														
qHvDRR47-PH-2.1	2H	JHI-Hv50k-2016-77567	74.8	41785355	6.5	JHI-Hv50k-2016-75229	48.9	30738391	JHI-Hv50k-2016-77956	77.1	43701749	3.6	Sissy	22.7	*2H.2 (Nice et al., 2017)*
qHvDRR47-PH-3.1	3H	JHI-Hv50k-2016-211559	339.8	585397421	4.2	JHI-Hv50k-2016-206035	296.7	567852591	SCRI_RS_230717	401.3	611216678	2.8	IG31424	14.1	*sdw1*
HvDRR47														34.5	
qHvDRR48-PH-2.1	2H	JHI-Hv50k-2016-73692	35.9	26152710	4.9	JHI-Hv50k-2016-72920	31.3	24495630	JHI-Hv50k-2016-74094	46.9	27574925	3.0	HOR1842	20.0	*Ppd-H1*
qHvDRR48-PH-4.1	4H	JHI-Hv50k-2016-228890	41.7	8817372	4.8	JHI-Hv50k-2016-228195	21.4	5728553	JHI-Hv50k-2016-229257	43.9	9515964	2.8	HOR7985	19.5	
HvDRR48														34.9	

Supplementary Table 7: Prediction ability of the genomic SNP marker data for flowering time and plant height without cross-validation (CV) and with five fold cross-validation across all sub-populations. SD indicates the standard deviation.

	Prediction ability across sub-populations		SD
	Without CV	5 Fold CV 20 runs	5 Fold CV 20 runs
Flowering time	0.89	0.766	0.015
Plant height	0.874	0.773	0.014

Supplementary Table 8: Genome-wide epistatic loci detected in the HvDRR population. LOD indicates the logarithm of odds of the interaction.

Trait	Population	Chromosome locus 1	Position locus 1 (cM)	Chromosome locus 2	Position locus 2 (cM)	LOD	p-value
Flowering time	HvDRR13	5H	107.5	6H	87.5	6.74345	0.006
Plant height	HvDRR02	5H	205.0	7H	72.5	11.5203	0
Plant height	HvDRR09	1H	172.5	7H	97.5	4.273374	0.042
Plant height	HvDRR17	1H	2.5	1H	7.5	4.125857	0.046
Plant height	HvDRR34	4H	165.0	5H	180.0	4.260018	0.034
Plant height	HvDRR34	4H	160.0	7H	215.0	4.484935	0.022
Plant height	HvDRR41	1H	122.5	5H	225.0	3.985981	0.042
Plant height	HvDRR44	2H	75.0	5H	262.5	11.46462	0.002
Plant height	HvDRR44	5H	262.5	7H	195.0	11.14014	0.002
Plant height	HvDRR45	1H	85.0	5H	197.5	5.781251	0.032

Supplementary Table 9: Lists of primers used to amplify *Ppd-H1* and *Vrn-H2*. The *Ppd-H1* primers are listed for each parental inbred. N-ter primers were used to amplify the start while the C-ter primers the end of the coding sequences. The primers pairs marked with * amplified the whole gene. Primers used to amplify *Vrn-H2* have the same nomenclature as described in Karsai *et al*. (2005).

Parental inbred	N-ter		Middle 1st		Middle 2nd		C-ter	
	Forward primer	Reverse primer	Forward primer	Reverse prime	Forward primer	Reverse primer	Forward primer	Reverse primer
Ancap2	ATCGAATCACCCGTTTCAATC	GACACCATCAGAGATAGTAAC	CAAATGTTCATCTGCTCCACC	CGCACACATATTGTACCTTGC	AGATGCTCCTAACTGCTCCT	ACCCATTTCTTTCGCTGCTG	ATCGAATCACCCGTTTCAATC*	TCCACACGCTCGTACTATGT*
CM67	ATCGAATCACCCGTTTCAATC	GACACCATCAGAGATAGTAAC	CAAATGTTCATCTGCTCCACC	CGCACACATATTGTACCTTGC	AGATGCTCCTAACTGCTCCT	ACCCATTTCTTTCGCTGCTG	TGGTGACCAAGCCCTGTG	AGCACAATACTCACTCATACTGC
Georgie	ATCGAATCACCCGTTTCAATC	GACACCATCAGAGATAGTAAC	CAAATGTTCATCTGCTCCACC	CGCACACATATTGTACCTTGC	AGATGCTCCTAACTGCTCCT	ACCCATTTCTTTCGCTGCTG	CTGAACCAAAAGCTGCCTGT	GCCGGCATGTTCTATGGTAG
HOR12830	ATCGAATCACCCGTTTCAATC	GACACCATCAGAGATAGTAAC	CAAATGTTCATCTGTTCCAGC	CGCACACATATTGTACCTTGC	AGATGCTCCTAACTGCTCCT	ACCCATTTCTTTCGCTGCTG	TGGTGACCAAGCCCTGTG	AGCACAATACTCACTCATACTGC
HOR1842	ATCGAATCACCCGTTTCAATC	GACACCATCAGAGATAGTAAC	CAAATGTTCATCTGCTCCACC	CGCACACATATTGTACCTTGC	AGATGCTCCTAACTGCTCCT	ACCCATTTCTTTCGCTGCTG	TCCGTATGTTGCATACTAACC	CTCCCAATGATCCATGGCC
HOR383	ATCGAATCACCCGTTTCAATC	GACACCATCAGAGATAGTAAC	CAAATGTTCATCTGCTCCACC	CGCACACATATTGTACCTTGC	AGATGCTCCTAACTGCTCCT	ACCCATTTCTTTCGCTGCTG	TCCGTATGTTGCATACTAACC	CTCCCAATGATCCATGGCC
HOR7985	ATCGAATCACCCGTTTCAATC	GACACCATCAGAGATAGTAAC	CAAATGTTCATCTGCTCCACC	CGCACACATATTGTACCTTGC	AGATGCTCCTAACTGCTCCT	ACCCATTTCTTTCGCTGCTG	TGGTGACCAAGCCCTGTG	AGCACAATACTCACTCATACTGC
HOR8160	CTCTGTTTCCGCTCGATTGG	CGACGACATCACTGGAAACG	CAAATGTTCATCTGCTCCACC	CGCACACATATTGTACCTTGC	AGATGCTCCTAACTGCTCCT	ACCCATTTCTTTCGCTGCTG	TCCGTATGTTGCATACTAACC	CTCCCAATGATCCATGGCC
IG128104	ATCGAATCACCCGTTTCAATC	GACACCATCAGAGATAGTAAC	CAAATGTTCATCTGCTCCACC	CGCACACATATTGTACCTTGC	AGATGCTCCTAACTGCTCCT	ACCCATTTCTTTCGCTGCTG	TCCGTATGTTGCATACTAACC	CTCCCAATGATCCATGGCC
IG128216	ATCGAATCACCCGTTTCAATC	GACACCATCAGAGATAGTAAC	CAAATGTTCATCTGCTCCACC	CGCACACATATTGTACCTTGC	AGATGCTCCTAACTGCTCCT	ACCCATTTCTTTCGCTGCTG	TCCGTATGTTGCATACTAACC	CTCCCAATGATCCATGGCC
IG31424	CTCTGTTTCCGCTCGATTGG	CGACGACATCACTGGAAACG	CAAATGTTCATCTGTTCCAGC	CGCACACATATTGTACCTTGC	AGATGCTCCTAACTGCTCCT	ACCCATTTCTTTCGCTGCTG	TGGTGACCAAGCCCTGTG	AGCACAATACTCACTCATACTGC
ItuNat ve	CTCTGTTTCCGCTCGATTGG	CGACGACATCACTGGAAACG	CAAATGTTCATCTGCTCCACC	CGCACACATATTGTACCTTGC	AGATGCTCCTAACTGCTCCT	ACCCATTTCTTTCGCTGCTG	CCAATTGTTCGAGCTGCTGA	TCTTCCAGGAGATGAGACGAG
K10693	ATCGAATCACCCGTTTCAATC	GACACCATCAGAGATAGTAAC	CAAATGTTCATCTGCTCCACC	CGCACACATATTGTACCTTGC	AGATGCTCCTAACTGCTCCT	ACCCATTTCTTTCGCTGCTG	TCCGTATGTTGCATACTAACC	CTCCCAATGATCCATGGCC
K10877	CTCTGTTTCCGCTCGATTGG	CGACGACATCACTGGAAACG	CAAATGTTCATCTGTTCCAGC	CGCACACATATTGTACCTTGC	AGATGCTCCTAACTGCTCCT	ACCCATTTCTTTCGCTGCTG	ATCGAATCACCCGTTTCAATC*	TCCACACGCTCGTACTATGT*
Kharsila	ATCGAATCACCCGTTTCAATC	GACACCATCAGAGATAGTAAC	CAAATGTTCATCTGCTCCACC	CGCACACATATTGTACCTTGC	AGATGCTCCTAACTGCTCCT	ACCCATTTCTTTCGCTGCTG	TCCGTATGTTGCATACTAACC	CTCCCAATGATCCATGGCC
Kombyne	ATCGAATCACCCGTTTCAATC	GACACCATCAGAGATAGTAAC	CAAATGTTCATCTGCTCCACC	CGCACACATATTGTACCTTGC	AGATGCTCCTAACTGCTCCT	ACCCATTTCTTTCGCTGCTG	TCCGTATGTTGCATACTAACC	CTCCCAATGATCCATGGCC
Lakhan	CTCTGTTTCCGCTCGATTGG	CGACGACATCACTGGAAACG	CAAATGTTCATCTGTTCCAGC	CGCACACATATTGTACCTTGC	AGATGCTCCTAACTGCTCCT	ACCCATTTCTTTCGCTGCTG	CAGGAGGAACAGAGGAACGT	TCTTCCAGGAGATGAGACGAG
Namhaebori	ATCGAATCACCCGTTTCAATC	GACACCATCAGAGATAGTAAC	CAAATGTTCATCTGCTCCACC	CGCACACATATTGTACCTTGC	AGATGCTCCTAACTGCTCCT	ACCCATTTCTTTCGCTGCTG	TGGTGACCAAGCCCTGTG	AGCACAATACTCACTCATACTGC
Sanalta	ATCGAATCACCCGTTTCAATC	GACACCATCAGAGATAGTAAC	CAAATGTTCATCTGCTCCACC	CGCACACATATTGTACCTTGC	AGATGCTCCTAACTGCTCCT	ACCCATTTCTTTCGCTGCTG	TCCGTATGTTGCATACTAACC	CTCCCAATGATCCATGGCC
Sissy	ATCGAATCACCCGTTTCAATC	GACACCATCAGAGATAGTAAC	CAAATGTTCATCTGCTCCACC	CGCACACATATTGTACCTTGC	AGATGCTCCTAACTGCTCCT	ACCCATTTCTTTCGCTGCTG	TCCGTATGTTGCATACTAACC	CTCCCAATGATCCATGGCC
Sprat Archer	ATCGAATCACCCGTTTCAATC	TACACCATCAGAGATAGTAAC	CAAATGTTCATCTGTTCCAGC	CGCACACATATTGTACCTTGC	AGATGCTCCTAACTGCTCCT	ACCCATTTCTTTCGCTGCTG	TCCGTATGTTGCATACTAACC	CTCCCAATGATCCATGGCC
Unumli-Arpa	ATCGAATCACCCGTTTCAATC	GACACCATCAGAGATAGTAAC	CAAATGTTCATCTGCTCCACC	CGCACACATATTGTACCTTGC	AGATGCTCCTAACTGCTCCT	ACCCATTTCTTTCGCTGCTG	TCCGTATGTTGCATACTAACC	CTCCCAATGATCCATGGCC
W23829/803911	ATCGAATCACCCGTTTCAATC	GACACCATCAGAGATAGTAAC	CAAATGTTCATCTGCTCCACC	CGCACACATATTGTACCTTGC	AGATGCTCCTAACTGCTCCT	ACCCATTTCTTTCGCTGCTG	TCCGTATGTTGCATACTAACC	CTCCCAATGATCCATGGCC

Primer name	Primer sequence
HvZCCT.06F	CCTAGTTAAAACATATATCCATAGAGC
HvZCCT.07R	GATCGTTGCGTTGCTAATAGTG
HvZCCT.HcF	CACCATCGCATGATGCAC
HvZCCT.HcR	TCATATGGCGAAGCTGGAG

Supplementary Table 10: List of candidate genes in the confidence interval of selected QTL that carried a polymorphism among the parental lines. IN/DEL indicates an insertion or a deletion, SV indicates predicted structural variants.

Trait	QTL	Gene name	Annotation	Polymorphism	Start (bp)	End (bp)
Flowering time	*qHvDRR02-FT-5.1*	HORVU.MOREX.r3.5HG0511790	WRKY transcription factor	IN/DEL	529688151	529692066
Flowering time	*qHvDRR28-FT-2.2*	HORVU.MOREX.r3.2HG0170150	pseudo-response regulator 3	SNP	489043031	489043723
Flowering time	*qHvDRR28-FT-2.2*	HORVU.MOREX.r3.2HG0170460	Ethylene responsive transcription factor	SV	491338258	491338785
Flowering time	*qHvDRR28-FT-2.2*	HORVU.MOREX.r3.2HG0172990	Receptor kinase-like protein	IN/DEL	508602510	508608623
Flowering time	*qHvDRR28-FT-2.2*	HORVU.MOREX.r3.2HG0173600	Receptor-like kinase	SNP	513985255	513987841
Flowering time	*qHvDRR28-FT-2.2*	HORVU.MOREX.r3.2HG0173720	F-box protein	SNP	514884459	514886953
Flowering time	*qHvDRR41-FT-2.2*	HORVU.MOREX.r3.2HG0172990	Receptor kinase-like protein	SNP	508602510	508608623
Flowering time	*qHvDRR41-FT-2.2*	HORVU.MOREX.r3.2HG0173600	Receptor-like kinase	IN/DEL	513985255	513987841
Flowering time	*qHvDRR41-FT-2.2*	HORVU.MOREX.r3.2HG0173720	F-box protein	SNP	514884459	514886953
Flowering time	*qHvDRR42-FT-3.1*	HORVU.MOREX.r3.3HG0294500	F-box family protein	IN/DEL	514548165	514552750
Flowering time	*qHvDRR42-FT-3.1*	HORVU.MOREX.r3.3HG0295240	Transcription factor	SNP	518705563	518707116
Plant height	*qHvDRR18-PH-7.1*	HORVU.MOREX.r3.7HG0647440	Cytochrome P450 family protein, expressed	IN/DEL	24114355	24116823
Plant height	*qHvDRR18-PH-7.1*	HORVU.MOREX.r3.7HG0650260	WRKY family transcription factor	IN/DEL	30228811	30233849
Plant height	*qHvDRR21-PH-7.1*	HORVU.MOREX.r3.7HG0679760	Basic helix-loop-helix transcription factor	IN/DEL	174290744	174293655
Plant height	*qHvDRR21-PH-7.1*	HORVU.MOREX.r3.7HG0679780	ETHYLENE INSENSITIVE 3-like 3 protein	IN/DEL	174906435	174909757
Plant height	*qHvDRR21-PH-7.1*	HORVU.MOREX.r3.7HG0679980	Squamosa promoter binding protein	IN/DEL	175604764	175609951
Plant height	*qHvDRR21-PH-7.1*	HORVU.MOREX.r3.7HG0681550	Auxin response factor	IN/DEL	186801101	186809084
Plant height	*qHvDRR21-PH-7.1*	HORVU.MOREX.r3.7HG0685230	Ethylene-responsive transcription factor	IN/DEL	214418007	214419708
Plant height	*qHvDRR21-PH-7.1*	HORVU.MOREX.r3.7HG0685870	Ankyrin repeat domain containing protein	IN/DEL	217930102	217934698
Plant height	*qHvDRR21-PH-7.1*	HORVU.MOREX.r3.7HG0687530	F-box protein	SNP	237430504	237431780
Plant height	*qHvDRR21-PH-7.1*	HORVU.MOREX.r3.7HG0692330	Basic helix-loop-helix transcription factor	SNP	287414769	287415368
Plant height	*qHvDRR21-PH-7.1*	HORVU.MOREX.r3.7HG0693000	Receptor-like protein kinase 1	IN/DEL	298396043	298396558
Plant height	*qHvDRR21-PH-7.1*	HORVU.MOREX.r3.7HG0695760	Cytochrome P450 family protein	SNP	335129415	335134705
Plant height	*qHvDRR21-PH-7.1*	HORVU.MOREX.r3.7HG0701240	Receptor-like kinase	SNP	395316354	395317058
Plant height	*qHvDRR21-PH-7.1*	HORVU.MOREX.r3.7HG0706930	F-box family protein	SV	441359842	441361274
Plant height	*qHvDRR22-PH-7.1*	HORVU.MOREX.r3.7HG0679760	Basic helix-loop-helix transcription factor	SV	174290744	174293655
Plant height	*qHvDRR22-PH-7.1*	HORVU.MOREX.r3.7HG0681550	Auxin response factor	IN/DEL	186801101	186809084
Plant height	*qHvDRR22-PH-7.1*	HORVU.MOREX.r3.7HG0684710	Leucine-rich repeat receptor-like protein kinase	IN/DEL	211389528	211390699
Plant height	*qHvDRR22-PH-7.1*	HORVU.MOREX.r3.7HG0685230	Ethylene-responsive transcription factor	SNP	214418007	214419708
Plant height	*qHvDRR22-PH-7.1*	HORVU.MOREX.r3.7HG0685360	Receptor protein kinase, putative	IN/DEL	215316327	215319934
Plant height	*qHvDRR22-PH-7.1*	HORVU.MOREX.r3.7HG0685720	basic helix-loop-helix (bHLH) DNA-binding superfamily protein	SNP	217520399	217520773
Plant height	*qHvDRR22-PH-7.1*	HORVU.MOREX.r3.7HG0685870	Ankyrin repeat domain containing protein	SNP	217930102	217934698
Plant height	*qHvDRR22-PH-7.1*	HORVU.MOREX.r3.7HG0687530	F-box protein	SNP	237430504	237431780
Plant height	*qHvDRR22-PH-7.1*	HORVU.MOREX.r3.7HG0692330	Basic helix-loop-helix transcription factor	SNP	287414769	287415368
Plant height	*qHvDRR22-PH-7.1*	HORVU.MOREX.r3.7HG0693000	Receptor-like protein kinase 1	IN/DEL	298396043	298396558
Plant height	*qHvDRR22-PH-7.1*	HORVU.MOREX.r3.7HG0695760	Cytochrome P450 family protein	SNP	335129415	335134705
Plant height	*qHvDRR23-PH-7.1*	HORVU.MOREX.r3.7HG0679350	Leucine-rich repeat receptor-like protein kinase family	IN/DEL	171303078	171304775
Plant height	*qHvDRR23-PH-7.1*	HORVU.MOREX.r3.7HG0679760	Basic helix-loop-helix transcription factor	IN/DEL	174290744	174293655
Plant height	*qHvDRR23-PH-7.1*	HORVU.MOREX.r3.7HG0679780	ETHYLENE INSENSITIVE 3-like 3 protein	IN/DEL	174906435	174909757
Plant height	*qHvDRR23-PH-7.1*	HORVU.MOREX.r3.7HG0681550	Auxin response factor	IN/DEL	186801101	186809084
Plant height	*qHvDRR23-PH-7.1*	HORVU.MOREX.r3.7HG0684710	Leucine-rich repeat receptor-like protein kinase	IN/DEL	211389528	211390699
Plant height	*qHvDRR23-PH-7.1*	HORVU.MOREX.r3.7HG0685230	Ethylene-responsive transcription factor	IN/DEL	214418007	214419708
Plant height	*qHvDRR23-PH-7.1*	HORVU.MOREX.r3.7HG0685360	Receptor protein kinase, putative	SNP	215316327	215319934
Plant height	*qHvDRR23-PH-7.1*	HORVU.MOREX.r3.7HG0685720	basic helix-loop-helix (bHLH) DNA-binding superfamily protein	SNP	217520399	217520773
Plant height	*qHvDRR23-PH-7.1*	HORVU.MOREX.r3.7HG0685870	Ankyrin repeat domain containing protein	IN/DEL	217930102	217934698
Plant height	*qHvDRR23-PH-7.1*	HORVU.MOREX.r3.7HG0687530	F-box protein	IN/DEL	237430504	237431780
Plant height	*qHvDRR23-PH-7.1*	HORVU.MOREX.r3.7HG0692330	Basic helix-loop-helix transcription factor	SNP	287414769	287415368
Plant height	*qHvDRR23-PH-7.1*	HORVU.MOREX.r3.7HG0693000	Receptor-like protein kinase 1	IN/DEL	298396043	298396558
Plant height	*qHvDRR23-PH-7.1*	HORVU.MOREX.r3.7HG0695760	Cytochrome P450 family protein	SNP	335129415	335134705
Plant height	*qHvDRR23-PH-7.1*	HORVU.MOREX.r3.7HG0701080	MYB transcription factor	IN/DEL	393617557	393619314
Plant height	*qHvDRR23-PH-7.1*	HORVU.MOREX.r3.7HG0701240	Receptor-like kinase	SNP	395316354	395317058
Plant height	*qHvDRR23-PH-7.1*	HORVU.MOREX.r3.7HG0702010	BHLH transcription factor	IN/DEL	402393931	402398482
Plant height	*qHvDRR23-PH-7.1*	HORVU.MOREX.r3.7HG0704030	Leucine-rich repeat (LRR) family protein	IN/DEL	418434701	418435006
Plant height	*qHvDRR24-PH-3.1*	HORVU.MOREX.r3.3HG0222140	Abscisic acid-deficient 4	SNP	7879841	7881157
Plant height	*qHvDRR24-PH-3.1*	HORVU.MOREX.r3.3HG0222500	F-box family protein	SNP	8689676	8690920
Plant height	*qHvDRR24-PH-3.1*	HORVU.MOREX.r3.3HG0224910	Receptor-like protein kinase	IN/DEL	12550264	12558296
Plant height	*qHvDRR24-PH-3.1*	HORVU.MOREX.r3.3HG0225310	Leucine-rich repeat receptor-like protein kinase family protein	IN/DEL	13210488	13214494
Plant height	*qHvDRR26-PH-4.1*	HORVU.MOREX.r3.4HG0340090	GATA transcription factor	SNP	28519563	28523383
Plant height	*qHvDRR29-PH-2.1*	HORVU.MOREX.r3.2HG0182430	AP2-like ethylene-responsive transcription factor SNZ	SNP + SV	561922125	561924536
Plant height	*qHvDRR29-PH-2.1*	HORVU.MOREX.r3.2HG0184300	Receptor kinase, putative	IN/DEL	568960838	568965967
Plant height	*qHvDRR31-PH-1.1*	HORVU.MOREX.r3.1HG0094840	Leucine-rich repeat receptor-like protein kinase family protein	SNP	514742923	514744137
Plant height	*qHvDRR47-PH-2.1*	HORVU.MOREX.r3.2HG0110400	F-box family protein	IN/DEL	32468345	32469451
Plant height	*qHvDRR47-PH-2.1*	HORVU.MOREX.r3.2HG0111100	Ethylene insensitive 3	SNP	34542934	34544805
Plant height	*qHvDRR47-PH-2.1*	HORVU.MOREX.r3.2HG0111780	Cytochrome P450 family protein, expressed	IN/DEL	38503489	38507833
Plant height	*qHvDRR47-PH-2.1*	HORVU.MOREX.r3.2HG0111790	Receptor-like kinase	IN/DEL	38585238	38590568
Plant height	*qHvDRR47-PH-2.1*	HORVU.MOREX.r3.2HG0111960	WRKY transcription factor	IN/DEL	39128713	39130996
Plant height	*qHvDRR47-PH-2.1*	HORVU.MOREX.r3.2HG0112180	Receptor-like kinase	SNP	40089781	40091197
Plant height	*qHvDRR47-PH-2.1*	HORVU.MOREX.r3.2HG0112200	F-box family protein	SNP	40165471	40167198
Plant height	*qHvDRR47-PH-2.1*	HORVU.MOREX.r3.2HG0113130	F-box family protein	SNP	43185684	43187206
Plant height	*qHvDRR48-PH-4.1*	HORVU.MOREX.r3.4HG0333850	basic helix-loop-helix (bHLH) DNA-binding superfamily protein	IN/DEL	6499457	6502480
Plant height	*qHvDRR48-PH-4.1*	HORVU.MOREX.r3.4HG0334320	F-box family protein	IN/DEL	8320765	8323470

Supplementary Figure 1: Histogram and correlation plot between flowering time (FT) and plant height (PH) across all 45 HvDRR sub-populations. Flowering time is reported in days after sowing (DAS) and plant height in cm.

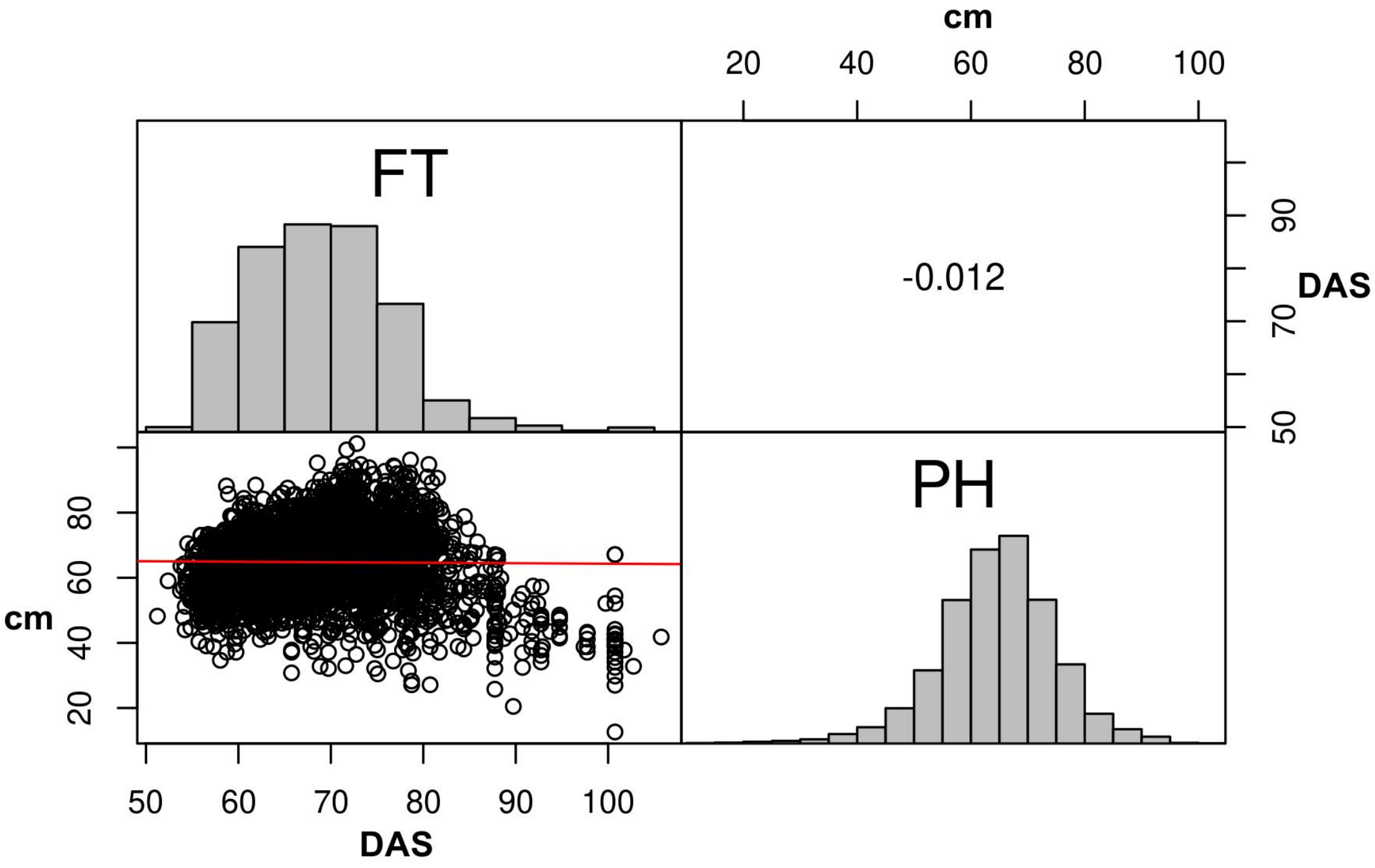

Supplementary Figure 2: Histograms and correlation plots between flowering time (FT, in days after sowing) and plant height (PH, in cm), for each of the 45 HvDRR sub-populations.

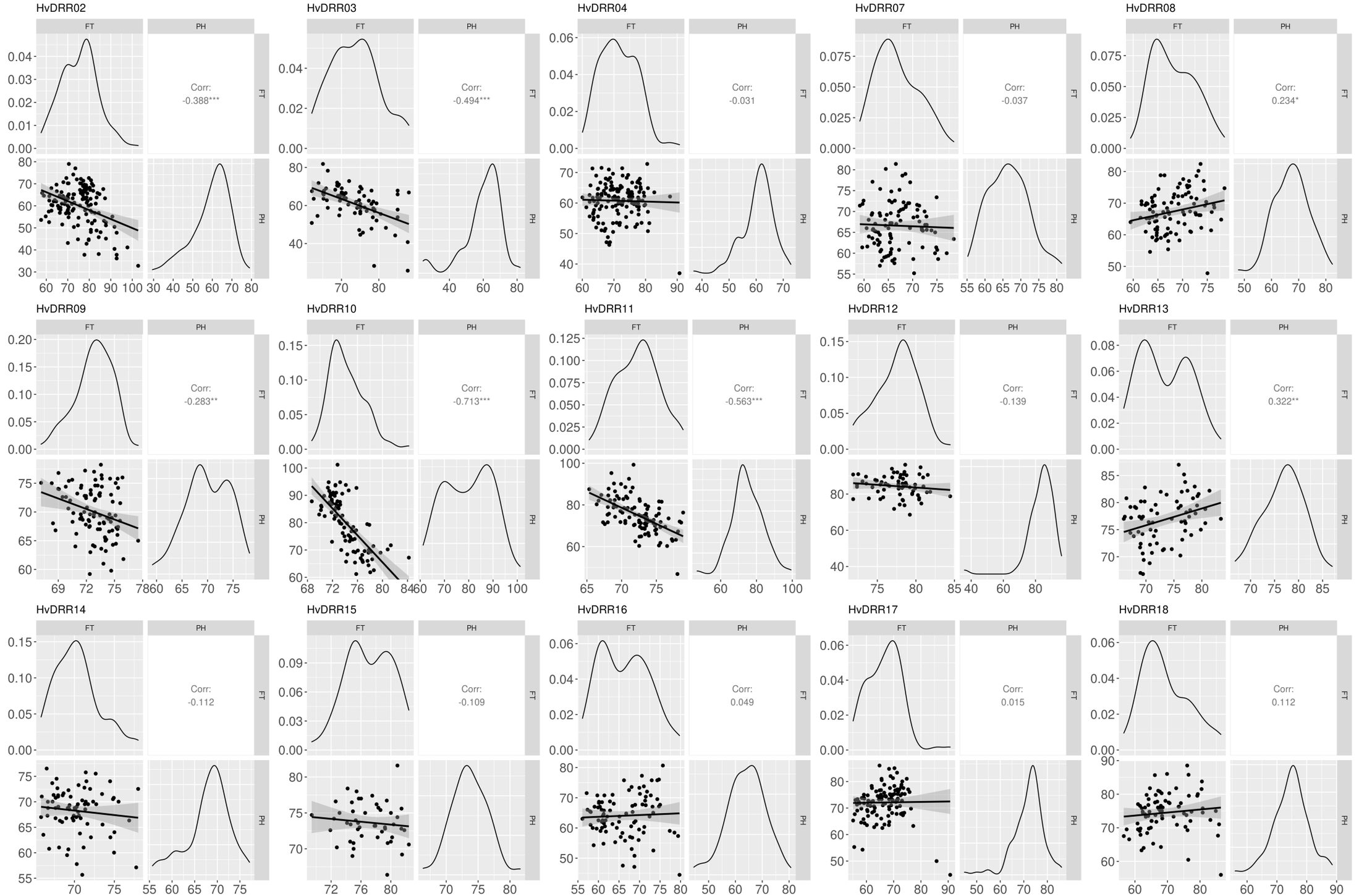

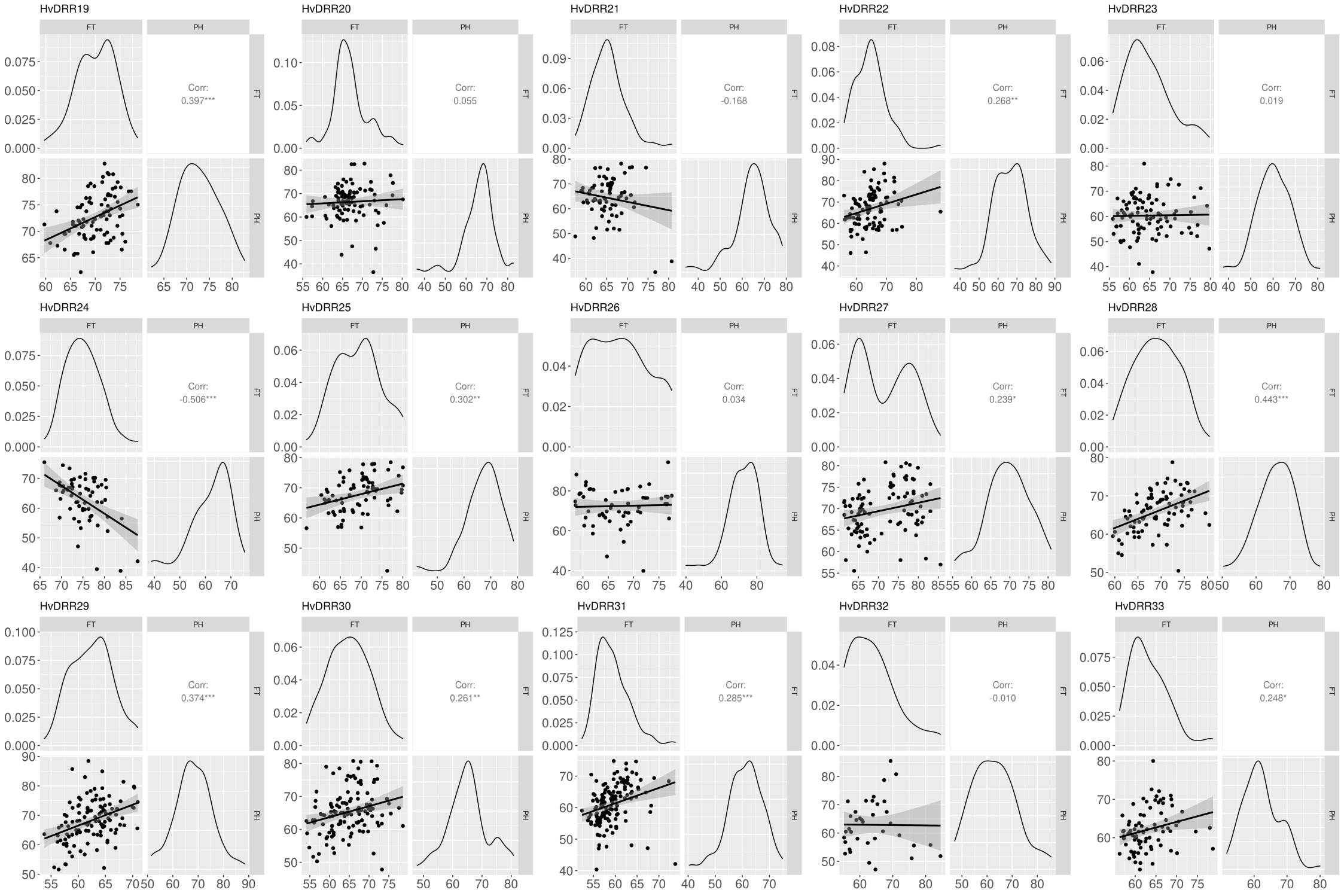
HvDRR19
HvDRR20
HvDRR21
HvDRR22
HvDRR23
HvDRR24
HvDRR25
HvDRR26
HvDRR27
HvDRR28
HvDRR29
HvDRR30
HvDRR31
HvDRR32
HvDRR33
FT
PH
Corr:
0.397***
Corr:
0.055
Corr:
-0.168
Corr:
0.268**
Corr:
0.019
Corr:
-0.506***
Corr:
0.302**
Corr:
0.034
Corr:
0.239*
Corr:
0.443***
Corr:
0.374***
Corr:
0.261**
Corr:
0.285***
Corr:
-0.010
Corr:
0.248*

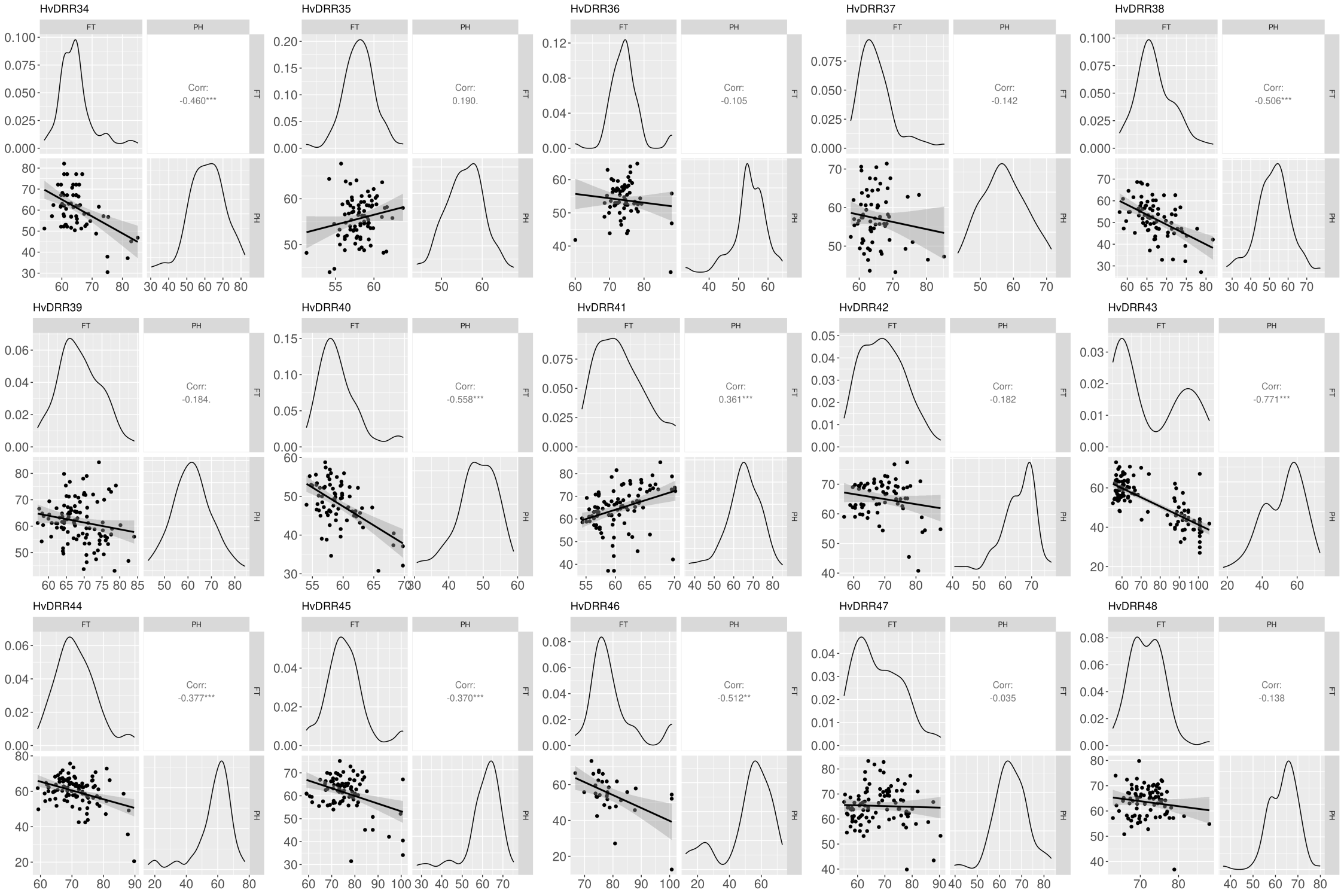
HvDRR34
HvDRR35
HvDRR36
HvDRR37
HvDRR38
HvDRR39
HvDRR40
HvDRR41
HvDRR42
HvDRR43
HvDRR44
HvDRR45
HvDRR46
HvDRR47
HvDRR48
FT
PH
Corr:
-0.460***
Corr:
0.190.
Corr:
-0.105
Corr:
-0.142
Corr:
-0.506***
Corr:
-0.184.
Corr:
-0.558***
Corr:
0.361***
Corr:
-0.182
Corr:
-0.771***
Corr:
-0.377***
Corr:
-0.370***
Corr:
-0.512**
Corr:
-0.035
Corr:
-0.138

Supplementary Figure 3: Effect size of the QTL detected through multi-parent population analysis for flowering time (top, in days after sowing) and plant height (bottom, in cm), for each of the parental lines.

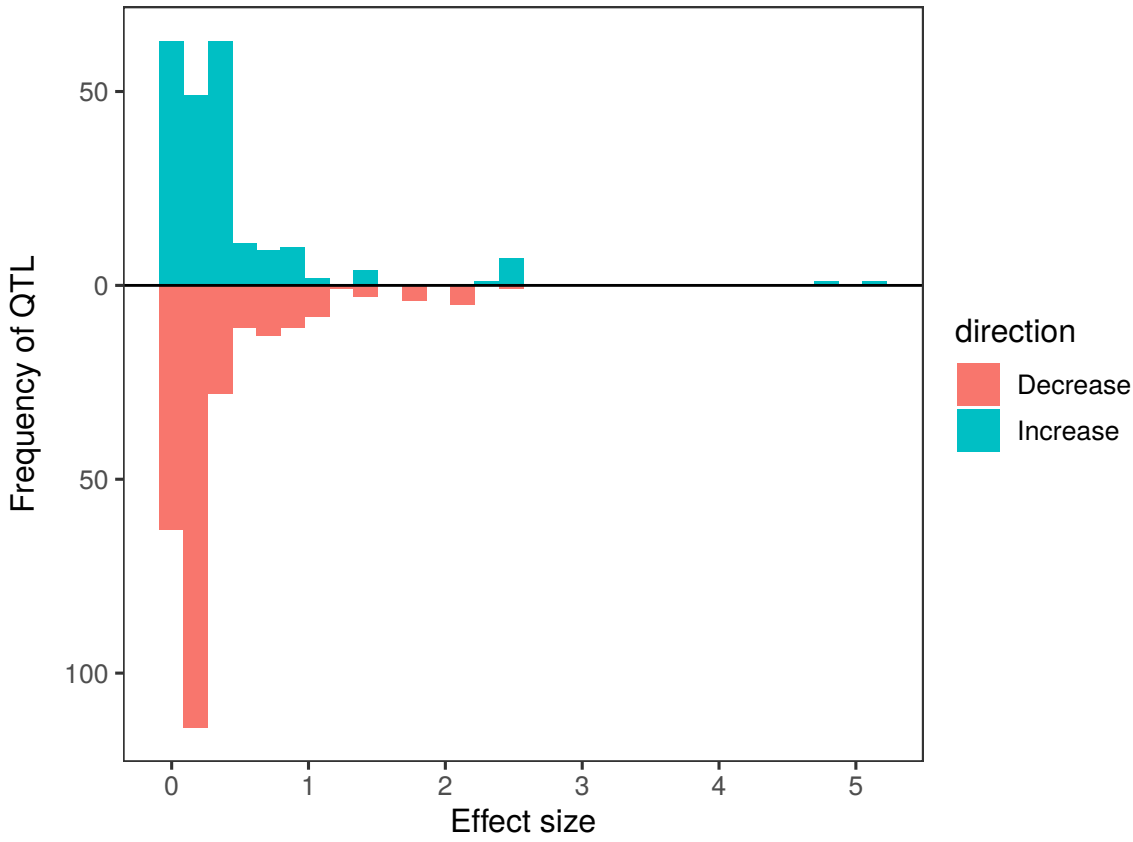

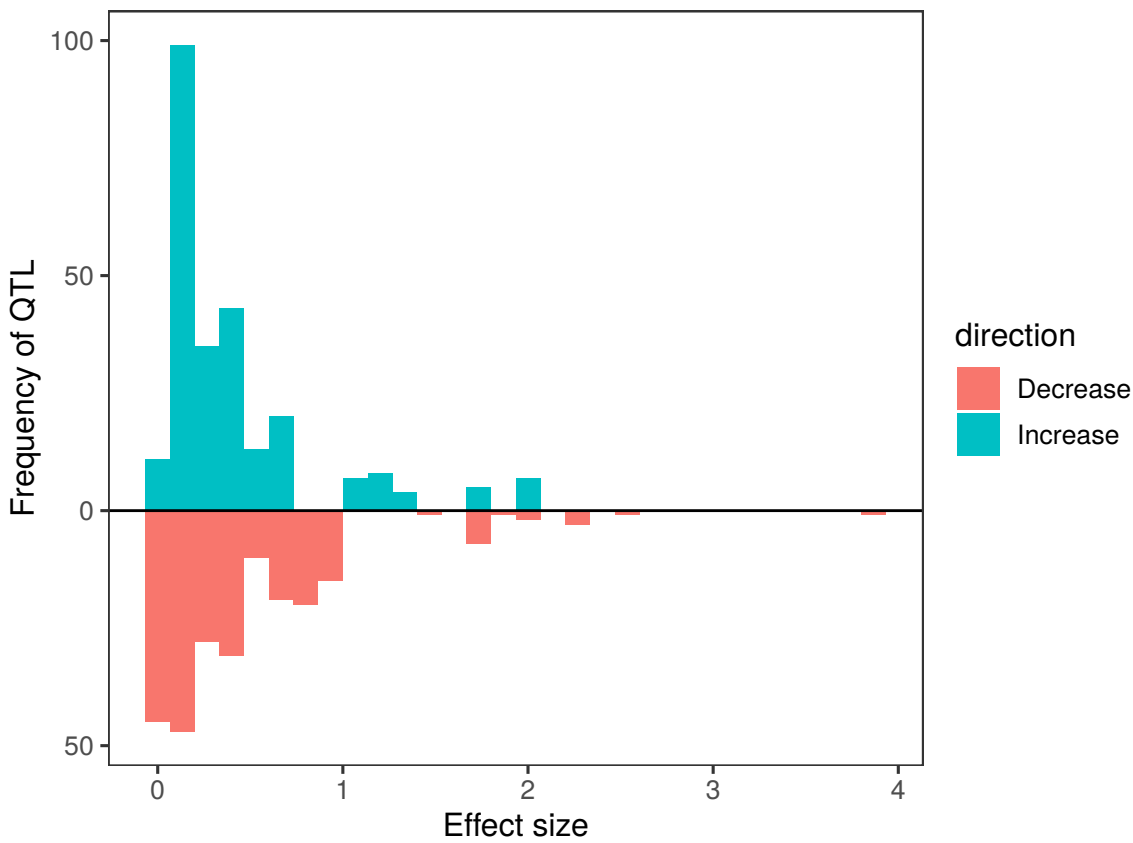

Supplementary Figure 4: Amino acid sequence of the terminal region of *Ppd-H1* of Morex, Igri, Optic, Golden Promise, Triumph, and the 23 parental inbreds of the HvDRR population. The amino acid synthesized by the triplet containing SNP 22 is highlighted in yellow, the one synthesized by the triplet containing SNP 1945 is highlighted in blue.

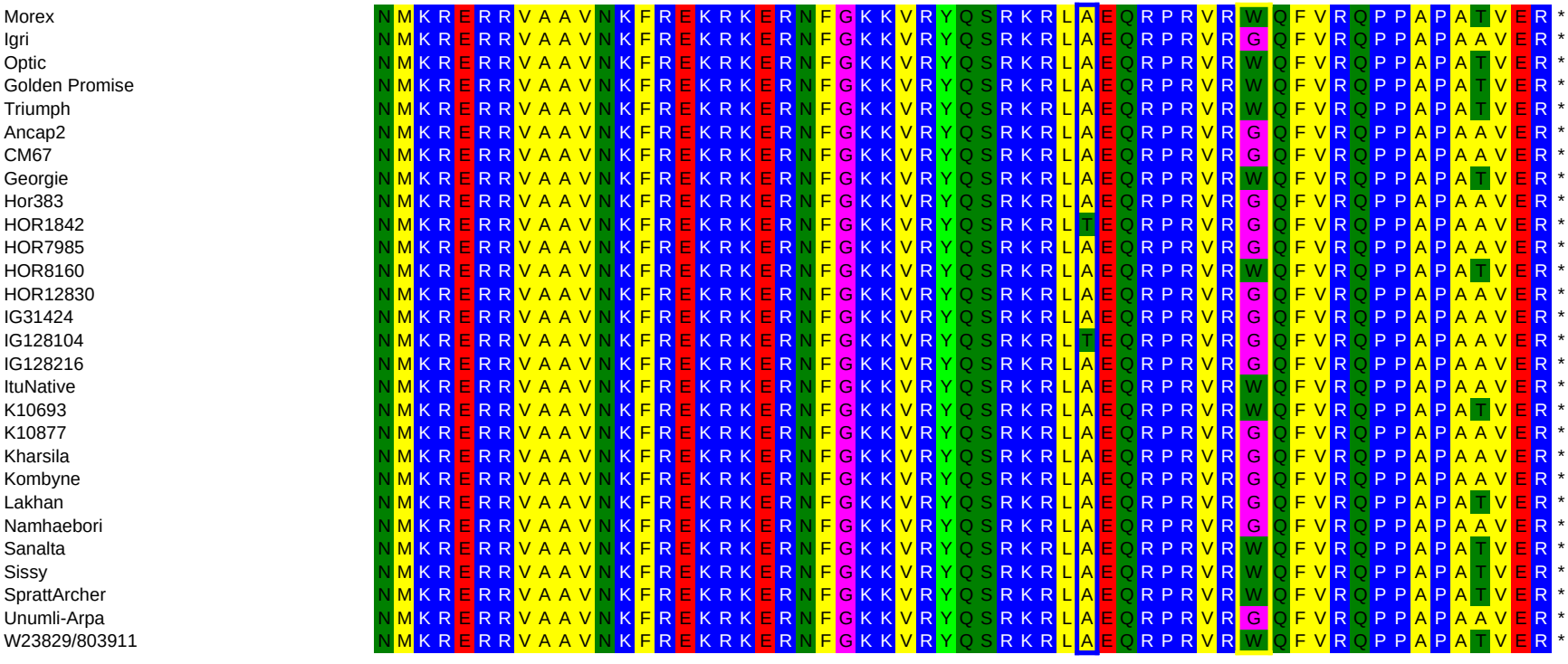

Supplementary Figure 5: Gel pictures of PCRs performed to detect the presence/absence of *ZCCT-Ha:b* (top) and *ZCCT-Hc* (bottom) as described in Karsai *et al*. (2005). The analyzed genotypes are Bowman (control spring variety), Antonella (control winter variety), Igri (control winter variety), and the parental inbreds of the sub-populations for which a QTL co-localizing with *Vrn-H2* was detected.

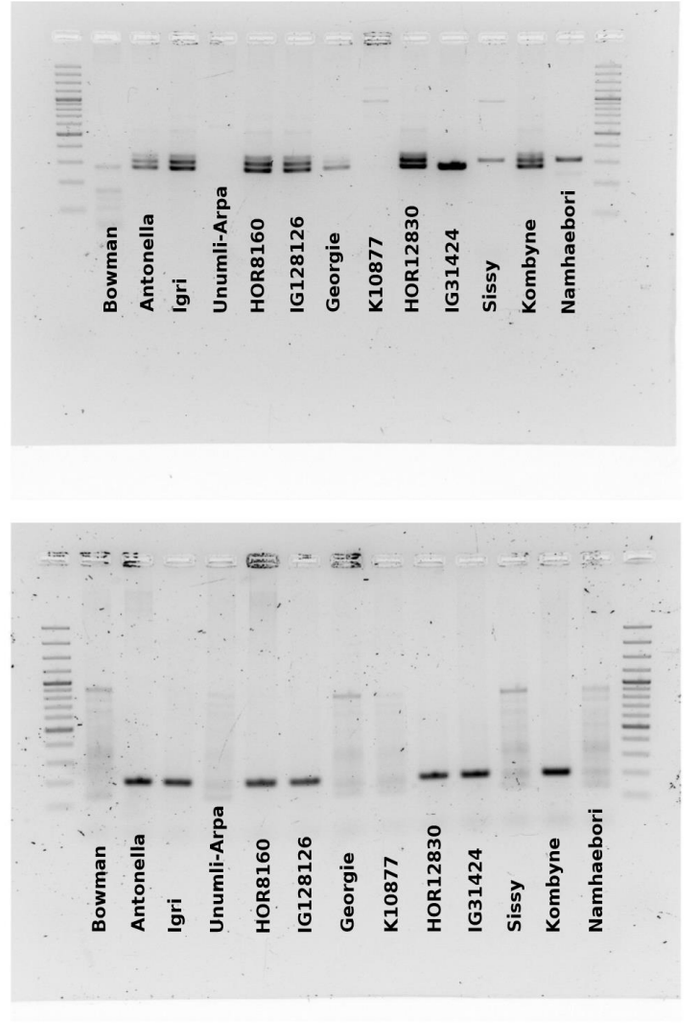

Supplementary Figure 6: Heat map of the module-trait relationships for plant height (PH) and flowering time (FT). On the y axis, the 27 detected modules are reported. For each module-trait correlation p-values are given in bracket

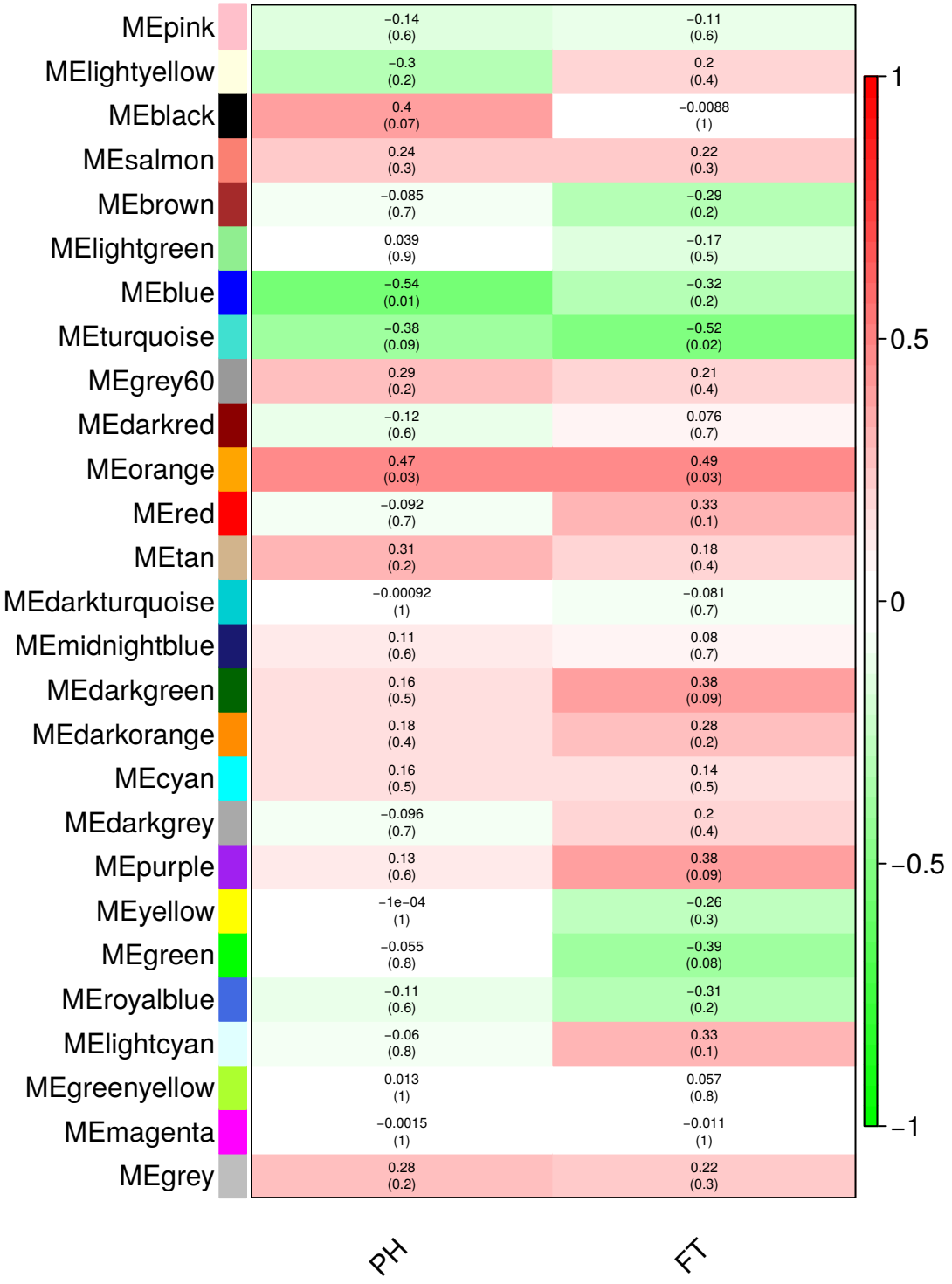

Supplementary Figure 7: Network predictions for modules “orange” (a), “black” (b), “darkgreen” (c), “purple” (d), “tan” (e), “lightyellow” (f), “green” (g), “blue” (h), and “turquoise” (i). Gene names with a gene-module membership p-value < 0.01 are indicated in the orange circles. Gene-gene interactions are represented by grey lines.

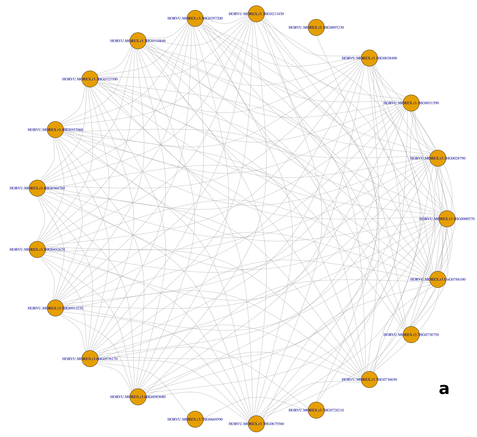

a

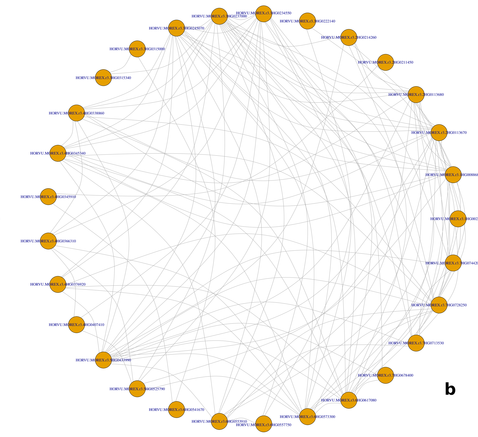

b

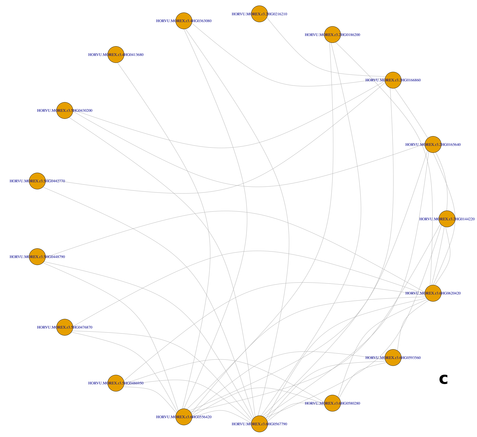

c

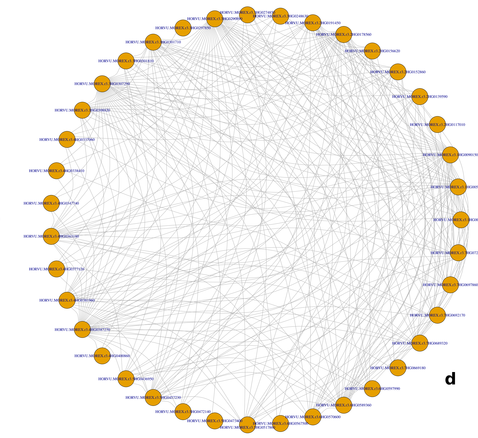

d

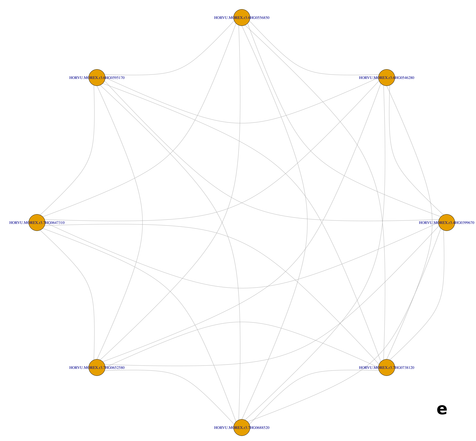

e

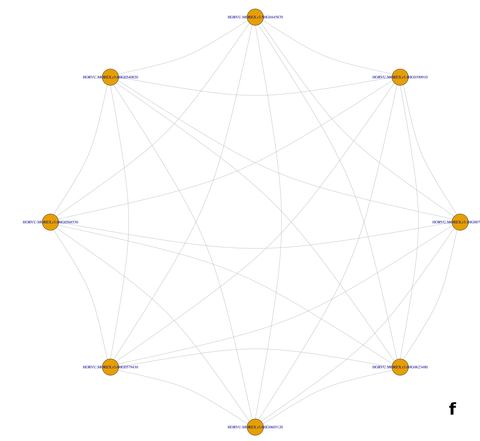

f

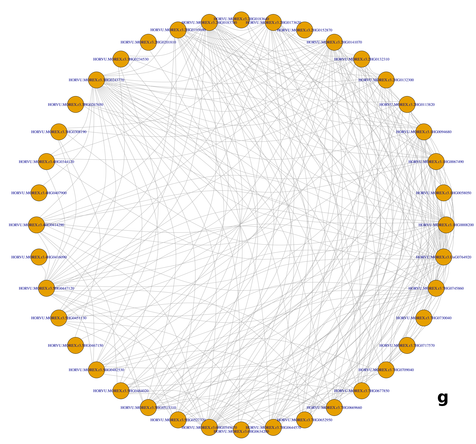

g

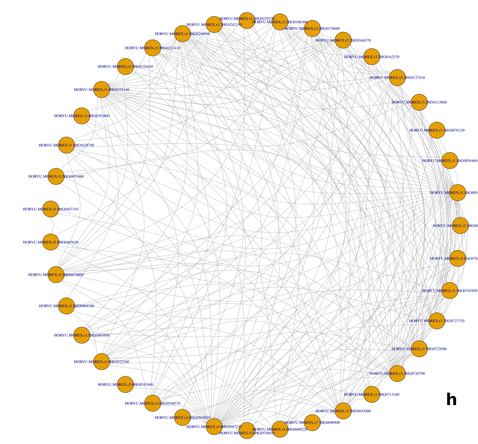

h

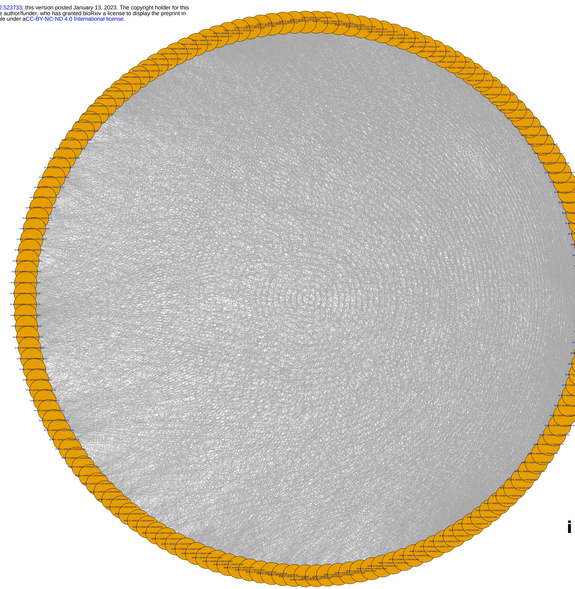

i

Supplementary Figure 8: Negative decadic logarithm of the p-value for association tests of sequence variants in QTL without previously reported genes for the control of the trait within their interval, explaining ≥ 15% variance, and with interval ≤ 30 cM for flowering time (left) and plant height (right). The QTL confidence intervals from single population analyses are indicated by colored bars.